

University of Trento

CIMeC, Centre for Mind/Brain Sciences



Doctoral School
in Cognitive and Brain Sciences

PhD Dissertation

THE ROLE OF NOISE
IN BRAIN DYNAMICS PROCESSES

Student: Andrea Vilardi

First supervisor: Dott. Leonardo Ricci

Second supervisor: Prof. Massimo Turatto

2006 – 2009 class

Contents

1	Introduction	1
I	Stochastic Resonance in Acoustic Perception	5
2	“Yes/No” discrimination paradigms	7
2.1	Introduction	8
2.2	Model for discrimination	10
2.2.1	Neural encoding	10
2.2.2	Discrimination ability	13
2.3	Psychometric function and perceptual threshold	15
2.4	Conclusions	19
3	Noise and acoustic perception	21
3.1	Introduction	22
3.2	experiments with exogenous noise	22
3.2.1	detrimental and non-detrimental role of noise	25
3.3	positive role of noise in non-linear systems	26
3.3.1	introduction	26
3.3.2	SR in biological systems	28
3.3.3	SR in human brain	29
3.3.4	SR and perceptual system	29
3.4	The experiment	31
3.4.1	Introduction	31
3.4.2	Participants and experimental setup	32
3.4.3	The model	33
3.5	Experimental procedure	35
3.6	Data Analysis	38
3.6.1	Analysis on single subject	38
3.6.2	Average procedure	42
3.7	Conclusions	45

II	Criterion Setting Dynamics	47
4	Signal Detection Theory	49
4.1	Introduction	50
4.2	SDT assumptions	51
4.2.1	Noise	52
4.2.2	Criterion	52
4.3	Stimulus/Response matrix and $p(c)$	52
4.4	Definition of d' and χ	54
4.5	H-F space	56
4.5.1	<i>Receiver Operating Characteristics (ROC)</i>	57
4.6	The role of Criterion	58
4.6.1	A model for stochastic resonance in perception	58
4.7	Conclusions	60
5	Feedback Control over Criterion Setting	63
5.1	Introduction	64
5.2	State of the art	65
5.3	Model	66
5.4	Experiment 1	71
5.4.1	Stimuli	71
5.4.2	Criterion shift	73
5.4.3	Experimental apparatus	76
5.4.4	Trial time-flow	76
5.4.5	Subjects	77
5.4.6	Time-line of the experimental session	78
5.4.7	Instructions	82
5.4.8	Criterion modulation	83
5.4.9	Data analysis	83
5.4.10	Results	84
5.5	Experiment 2	89
5.5.1	Motivations	89
5.5.2	Experimental setup	89
5.5.3	Subjects	91
5.5.4	Results	92
5.6	Merging of the two Experiments	99
5.7	Non-linear components of criterion dynamics	102
5.7.1	Results	106
5.8	Final discussion	108

III	General Discussion	109
6	Conclusions	111
A	Preliminar statement, instruction and final questions	115
B	Linear model for feedback loops	121

Chapter 1

Introduction

Noise is ubiquitous in nature. For this reason, it makes up a widely investigated topic [1]. Taking into account experimental physics, whatever the measurement process under investigation, noise, defined as a random fluctuation of the measured signal, is usually considered to be detrimental. Thus, many techniques have been developed to reduce its impact: for example, the most common post-processing procedure to improve a noisy measurement consists in averaging the measured signal over repeated sessions.

Rather surprisingly, the opposite, non-detrimental effect has been also observed: the response of a nonlinear system to a weak input signal is, under suitable conditions, optimized by the presence of a particular, non-vanishing noise level. In the last decades, the wide spectrum [2] of such phenomena has been referred to as *stochastic resonance* [3].

With regard to neuroscience, noise can be considered ubiquitous also in the brain processes. Theoretical considerations, as well as a robust experimental evidence, demonstrate its role in many phenomena occurring at different levels in neural system [4]: for example, firing rate of neurons is not predictable by reason of their intrinsic variability [1, 5, 6]; measurements of brain activity with imaging techniques, like EEG [7], MEG [8] or fMRI [9], are always affected by inner, noisy mechanisms.

Recently, neuroscientists put forward the idea that stochastic fluctuations of neural activity have a functional role in brain dynamics [10, 11]. However, this functional role has been thus far observed in very few experimental situations [12]. Regarding the human behaviour, decision making (representing our main field of investigation) is also influenced by several noisy processes [13]. Also in this case, random fluctuations of brain processes typically have a detrimental role, limiting, for example, the possibility to exactly predict the human behaviour not only in everyday life, but also under controlled conditions, such as psychophysical experiments [14, 15].

*Noise in
neuroscience*

*Different kinds
of noise*

Aim of this work is to gain insight into the problem of how noise influences the decisional mechanisms. In this framework, two different kinds of noise were investigated, namely *endogenous* and *exogenous*. The *endogenous* noise refers to stochastic fluctuations that are present within the neural system [4], whereas with *exogenous* some form of environmental noise, external to the perceptual system, are meant. These two distinct types of noise define two independent research fields, that were both investigated by means of behavioural experiments. In other words, we were interested in investigating how noise acts on human behavior, in particular in case of discrimination processes. To this purpose, psychophysical experiments were carried out, addressing both the acoustic and the visual modality.

*Noise improves
perception*

To investigate how **a proper amount of exogenous noise can act positively on human perception, improving performance in detection experiments**, – an effect that, as mentioned above, is interpreted as an occurrence of stochastic resonance – we carried out experiments in the acoustic modality. This is the topic of the first part of this work. In particular, we used a detection paradigm where pure tone stimuli were superimposed with different levels of noise and subjects were requested to signalize the presence of the tone. Usually a sufficient noise level masks the signal. However, what we observed [16] was a tiny, yet statistically significant improvement of stimulus detection ability in correspondence to a specific noise level.

The used experimental approach – “Yes/No” experiments – is usually interpreted in terms of Signal Detection Theory (SDT) [14, 15]. The two most important SDT parameters are the sensitivity d' and the decisional *criterion*. Since improvement of detection ability driven by noise is, if any, a tiny effect, all the ingredients combined to formulate a decision must lay under the experimenter’s control. In particular, in addition to the stimulus detectability, also the knowledge of the decisional strategy at any time is crucial so as to achieve reliable data.

*Criterion setting
dynamics*

In other words, the demand of criterion stability, and more in general the problem of its dynamics, turned out to have a critical role and urged us to focus our attention to the specific topic of criterion dynamics. The scientific literature on the possibility to condition the subject’s criterion and reconstruct its dynamics with the highest possible time resolution (the single trial) is extremely scant: the only two works on this subject do not provide robust methods to tackle the issue. The second part of the dissertation is completely focused on our theory of criterion setting dynamics and the related experimental evidence.

An *ad-hoc* experiment involving the visual perceptual modality allowed to test a model for trial-by-trial criterion dynamics based on the theory of feedback [17]. Feedback loop were implemented by informing the sub-

ject, after each trial, relatively to his/her performance. When requested to maximize the rate of correct response in an orientation discrimination experiment, subjects showed the ability to continuously change their internal criterion. More in detail, the optimal criterion position oscillates at a certain frequency, set **a-priori** by the experimenter; we observed that subjects were able to modify their decisional criterion in order “to follow” the optimal position. Two main assumptions of our model are that the subject stores information coming from previous trials, and is willing of in improving his/her performance.

One of the most important assumption of SDT is that the adopted strategy, i.e. the criterion positioning, by an observer performing a task is completely independent from his/her discrimination ability. We implemented this consideration in a model for criterion dynamics so that this parameter turns out to be completely independent from d' . The possibility to disentangle sensitivity and criterion allows the experimenter to force the subject's inclination to be more liberal or conservative, independently from his/her ability in performing the task, and monitor at each trial the result of this conditioning.

The problem of how the human neural system set and maintain a decision criterion over time is still an open question. This problem recently received particular attention, within the more general context of the neural mechanisms underlying the decision process [13]. Our approach, based on behavioural experiments, provides an novel investigation tool to tackle the issue.

*Criterion setting
&
decision making*

The present dissertation is organized as follows: the model relative to the experimental situation described by a stimulus presentation and a decision between two mutually-exclusive classes of response is presented in Chap. 2. This model was applied to an experiment in which noise showed a positive role in acoustic perception. The phenomenon we were interested in, referred to as *stochastic resonance*, corresponds to an improvement of the subject's ability to perceive stimuli when a certain amount of noise is superimposed to the stimulus itself. Experimental results are discussed in Chap. 3: the effect we observed was tiny – a weak drop of the perceptual threshold only for specific levels of noise – but very robust from the statistical point of view.

In the second part of the work (Chap. 4 and Chap. 5), the attention is focussed to dynamical aspects of the SDT decisional mechanism. This mechanism is modeled by two main ingredients: the intrinsic variability of the neural activity evoked by a stimulus presentation and a threshold, usually called *decision criterion*: in particular, in Chap. 4 we provide an overview of SDT, whereas two experiments performed to investigate the criterion dynamics are presented in Chap. 5.

Final conclusions and remarks are reported in Chap. 6.

Part I

Stochastic Resonance in Acoustic Perception

Chapter 2

“Yes/No” discrimination paradigms

Abstract The present chapter provides a description of the process of discrimination in the human brain by applying a *black-box* perspective. The model presented here accounts both for the encoding within the brain of the stimulus-related information, and the subject ability to produce a response. The neural activity evoked by the stimulus presentation is interpreted in terms of a stochastic variable, whereas for the choice between two mutually exclusive classes of response is introduced a threshold. Within this theoretical framework we provide also a definition of perceptual threshold and a model for the psychometric function.

2.1 Introduction: link between stimuli and responses

The link between perception of a stimulus and decision making is a widely investigated topic in the field of neuroscience [13]. Depending on the different techniques used to measure the brain response to a stimulus, at least three different approaches can be identified. In this section we present these investigation techniques moving from a microscopic to a macroscopic point of view.

Electrophysiological approach

With microscopic we mean the electrophysiological approach. The direct measurement of neuronal electrical activity, through arrays of electrodes implanted into well-defined areas of an animal brain¹, started in 1959 with the work by the Nobel laureates David Hubel and Torsen Wiesel [18, 19, 20], and still represents a promising research field. Many recent works discuss the possibility to correlate variations of the measured electrical activity with different stimuli and/or experimental conditions [21, 22, 23, 24]. Unfortunately, unresolved problems strongly limit the possibility to provide a complete and exhaustive view of the discrimination process by using this methodology. In addition to the local degeneration of involved brain tissue [25], the most important constrains regard both the high number of neurons involved into the computation and the high complexity of the network of connections into the brain [26].

A second interesting approach to the problem of how the brain interprets stimuli, is the study of specific functions of different areas into the cerebral cortex. The main hypothesis underlying this approach is that the brain is organized in specific functional areas, each of them carries out a specific task [27]. After a long period in which this type of investigation was limited to the study of how well-known brain damages² affect the behaviour, some recent technological improvements provide the possibility to investigate living and healthy brains. Two important examples are the Magneto-Encephalography (MEG) [28] and the functional-Magnetic Resonance Imaging (f-MRI) [29]. In this context, f-MRI represents the most important and popular contribution both to anatomical investigations and to studies of the functional organization of the brain.

Imaging techniques

Despite its popularity and its recently-acquired importance in neuro-

¹The most frequently used animal in this type of experiments are monkeys or rats.

²Before the advent of the possibility to study the living brain with imaging technologies like the functional magnetic resonance, this type of investigation was only possible by looking *post-mortem* to the brain of the patient and subsequently correlating the anomalous behaviour with brain damages.

science, the functional magnetic resonance imaging is intrinsically strongly limited by the nature of the detected signal. The quantification of the blood flow variations in well-defined brain areas offers only an indirect measure of the neuronal activity: a robust model linking together the electrical activity with the blood perfusion is not yet available [30, 31, 32, 33, 34]. In addition, the temporal dynamics of the signal measured by the fMRI is typically three order of magnitude slower than the firing rate of the neurons.

A third possible approach to investigate the human ability to interpret a stimulus and provide a response is the so called “black-box” analysis performed through psychophysical behavioural experiments [35]. A model is built by taking into account some statistical properties of the entire neuronal activity, in response to a stimulus presentation, without considering its local properties. Each *stimulus/response* couple is interpreted on the basis of the parameters of a model [36], as discussed in details in the rest of the present chapter. Many psychophysical studies are based on this experimental methodology. The standard way to implement a behavioural experiment is schematically shown in Fig. 2.1.

*Behavioural
experiments*



Figure 2.1: Schematic view of a standard behavioural experiment: the participant’s neural system is represented by the green rectangle.

In the rest of the present chapter we present the details of the standard model used to interpret the discrimination ability in psychophysical experiments. The model provides an answer to two important questions related to this topic:

1. How does the brain encode the stimulus-related information?

2. How does the model represent the ability to produce a response to a task?

2.2 Model for discrimination

Psychophysical experiments primarily differ on the basis of the type of stimuli presented to the subject. Depending on the goal of the experiment, different sensorial modalities can be involved in the perceptual process: for example, possible stimuli involving the acoustic modality can be pure tones [16] or more complex acoustic pattern, like speech [37, 38] or music [39, 41, 40]. Similarly, two or more perceptual modalities can be exploited at the same time: in this case stimuli are referred to as cross-modal [42].

*Stimuli
&
task*

In addition to the stimulus presentation, a behavioural experiment is characterized by the task the subject is requested to solve [43]. For example, a possible question, concerning either an acoustic or visual stimulus, is: *did you perceive it?* For this reason, this type of discriminations are usually referred to as “Yes/No” experiments.

2.2.1 Neural encoding

Stimuli are physical events characterized by one or more physical quantities and linked to the sensorial perceptual modality with which they interact into the observer’s brain. For example, a pressure wave acting to the subject’s ear defines an acoustic stimulus. Similarly, a visual pattern appearing on a screen and characterized by the luminosity or color of a set of pixels is associated with a visual stimulus.

So, stimuli are classified by the intensity of their physical parameters (in the previously cited examples, the acoustic intensity and the contrast with the background luminosity). These physical features have to be under the experimenter’s control. In order to investigate the effect of a stimulus presentation on the subject’s response it is important to control and possibly stabilize the influence of the boundary conditions (environmental noise or uncontrolled variations of the luminosity, for example).

In a standard “Yes–No” discrimination experiment, on each trial a single stimulus³ per trial is presented to the subject. The stimulus presented to the subject evokes a certain neural response, which is commonly considered slightly different from the basal brain activity. This neural response can

*Neural
activity*

³“Single stimulus” does not necessarily mean “single object” in case of visual stimuli, or “single tone” in case of acoustic experiment. More complex stimuli can be used, depending on the aim and the design of the experiment.

2. “YES/NO” DISCRIMINATION PARADIGMS

be encoded into a variable, that we labeled with x [36]. Here we assume that, although each stimulus is characterized by many physical features (for example, in case of acoustic stimuli, intensity, frequency, duration, etc.) only a single feature is of interest for the experimenter.

Because of the presence of noise, ubiquitous in the neural activity, x is a stochastic variable. For the sake of clarity, in the rest of the discussion we will use a pure tone of a well-defined duration and intensity as an example of acoustic stimulus: the physical features of that stimulus are, in general, under the experimenter’s control. Repeated presentations of the same stimulus to a subject, evoke different values of x at each trial. More in particular, the distribution underlying this variable is assumed to be *Gaussian* (or *normal*), with mean value μ and standard deviation σ . In other words, the probability distribution $P(x)$ associated with the variable x is

$$P(x) = \frac{1}{\sigma\sqrt{2\pi}} \exp\left[-\frac{(x-\mu)^2}{2\sigma^2}\right]. \quad (2.1)$$

The link between neural activity and the physical features of the stimuli is modelled by the statistical parameters of its distribution. In particular, the mean μ is proportional to the amplitude of the stimulus intensity, whereas σ is usually assumed to be independent from the stimulus presentation.

It is important to remark a strong argument supporting the assumption of normally-distributed neural responses. The intrinsic variability of x is mainly caused by internal sources of noise. Thus, if noise derives from a number of independent sources that combine additively, a Gaussian-distributed random variable is produced by virtue of the Central Limit Theorem [44]. Embedding a signal into this noise is assumed to shift the noise distribution by a positive quantity⁴, reflecting the strength of the signal.

In Fig. 2.2 the effect of multiple repetition of a restricted number of classes of stimuli (here labeled with the numbers “0”, “1” “2” and “3”), on the variable x supposed to encode the neural activity is shown. The presentation of the i -th class of stimuli evokes an occurrence probability $P_i(x)$ for the neuronal activity x . $P_i(x)$ distributions differ by small variations of the parameter μ_i . It is important to note that the model accounts also for the case of trials in which the stimulus is absent and only background noise is presented to the subject: in Fig. 2.2, the class of stimuli labelled with “0” can be considered as the “no-stimulus” case. During “only-noise” trials the variable x encodes the basal neuronal activity.

Why Gaussian distributions?

no-stimulus trials

⁴This quantity is linked with the d' -parameter of the Signal Detection Theory [14, 15]. More details about this point will be provided in Chap. 4.

2.2. MODEL FOR DISCRIMINATION

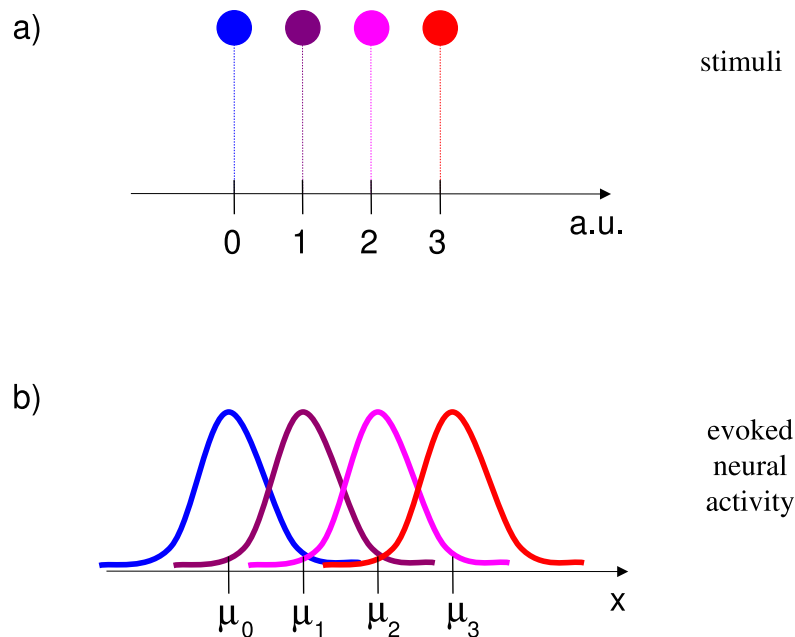


Figure 2.2: Neural activity related with the physical feature of the stimulus. In part *a* of Fig. 2.2 the dots represent multiple repetition of the same stimulus. For the sake of clarity, each amplitude of the physical feature that characterizes the stimulus (e.g. the intensity of acoustic stimuli) is drawn with a different color. Then, as shown in part *b*, each stimulus evokes a neural response encoded in a normally-distributed stochastic variable x . Standard deviation σ of the probability distributions $P(x)$ is supposed to be independent from the stimulus intensity, whereas the shift of the mean μ of the different distributions is proportional to the intensity of the stimulus.

Multidimensional case

A generalization of the unidimensional case presented so far is given when more features are considered at the same time [45]. Then, the variable x becomes the vectorial quantity \vec{x} , whose components behave singularly as the unidimensional case described above [15]. For example, the internal representation of an acoustic stimulus can be modulated by changing its intensity and duration. Regarding the underlying probability distribution of the \vec{x} components, all the arguments supporting the model based on a normal distribution remain valid.

In Fig. 2.3, the two different stimulus characteristics are labeled with x_a and x_b . The resulting occurrence probability distribution P_{occ} is a two-dimensional Gaussian distribution.

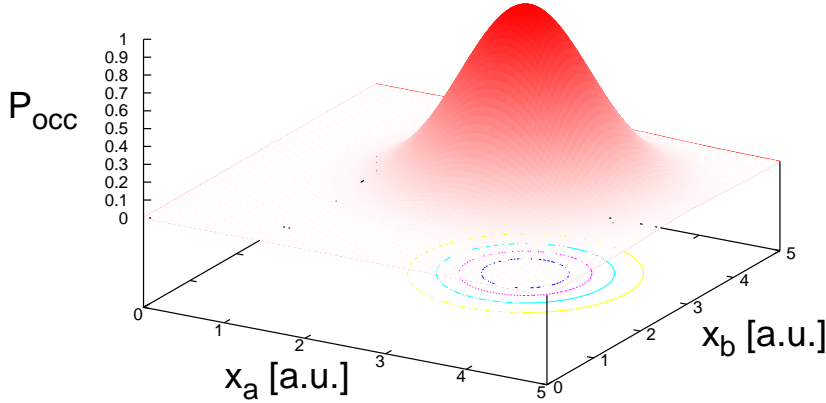


Figure 2.3: In the multidimensional case the decision variable x is generalized to a random vector \vec{x} , whose components correspond to the perceived attributes of the presented stimulus.

To investigate the multidimensional level of neuronal encoding, it is necessary to ask the subject to produce an answer relative to all features of interest. The work presented in this dissertation is completely focused on the unidimensional case⁵.

2.2.2 Discrimination ability

In case of behavioural experiments, the only possibility to monitor a subject’s perception of a certain stimulus is to formulate a question the subject has to answer. A “Yes/No” discrimination paradigm is defined on the basis of the type of response the subject has to provide: only two mutually exclusive classes of response are possible. This is defined as a dichotomic answer. For example, the question *Did you perceive the stimulus?* is very common in “Yes/No” experiments and only one of the two possible response (*the stimulus was present/absent*) is allowed.

*Dichotomic
answers*

It is important to point out, that for healthy human subjects, it is always

⁵Traditionally, in psychophysical experiments only very few characteristics of the different classes of stimuli are investigated at the same time. The reason is the need to reduce the dimensionality of the experimental design, and, as a consequence, to limit the duration of each experimental session.

2.2. MODEL FOR DISCRIMINATION

possible to produce an outcome, in form of a motor (verbal) response, by performing this type of discrimination tasks. Subjects choose one of the two possible classes of responses, independently from the correctness of their answers or their confidence about it. The ability to produce an answer is a very basic characteristic, not only in humans.

The most automatic way to implement the decision mechanism in the model is to set a threshold (labeled with χ in Fig. 2.4), usually defined as *perceptual threshold* [14, 15]. If the neural activity evoked by the stimulus overcomes the threshold, the subject will produce a certain response (“Yes, the signal was present”). On the contrary if the value of the variable x remains below the threshold the subject will choose the opposite class of outcomes (“No, there was merely a presentation of noise alone”).

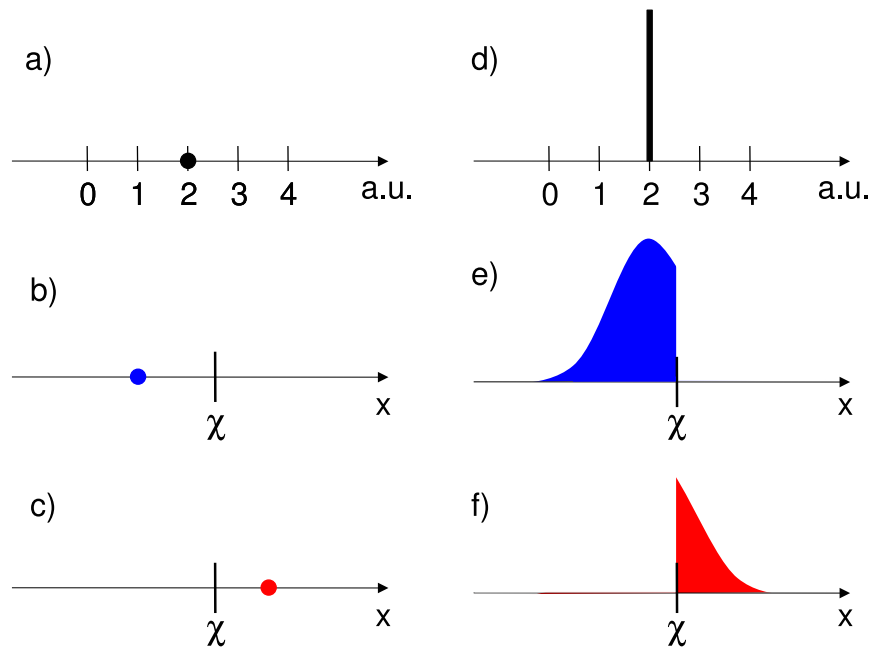


Figure 2.4: Effect of threshold χ on the rates of both the classes of responses: in *b* and *c* are drawn two possible values of neural activity x , associated with a single presentation of a certain stimulus (*a*), whose intensity is given in arbitrary units (a.u.). Depending on criterion position, subject provides two possible responses: “No” (*b*) or “Yes” (*c*). In the right part, the same stimulus is presented many times to the subject (*d*). The blue and red shaded areas of part *e* and *f* represent the rates of “No” and “Yes” responses, respectively.

The pictures in the left part of Fig. 2.4, labeled with *a*, *b* and *c*, represent the case of single presentation of a certain stimulus (*a*). The stimulus evokes

a stochastic neural response, that can be smaller (b) or larger (c) than the threshold χ . The blue dot (b) represents the response “No”, whereas the red one (c) represent the response “Yes”. In the right part is represented the case of multiple repetition (d) of the same stimulus, whereas e and f represent the probability of “No” and “Yes” response, respectively. It is important to note that the threshold χ is not necessarily set to the mean value μ of the distribution relative to the evoked neural activity.

2.3 Psychometric function and perceptual threshold

Aim of the present section is to introduce the psychometric function, widely used to measure the subject’s discrimination ability in “Yes/No” experiments. In addition the perceptual threshold, defined as the stimulus intensity at which the probability to obtain a response “Yes” assumes a well-defined value, will be compared with the threshold χ , assumed in the model presented in Sec. 2.2.2.

Trial time-line The trial time-line, defined as the sequence of events occurring at each trial, depends on the aim and the structure of the experiment. The picture in Fig. 2.5 schematizes the most basic implementation of a typical single trial: after each stimulus presentation the subject is requested to produce a response; prior to the stimulus, an attentional cue can be presented while, after the response, a feedback with information about subject’s performance can be provide to the subject.

A single trial

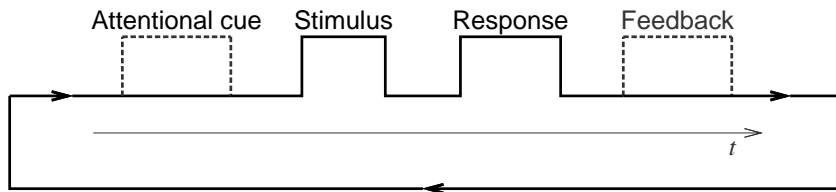


Figure 2.5: Schematic view of the standard trial time-line in “Yes/No” experiments: with solid (dashed) lines two basic (optional) blocks are shown. After the presentation of an attentional cue, for example a fixation cross in the center of a screen, the stimulus is presented. Then, the subject provides his/her response. Finally, in particular cases, an additional feedback containing information about the performance is provided to the subject.

2.3. PSYCHOMETRIC FUNCTION AND PERCEPTUAL THRESHOLD

The trial time-line can be repeated as long as the initial experimental conditions remain unchanged: typically, after around one hour, subjects get tired or meet difficulties to focus their attention to the task [46].

Psychometric function: In the previous section we presented the case of multiple repetition of the same stimulus. As shown in Sec. 2.2.1, the probability distribution of the evoked neural activity x is given by a Gaussian distribution with standard deviation σ and mean μ_I , depending on the intensity I ,

$$P(x|I) = \frac{1}{\sigma\sqrt{2\pi}} \exp\left[-\frac{(x - \mu_I)^2}{2\sigma^2}\right]. \quad (2.2)$$

Given a certain threshold χ on the axis of the neural activity x , the parameters μ and σ of the distribution define the rates (or probability) of response “Yes”, given by the cumulative function of the underlying distribution. In particular

Rates of response “Yes”

$$P_{yes} = \int_{\chi}^{+\infty} P(x) dx = \Phi\left[\frac{\mu_I - \chi}{\sigma}\right] \quad (2.3)$$

where

$$\Phi(x) = \frac{1 + \operatorname{erf}(x)}{2} \quad (2.4)$$

Multiple repetitions of stimuli belonging to four distinct classes of intensity (from “0” to “3”) are drawn in the upper part of Fig. 2.6. At each stimulus presentation subjects provide their response: the number of response “Yes” depends on the stimulus intensity, as showed in the intermediate plot of Fig. 2.6.

As usual,

$$\lim_{N \rightarrow \infty} \frac{\#Yes}{N} = P_{yes} \quad (2.5)$$

where N is the number of repetition of the stimulus presentation and “#Yes” the number of response “Yes”.

Given the definition provided in the previous section of “Yes/No” experimental paradigm, with mutually exclusive classes of responses, it is $P_{no} = 1 - P_{yes}$.

The possibility of multiple repetition of either the same stimulus or stimuli of different classes allows the experimenter to interpret the “stimulus/response” couples in terms of occurrence probability of a certain class of response. Thus, the psychometric function is defined as the probability to obtain a well-defined class of responses as a function of the intensity of the physical feature that characterizes the stimulus. In other words, if “Yes” is the response

Definition of psychometric function

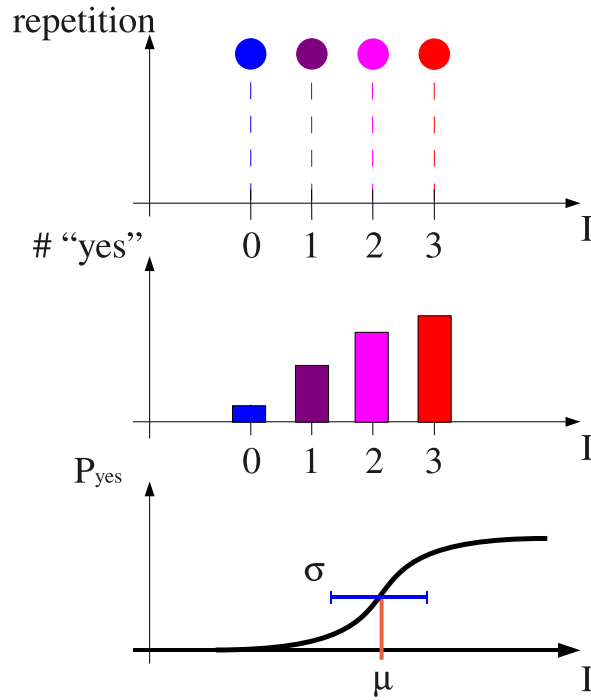


Figure 2.6: (Upper part) four classes of stimuli. Histograms (middle part) represent the number of “Yes” responses as a function of the stimulus intensity I . The psychometric function is shown in the bottom part. Both the perceptual threshold μ , set between stimulus “1” and stimulus “2”, and the standard deviation σ of the distribution are schematically drawn.

of interest and I the intensity of the stimulus, the psychometric function is defined by the probability $P_{yes}(I)$.

The most frequently adopted model for this function is the Gaussian cumulative distribution as in Eq. (2.3), so that

$$P_{yes}(I) = \Phi\left(\frac{I - I_{th}}{\sigma}\right). \quad (2.6)$$

Then, an operative definition of perceptual threshold can be introduced by comparing Eq. (2.3) with Eq. (2.6), as follows.

Perceptual threshold: I_{th} is defined as the intensity level at which the probability to obtain a response “Yes” is 0.5. Of course, the choice of this rate is completely arbitrary: sometimes, in the literature the proportion of 75%

Definition of perceptual threshold

2.3. PSYCHOMETRIC FUNCTION AND PERCEPTUAL THRESHOLD

of detection rate is alternatively used to set the perceptual threshold⁶ [47].

The psychometric function is typically used to compare the ability of different subjects to perform a task. By comparing parameters μ and σ for each subject of the experimental sample, it is possible to quantify the discrimination ability and to interpret **a posteriori** the results of the experiment, for example, through an **ad hoc** renormalization of the data.

A critical point to this aim regards the fitting procedure that has to be applied in order to evaluate the parameters of the psychometric function. The distribution of each rate value is binomial. For this reason, the standard method based on χ^2 minimization, by means of the Levenberg–Marquardt algorithm [48] are not allowed to fit the experimental data. We instead used computational techniques based on Maximum Likelihood Estimation (*MLE*).

*Maximum
Likelihood
Estimation*

For each stimulus intensity I , the probability to obtain K_I “Yes” responses depends on $P_{yes}(I)$. Given a couple of parameters \tilde{I}_{th} and $\tilde{\sigma}$, the likelihood for the data, at each intensity I , is given by

$$\mathcal{L}(I; \tilde{I}_{th}, \tilde{\sigma}) = \left[\Phi\left(\frac{I - \tilde{I}_{th}}{\tilde{\sigma}}\right) \right]^{K_I} \cdot \left[1 - \Phi\left(\frac{I - \tilde{I}_{th}}{\tilde{\sigma}}\right) \right]^{N - K_I} \quad (2.7)$$

where N , the number of repetitions, is taken to be the same for each stimulus intensity I . The likelihood \mathcal{L} relative to the entire sample of K_I is then

$$\mathcal{L}(\tilde{I}_{th}, \tilde{\sigma}) = \prod_{I=I_{min}}^{I_{max}} \mathcal{L}(I; \tilde{I}_{th}, \tilde{\sigma}) \quad (2.8)$$

The method generally adopted in our work consists in looking for the maximum of $\mathcal{L}(\tilde{I}_{th}, \tilde{\sigma})$ by varying the parameters I_{th} and σ on a pre-assigned two-dimensional lattice.

*Errors on
parameters*

Finally, regarding the errors dI and $d\sigma$ on the psychometric function’s parameter I and σ , they are defined as the interval causing a variation of the 5% of the likelihood \mathcal{L} , so that

$$\begin{aligned} \mathcal{L}(|I_{th} + dI|, \sigma) &= 0.95 \cdot \mathcal{L}(I_{th}, \sigma) \\ \mathcal{L}(I_{th}, |\sigma + d\sigma|) &= 0.95 \cdot \mathcal{L}(I_{th}, \sigma) \end{aligned} \quad (2.9)$$

⁶Here and the subsequent chapters the perceptual threshold is intended as the intensity level corresponding to the 50% of the proportion of response “Yes”.

2.4 Conclusions

We provided mathematical details of a model widely used to interpret the discrimination process. By adopting a *black-box* perspective, only the *stimulus/response* pairs are object of investigation. The model presented here accounts both for the encoding, into the human brain, of the stimulus-related information and the subject ability to produce a response. The neural activity evoked by the stimulus presentation is interpreted in terms of a stochastic variable, whereas the decision is modeled by a simple threshold model.

In addition, a possible definition of perceptual threshold, related to the psychometric function, has been provided.

Finally, mathematical and computational problems linked to the evaluation of the psychometric function have been presented, with the solution adopted in the rest of the present dissertation.

2.4. CONCLUSIONS

Chapter 3

The role of exogenous noise in human auditory perceptual system

Abstract In perception, exogenous noise is known to yield a masking effect, i.e. an increase of the perceptual threshold proportional to the noise intensity superimposed to the stimulus. However, somehow counter-intuitively, the opposite mechanism can occasionally occur: a decrease of the perceptual threshold for a non-vanishing, *virtuous* amount of noise. This phenomenon, that is referred to as stochastic resonance, is deemed to provide important information about the role of noise in the human brain.

3.1 Introduction

In the previous chapter, we presented the general framework of our investigation: decisional processes allowing the subject to produce a dichotomic response were interpreted in terms of the neural activity evoked by a stimulus presentation and an inner threshold. Noise was considered as the source of variability for the evoked neural response, encoded into the stochastic variable x . In addition to that, it is interesting to investigate the effect of noise on perception when the stimulus itself is superimposed to exogenous noise.

*Stochastic
Resonance
&
acoustic
perception*

Aim of the present chapter is to study the phenomenon of stochastic resonance (SR) within the human auditory perceptual system. The main idea underlying SR in psychophysical experiments is that a certain amount of external noise can improve the ability to detect stimuli: the most straightforward way to test this hypothesis is to measure the subject's performance detecting stimuli without superimposed noise and to compare his/her performance with the results of a similar experiment where stimuli are superimposed with noise. We applied this strategy by testing the effect on the human perception of pure tones.

It must be remarked that we implemented several experimental approaches to study SR in the acoustic modality. The experiment described here makes up our best attempt to this goal, from the point of view of repeatability and thus of scientific reliability.

The present chapter is organized as follows: we first describe the masking effect occurring when noise detrimentally acts on the stimulus perception in Sec. 3.2. Then, we present the phenomenon of SR: besides psychophysics of perception, this effect has been observed in different fields. A review of experimental situations in which SR-like phenomena have been observed is presented in Sec. 3.3. The experiment aimed to test the occurrence of SR in acoustic modality is described in details in Sec. 3.4, 3.5 and 3.6. Possible future perspectives are discussed in Sec. 3.7

3.2 General framework for experiments with exogenous noise

In the model for decision making described in Sec. 2.2, noise was taken into account by considering the intrinsic variability of the neural activity evoked by a stimulus presentation. In this case noise was defined as being endogenous.

*Endogenous
noise*

Fig. 3.1 shows a schematic graphical representation of the discrimination process: in the upper part (a) the experimental situation described in the

3. NOISE AND ACOUSTIC PERCEPTION

previous section is presented. From left to right, a stimulus presented to the observer enters into the discrimination block (the green rectangle in Fig. 3.1) and evokes a certain neural response. Internal (or “endogenous”) noise is included by summation. The resulting noisy neural response, labeled with x , is compared with the perceptual threshold, previously labeled with χ , in order to produce an outcome (response).

In Fig. 3.1.b the experimental situation in which additional noise is superimposed to the stimulus is shown. This type of noise is external to the subject and for this reason it is usually called *exogenous*. It is important to point out that with exogenous noise only a special kind of external noise is meant: for example, for acoustic stimuli it is impossible to completely avoid environmental noise, or in case of visual patches the screen itself produces a certain amount of noise. With “exogenous” we rather mean the amount and kind of noise that can be manipulated by the experimenter and is also under his/her control.

*Exogenous
noise*

Aim of this type of experiments is to investigate how exogenous noise acts on the subject’s response.

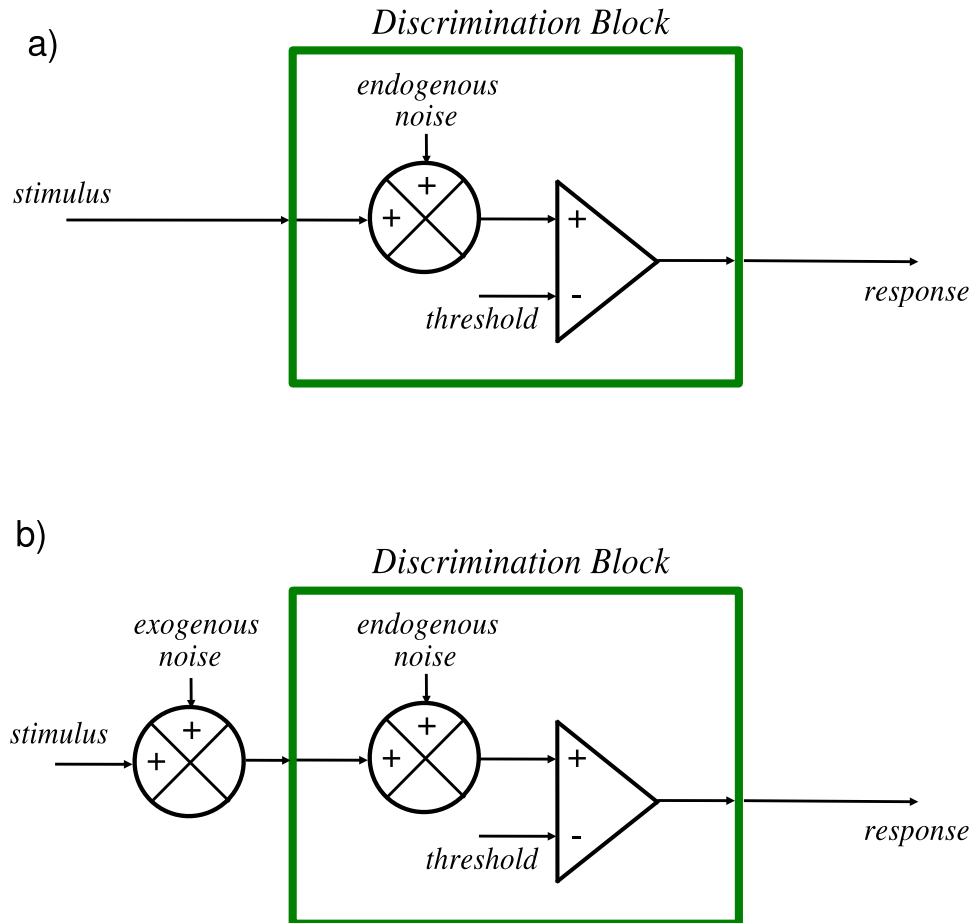


Figure 3.1: Response changes when exogenous noise is added. a) The discrimination block encoded in the human brain has here a different graphic representation of the same model described in the previous chapter and shown in Fig. 2.4: the stimulus evokes a noisy neural activity. The response is produced by comparison with the perceptual threshold. b) Exogenous noise is added to the stimulus presented to the subject. In the experimental situation described here, the amount and type of exogenous noise added to the stimulus is under the experimenter's control.

3.2.1 Two opposite mechanisms: detrimental and non-detrimental role of noise

In the rest of the present chapter we will focus our attention to behavioural experiments based on a detection task. Thus, subject's performance is interpreted in terms of psychometric function, as shown in Sec. 2.3. If noise is superimposed to the stimulus two opposite effects occur, namely the masking effect and the stochastic resonance.

Masking effect

The most frequent effect of noise on detection is usually referred to in the literature as masking effect: in this case, noise detrimentally acts on subject's performance and makes more difficult (masks) the perception of a stimulus. The subject's ability to detect the stimulus generally decreases proportionally to the exogenous noise amplitude. The masking effect typically takes place for values of noise intensity I_n higher than a critical value I_{nc} , and is measured as an increase of the perceptual threshold. Fig. 3.2 shows a typical profile of the perceptual threshold μ as a function of noise intensity.

*Noise masks
the signal*

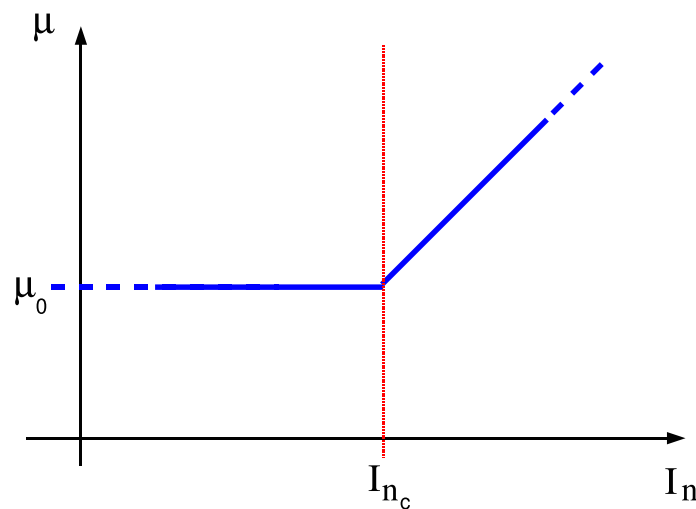


Figure 3.2: Masking effect: for noise intensities (I_n) smaller than I_{nc} , the perceptual threshold is noise-independent. In the masking regime, i.e. for noise intensities $I_n > I_{nc}$, the perceptual threshold μ typically increases linearly with I_n . If reported in a log-log scale, $\mu(I_n)$ has then unitary slope.

If logarithmic intensity scales are used (dB), the slope coefficient of $\mu(I_n)$

is unitary ($\frac{d\mu}{dI_n} = 1$) in the range of noise intensities in which the masking effect takes place. In other words, if $I_n > I_{nc}$

$$\mu(I_n) = \mu_0 + (I_n - I_{nc}) , \quad (3.1)$$

where μ_0 is the perceptual threshold without superimposed noise.

*Masking in
acoustic modality*

The masking effect in acoustic modality was investigated for the first time, to our knowledge, in 1950 by J.E. Hawkins and S.S. Stevens [49]. In their work the effect occurring when pure tones or speech were superimposed by white noise of different intensities was analyzed. The authors observed a profile of the masking effect similar to Fig. 3.2. Over the intervening years, many papers have taken inspiration from this seminal work: for example, studies focused on speech perception [50] or cochlear signal processing [51].

*Threshold
versus
Contrast*

In the literature, the profile of Fig. 3.2 is also called *Threshold versus Contrast*, or TvC, function. Because of its generality¹, TvC function recently received attention not exclusively in the field of acoustic perception: as an example, L.A. Lesmes and colleagues [54] proposed a Bayesian adaptive procedure, named *quick TvC*, to rapidly estimate multiple TvC functions independently from the sensorial modality. In this case the three parameters characterizing the TvC function are the perceptual threshold without noise, also called optimal threshold, the noise critical value (I_{nc} , in Fig. 3.2) and the slope of the masking as a function of noise.

Although the masking effect seems to be robust, to our knowledge no satisfactory theory was so far devised to interpret TvC function so as schematized in Fig. 3.2. An example of unresolved problem regarding the TvC function is the presence of a discontinuity around I_{nc} of difficult interpretation. On the other hand, a physical model for this effect is out of the scope of our work. We focused our attention to the occurrence of stochastic resonance phenomena in acoustic perception.

3.3 Stochastic Resonance: a positive role of noise in non-linear systems

3.3.1 Introduction: a counterintuitive phenomenon

In physics, an important parameter widely used to quantify to goodness of a measurement is the so-called Signal-to-Noise ratio ($\frac{S}{N}$), defined as the ratio between the amplitudes, typically expressed in dB, of signal and noise,

¹The profile of the perceptual threshold as a function of noise can be determined also in different sensorial modalities like, for example, in visual perception experiments [52, 53].

respectively. In case of linear systems, since the output signal directly proportional to the input, the $\frac{S}{N}$ ratio decreases if exogenous noise is superimposed, as in Fig. 3.1.b. Conversely, in case of non-linear systems, though the same detrimental effect generally takes place, there are particular situations in which a positive role of noise has been observed. An example was reported by L. *Gammaitoni et al.* [3]: the system under investigation was modelled by a quartic double-well potential, and a sinusoidal modulation was applied to the input of the system. If the modulation amplitude was kept slightly under the threshold defining the switch of the system from a state to another one, the output spectrum showed a pronounced peak at a suitable noise intensity.

*Noise in
non – linear
systems*

The phenomenon of stochastic resonance was described, for the first time, in 1981. The work by Benzi et al. [55] showed that a dynamical system subject to both a periodic forcing and a random perturbation may show a resonance that vanishes when either the forcing or the perturbation is absent. In that case, the resonance was observed as a peak in the output power spectrum. The mechanism of noise improving the information transfer through a nonlinear system was theoretically investigated in different conditions [56, 57, 58, 59, 60]: the general case of improved signal transmission through a static nonlinear system was investigated by F. *Chapeau-Blondeau* [61, 62]. In a different work [63], J. *Tougaard* studied the occurrence of SR in energy detectors, as a model for biological systems.

*First evidence
of SR*

Although the main ingredients of SR, as resulting in the most important reference on this topic [3], are a bistable system, an incoming signal slightly under the threshold, and noise, SR was theoretical predicted also in monostable systems [56] or in case of supra-threshold input signals [64, 65, 66].

SR, first described in the framework of non-linear physics, was demonstrated in a very wide range of research fields [3], all of them characterized by noise playing a non-detrimental role²: more in particular, SR was first described by looking at the dynamics of climate changes [69, 70]. More recently the phenomenon was studied in different experimental situations and theoretical approaches [2], from laser dynamics [71] to nanomechanical resonators [72], to quantum mechanical systems [73]. During 2009 a special issue of *European Physics Journal B* (Vol. 69, Nr. 1) was published, entirely dedicated to new observations of the SR phenomenon. The results of our work are included in this volume [16].

*SR in
different
research fields*

²Recently, many reviews on SR were published. In addition to the previously cited reference [3], the topic was reviewed with particular attention to the sensory information processing [67], to its occurrence in the human brain [68].

3.3.2 Stochastic resonance in biological systems

SR like effects are observed in many biological systems. Here we present an overview of experiments in which physiology or behaviour of different kinds of animals were interpreted as an improvement of performance driven by noise. As an example of investigation relative to the role of noise in animal physiology, in 2007 L. Martinez *et al.* [74] showed that the cat motor system, and in particular the pathway of monosynaptic reflex in the spinal cord, can be optimally driven by an external stimulation superimposed by a proper amount of noise. Of particular interest is also the work by K. Funke and colleagues [102], in which the results of physiological investigations showing SR effects in the cat primary visual cortex were reported.

*Animal
physiology*

In addition to physiology, experiments involving animal behaviour were carried out: in 2000, P. E. Greenwood *et al.* [75] claimed that the paddlefish prey capture system receives an optimal amount of information at specific noise intensities, depending on the distance of the prey. Few months later an analogous effect was observed also in juvenile paddlefish [76]. In these cases, the mechanism by which paddlefish locates, tracks and captures its prey remains largely unknown; nevertheless, it has been experimentally shown that it can be improved by noise.

Similarly, the possible occurrence of SR was investigated also in the mating behaviour: temporal and spectral analysis of calling song of *Nezara Viridula (L.)* female individuals were monitored by looking at noise-driven shifts of the threshold level for signal detection [77].

A new, promising research field relative to SR are medical applications. In this field, many studies are devoted to possible role of noise in therapy [78] or, at least, in controlling diseases [79]. For example, M. Rusconi *et al.* published in 2008 a work [80] in which SR-like effects were studied during bone formation in case of patients under osteopenic conditions.

*Medical
applications*

Of particular interest because of their wide application are studies on posture [81, 82] and human balance control, also in connection with pathological states such as diabetes or strokes [83]. Other types of health problems, in which noise was shown to act either positively or simply as an indicator of dysfunction, are the sensorimotor system's problems [84], and the pathologic cardiac dynamics [85].

Noise recently revealed its central role in pathological states involving the central neural system (*CNS*): Y. Yamamoto *et al.* in 2005 showed that noisy vestibular stimulations can improve responsiveness in central neurodegenerative disorders [86].

In the rest of the present section we will focus our attention to SR in the human brain, not only in case of specific pathologies, but also by looking at

the effect on healthy subjects.

3.3.3 Stochastic resonance and the human brain

In addition to behavioural experiments in which one or more perceptual modalities are involved, SR was observed at different levels in brain dynamics [68]. In 2000 a work by I. Hidaka *et al.* [12] documented the functional role of SR in human baroreflex system. This work attracted strong interest in subsequent years because it represents, according to the authors, the first evidence of a functional role of noise in human brain.

*Baroreflex
system*

Similarly to the previously cited work, the experiment carried out by A. Priplata and colleagues [87], demonstrated a noise-enhanced balance control in humans. Differently from the work cited in the previous section [83], here the authors carried out their experiments on healthy, young and elderly individuals.

In addition, the electric brain activity was also monitored as a function of noise: an overall large-scale phase synchronization of brain activity, measured with EEG techniques [88], was observed when specific values of noise were superimposed to external signals.

*SR
&
EEG*

3.3.4 Stochastic resonance within the human perceptual system

This section is devoted to some results reported in the literature, that show a noise-driven improvement of a subject's performance in case of behavioural experiments.

Tactile sensation

Perhaps, the most famous work on this topic was published in 1996 by J.J. Collins *et al.* [47]. They showed that detection of tactile stimuli, a stepwise profile of variable height, improved when a certain amount of noise was added to the stimulus on the same perceptual modality. A similar experiment was also reported one year later [89].

An improvement of tactile sensation was also observed by C. Wells *et al.* [90] in an experiment in which stimuli of intensity closed to the perceptual threshold were presented on the foot sole of old and young (mean age 26(3) and 88(5), respectively) healthy subjects.

Finally, also EEG components elicited by tactile stimuli [91] were observed to increase at an optimal amount of superimposed noise.

Visual modality

*Visual
detection*

Evidence of SR was shown also in experiments addressing the visual modality. In 1997, E. Simonotto *et al.* [92] described a SR-like effect in an experiment of visual stimuli detection. The subject was presented a digitalized picture, composed by modulating the grey scale of each pixel of a screen; noise was introduced by fluctuations on the grey scale. The decoding of the picture was measured to be optimal at a non-zero value of noise.

Detection and discrimination of bidimensional visual stimuli were investigated in noisy conditions [93, 94, 95, 96]. In addition, the case of SR like effects was reported also in three-dimensional autostereograms perception [97].

*SR in
cognition*

Recent experiments in the visual modality tackled the problem of the role of noise on cognitive assessment [98, 99]: for example, a work by K. Kitajo *et al.* [100] was focused on the effect of SR in the framework of the attentional control. Incidentally, the role of internal noise was also investigated in this framework [101].

In addition to the unimodal case, in which noise and stimulus act on the same perceptual modality, some experiments addressed the case of a cross-modal interference occurring within the brain. For example, visual discrimination ability can be improved by acoustic noise: this is the so-called cross modal SR [42].

SR in acoustic modality

*Behavioural
experiments*

As mentioned above, our investigation was mainly focused on the occurrence of SR in human brain, with particular attention to the acoustic perception. SR in the human auditory system was observed at a physiological level [103, 104, 105]. In this works, it was investigated how transduction of mechanical stimulations into electrical signals depends on the amount of stochastic, mechanical fluctuations of hair cells. With regard to perception experiments, the first evidence of SR in the human auditory modality was described by Zeng *et al.* [106], in both normal hearing individuals and cochlear or brainstem implant recipients³. Subjects were asked to detect the presence of a signal superimposed to a specific level of white noise. The authors determined the perceptual threshold via a two-interval, forced-choice adaptive staircase procedure (*three-down, one-up*, pointing at a correct detection rate of 79.4 % [14]) and reported a non-monotonic profile of perceptual threshold vs. noise intensity, with a minimum at a non-vanishing noise value. A

³In the literature several works are available, concerning SR in cochlear implants recipients [107, 108]. Conversely, we investigated the effect only in case of healthy subjects. Thus, we limit here our overview to the literature relative to this type of experiments only.

similar experiment, with normal hearing subjects only, was carried out by Long *et al.* [109, 110]. Authors reported a somehow impressive improvement of human perception near the acoustic threshold. Finally, another recent work [111] addressed the role of different types of noise on acoustic perception, showing results similar to the work by Long [109].

All the works mentioned above claimed evidence of the occurrence of SR in human acoustic perception. However, the statistical robustness of these analyses appears to be questionable. In the work by Zeng [106], the standard deviation of the data collected from the normal hearing subjects was one order of magnitude larger than the claimed threshold shift, whereas in the work by Long [109] a quantification of the effect over the entire sample of subjects was lacking. Moreover, the conspicuous threshold shift presented by Long [109] seems to be incompatible with the faint effect shown by Zeng [106]. With regard to the work by Ries [111], the statistical test used did not show SR unless data were heavily *a-posteriori* rearranged.

*Open
problems*

The main goal of our investigation regarded a crucial question that was apparently overlooked by the previous works on the same topic [106, 109, 111]: whether the observed profiles of the subject's performance, with a maximum at a non-vanishing level of noise, are due to SR or, more soberly, to fluctuations.

Differently from the works available in the literature, we investigated shifts of the entire psychometric function as a function of noise intensity and described a statistically robust assessment of SR within the human auditory modality.

3.4 The experiment

3.4.1 Introduction

We investigated SR in the auditory modality, carrying out an extensive analysis of sensory response in the presence of white noise on 11 normal-hearing subjects. We founded SR in the auditory modality to be a tiny effect, largely masked by statistical fluctuations. Subjects performed an experiment, whose task consisted in the detection of an acoustic signal in presence of a varying amount of white noise. Rather than using adaptive methods for the assessment of the sensory threshold, we used a straightforward *Yes-No* procedure to determine the functional dependence of the entire psychometric function on the signal and noise intensity. Data were analyzed by means of a modified version of the Levenberg-Marquardt algorithm; we fitted the whole *threshold-vs-contrast* (TvC) curve [49]. Thus, the evidence of SR based on

The task

3.4. THE EXPERIMENT

χ^2 statistics can rely on a significant degree of confidence, rather than on a simple visual inspection⁴.

3.4.2 Participants and experimental setup

A set of 11 normal-hearing participants were recruited to take part in the experiment (7 female, 4 male, age from 19 to 27, average 22, standard deviation 3); 9 subjects were naïve as to the purpose of the experiment. Participants were students or members of the University of Trento; they all provided informed consent before taking part to the experiment. Two subjects performed the experiment two and three times, respectively. The experiment was conducted in a sound-attenuated room (Amplifon, Sisper Mod. G), located at the CIMEC's Psychophysics Laboratories in Rovereto. Acoustic stimuli were generated by means of C++ routines through an Audiophile 2496 PCI D/A converter (dynamic range 104 dB, dB relative to the full-scale) and monoaurally presented to the left ear of each participant through circumaural headphones (Sennheiser HD 580).

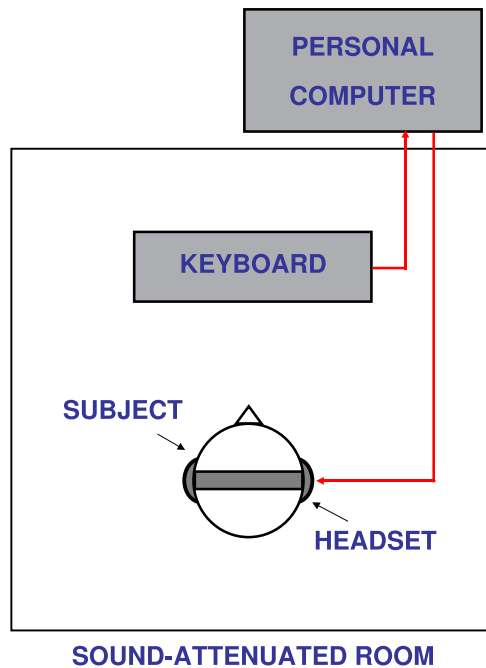


Figure 3.3: Schematic view of experimental setup

⁴In the previously cited works on the same topic [106, 109, 111], SR was often detected by simply observing a dip in the spectrum of noise-dependent perceptual threshold.

Each acoustic stimulus consisted of a *signal* and a *noise* component of intensity I_s and I_n , respectively. The signal was a pure tone of frequency 4000 Hz and duration 400 ms, whereas the noise was white Gaussian; henceforth, a stimulus will be identified by specifying the pair (I_n, I_s) of acoustic intensities of the noise and signal components, expressed in dB relatively to the full audio equipment range. After each stimulus presentation, the observer responded by pressing alternatively the “S” or “N” key on a computer keyboard, where “S” (*Si*) represented the response “*Yes, the signal was present*” and “N” (*No*) represented the opposite one: “*No, there was merely a presentation of noise alone*”. Reaction time was not taken into account in our experimental design. A new stimulus was presented 200 ms after the subject response. Attentional cue before the stimulus presentation and feedback about the subject’s performance were not included in the trial time–line (see Sec. 2.3).

Stimuli

3.4.3 The model

For each level of noise intensity I_n , the psychometric function was assumed to be modelled by a Gaussian cumulative distribution function with mean μ and standard deviation σ . The mean μ was considered, as shown in the previous chapter, as the subjective perceptual threshold, and assumed to be noise dependent. This is mathematically expressed by the function $\mu(I_n)$. Conversely, the standard deviation σ was assumed to be independent from the noise intensity.

We developed a model for parameter μ as a function of noise intensity by taking into account the two main effects occurring when stimuli are superimposed by noise: the masking effect and the stochastic resonance. The following session is focused on the masking effect.

*Model for
masking and
SR*

Masking effect

With masking we mean the effect occurring when noise covers the signal (stimulus) and makes the detection by the subject more difficult. We assumed the mean of the psychometric function to vary as an hyperbolic function of the noise level (see Fig. 3.4, top):

$$\mu(I_n) = \mu_0 + \frac{1}{2} \cdot (I_n - I_{nc}) + \frac{1}{2} \cdot \sqrt{(I_n - I_{nc})^2 + D^2} \quad (3.2)$$

This shape was chosen upon the following considerations: first, $\mu(I_n)$ tends to μ_0 if $I_n \ll I_{nc}$. Second, μ linearly depends on I_n if $I_n > I_{nc}$. Finally, the function has to be continuous. The profile of the TvC is significantly

3.4. THE EXPERIMENT

modified with respect to the standard case [54]: the additional parameter D was here introduced in order to avoid, in the case $D \neq 0$, the discontinuity (in the derivative) around I_{nc} .

*Our model
for the TvC*

Fig. 3.4 shows a color map of the *Threshold versus Contrast (TvC)* function, defined as the probability of a “Yes” response as a function of the noise and stimulus intensities (I_n, I_s) .

Stochastic resonance

Stochastic Resonance (SR) was experimentally highlighted by a decrement of the perceptual threshold around a certain noise intensity level (see bottom part of Fig. 3.4). Former works in the literature, based on behavioural experiments in acoustic modality [106, 109, 111], suggested to focus our analysis on the noise intensity interval around I_{nc} .

On the strength of phenomenological considerations and in absence of any theoretical clue, we built a model for the TvC considering a family of psychometric functions with constant standard deviation and noise-dependent perceptual threshold; in particular, we assumed the following hyperbolic profile for the threshold:

$$\mu(I_n) = \mu_0 + \frac{1}{2} [(1 - k)(I_n - I_{nc})] + \frac{1}{2} \left[(1 + k) \sqrt{(I_n - I_{nc})^2 + D^2} \right] \quad (3.3)$$

where, analogously to Eq. (3.2), μ_0 is the subjective threshold in absence of external noise, I_{nc} represents the critical noise intensity at which the masking effect starts to take place and D , as in Eq. 3.2, is proportional to the distance between the focus of the hyperbola and the point of coordinates (I_{nc}, μ_0) ; as discussed above, this last parameter avoids the discontinuity in (I_{nc}, μ_0) , usually overlooked in the scientific literature [54]. In addition, k corresponds to the slope of the negative (if $k > 0$) asymptote.

Fig. 3.4 shows a color map of our model for the TvC as reported in Eq. (3.2) (top), and in the case of occurrence of SR (bottom), expressed by Eq. (3.3).

For $I_n > I_{nc}$, the threshold is expected to linearly increase with the noise intensity [54]. Since the intensities are expressed in dB, the slope of the rightmost asymptote ($I_n \rightarrow +\infty$) is unitary. On the contrary, the slope k of the leftmost asymptote, is a free parameter for the fit procedure of the experimental data. Under standard circumstances, i.e. if masking is the only effect of noise, the parameter k would vanish: if $k = 0$, then Eq. (3.3) corresponds to Eq. (3.2). Moreover, there is no reason to expect negative values for k . On the other hand, a positive value of the parameter k would

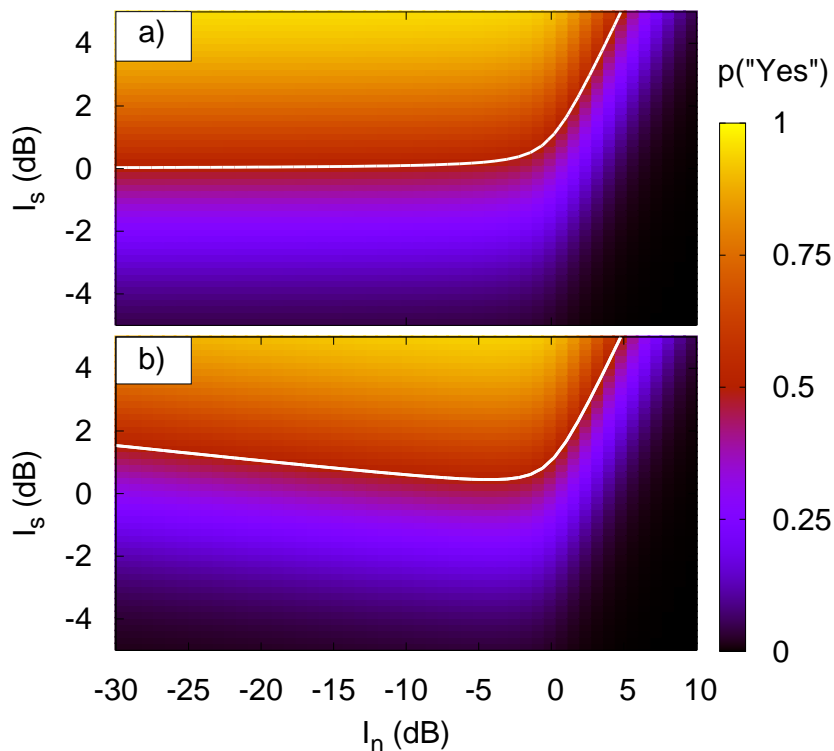


Figure 3.4: Color map of the TvC function; white solid lines correspond to the profile of $\mu(I_n)$. The surface parameters are $\mu_0 = 0$ dB, $I_{nc} = 0$ dB, $\sigma = 3.0$ dB, and $D = 2.0$ dB. In a), $k = 0$ and the TvC does not show SR. In b) $k = 0.05$; the profile shows a minimum, i.e. a clear evidence of SR.

correspond to a negative slope for the asymptote, yielding a minimum of Eq. 3.3 for I_n closed to I_{nc} . As SR is expected to occur if there is a minimum of the function $\mu = \mu(I_n)$ for a non-vanishing I_n value, a positive k value would be a sign of SR. The position of the minimum for $k > 0$, turns out to be closed to I_{nc} , in agreement with previous works [106, 109, 111].

Occurrence of SR

3.5 Experimental procedure

We measured the TvC function on a suitable set of intensity values (I_n, I_s) : for each experimental run, the 2-dimensional region of interest was chosen by taking as a reference the point (I_{nc}, μ_0) . To this purpose, prior to the main experimental phase, we first measured the psychometric function without noise in order to obtain numerical values for μ_0 also defined as $I_{s_0}^{th}$, and σ_0

Preliminary part

3.5. EXPERIMENTAL PROCEDURE

parameters⁵. Averaging the data over the entire set of experimental sessions yields $\langle \mu_0 \rangle = \langle I_{s_0}^{th} \rangle = -73(8)$ dB and $\langle \sigma_0 \rangle = 4(3)$ dB.

Then, we repeated the procedure with superimposed noise of intensity $I_n = \mu_0 + 30$ dB: we empirically found that, once this noise value was set, the resulting new threshold μ_1 , or $I_{s_1}^{th}$ lay within the masking region. New estimation of the psychometric function parameters $\mu_1 = I_{s_1}^{th}$ and σ_1 provided on average the numerical results $\langle \mu_1 \rangle = -61(8)$ dB and $\langle \sigma_1 \rangle = 6(6)$ dB. Since the slope in the masking region is unitary, disregarding SR effects ($k = 0$) and considering $D = 0$, it is easy to see that the critical noise value can be estimated by $I_{nc} = 2\mu_0 + 30 - \mu_1$. To speed-up this preliminary measurement and thus circumvent the need for a break before the main experimental session, we developed a quick adaptive procedure that, starting from a set of 3 signal intensities (each presented 4 times), rapidly converged to the subjective psychometric parameters by choosing step-by-step new signal intensities according to a maximum likelihood estimation (MLE). The average duration of this preliminary measurements was 6(1) minutes.

Main
part

The second session addressed the presence of SR by superimposing different levels of acoustic white Gaussian noise I_n to different stimulus intensities I_s in a two-dimensional region around $(I_{nc}, I_{s_0}^{th})$. More precisely, the region was defined as follows: the signal intensity interval was divided in 11 equispaced points covering the range from $I_{s_0}^{th} - 5$ dB to $I_{s_0}^{th} + 5$ dB ($\delta I_s = 1$ dB). Similarly, the noise intensity range ΔI_{n_0} was divided in a number N of equispaced points, the single step $\delta I_n = 2.5$ dB, covering three different intervals: from $I_{nc} - 3/4\Delta I_{n_0}$ to $I_{nc} + 1/4\Delta I_{n_0}$ (one single subject); from $I_{nc} - 2/3\Delta I_{n_0}$ to $I_{nc} + 1/3\Delta I_{n_0}$ (two different subjects); from $I_{nc} - 3/4\Delta I_{n_0} + \delta I_n$ to $I_{nc} + 1/4\Delta I_{n_0} - \delta I_n$ (three subjects). The number N was equal to 11 for each interval. The covered span was $\Delta I_{n_0} = 25$ dB.

Subsequently, three additional versions of the experiment were carried out, varying the number N of the noise values and keeping δI_n constant. Possible values for N were 12, 14 or 15, thus covering a range of $\Delta I_n = 27.5$, 32.5 or 35 dB, respectively. The intervals of noise values around I_{nc} were selected as follows: from $I_{nc} - 3/4\Delta I_{n_0} + \delta I_n$ to $I_{nc} + 1/4\Delta I_{n_0}$ ($N = 12$, two subjects), from $I_{nc} - 3/4\Delta I_{n_0} + 4 \cdot \delta I_n$ to $I_{nc} + 1/4\Delta I_{n_0} - \delta I_n$ ($N = 14$, four subjects) and, finally, from $I_{nc} - 3/4\Delta I_{n_0} + 4 \cdot \delta I_n$ to $I_{nc} + 1/4\Delta I_{n_0}$ ($N = 15$, two subjects). Fig 3.5 summarizes the number of different experimental sessions in which each value of noise intensity, relative to I_{nc} , was presented.

To sum up, each stimulus was defined by a pair (I_n, I_s) and a matrix-like sequence of 121, 132, 154 or 165 stimuli in case of N equal to 11, 12, 14 15, respectively, were presented.

⁵With the subscript “0” we mean *without superimposed noise*.

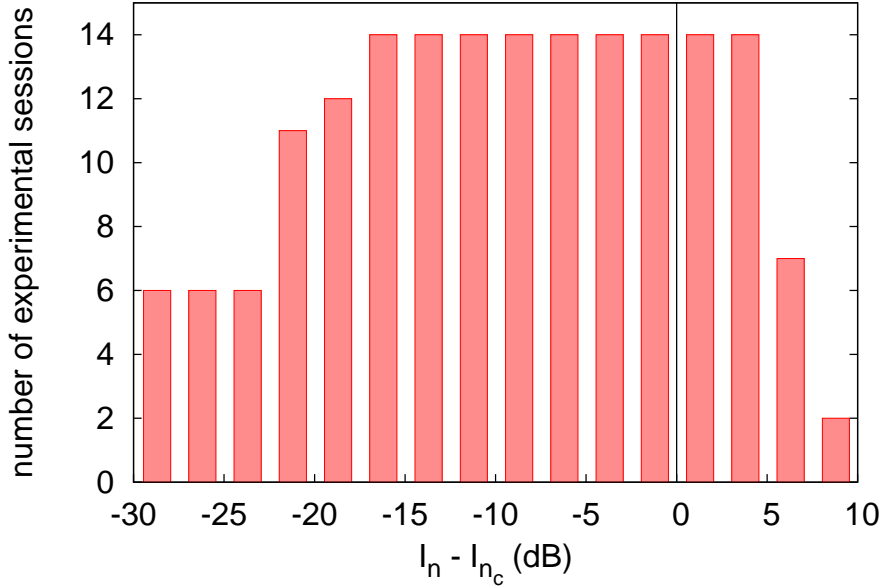


Figure 3.5: Histogram of the number of experimental sessions in which a particular value of noise intensity I_n was presented, measured relatively to I_{n_c} . The vertical black line shows the position of I_{n_c} on the x-axis.

In addition, 3 stimuli without signal for each I_n value (for a total number of 33, 36, 42 or 45, respectively) were included into the sequence of trial presented to the subject for further investigation. However, we did not taken into account the outcome of these stimuli for the data analysis presented in the rest of the present chapter. In conclusion, the total number of stimuli per each sequence was 154, 168, 196 or 210, depending on whether $N = 11, 12, 14$ or 15 , respectively.

In order to avoid any possible attentional bias we randomized the order of presentation of the stimuli. To improve statistics, the same sequence was presented four times to each subject within the same experimental session. No pauses were allowed during the experimental session.

The final result was a matrix of $P(\text{yes} | (I_s, I_n))$ values. The possible scores for each matrix element were 0, 0.25, 0.5, 0.75, 1. The average duration of the whole experiment was 25(5) minutes.

3.6 Data Analysis

Two different procedures were used to analyze the subject responses: in Sec. 3.6.1 we present the procedure, based on a modified version of the χ^2 analysis, applied to highlight the occurrence of SR in each data set (14 different results).

Subsequently, we developed a second data analysis technique, presented in Sec. 3.6.2, in order to investigate the occurrence of the effect by averaging the data over the entire sample of subjects.

3.6.1 Analysis on single subject

*Fit
procedure*

Results were summarized by a $N \times M$ histogram $R_{n,s}$ corresponding to the number of “Yes” responses provided for each stimulus on the grid; the possible values for each bin are 0, 1, 2, 3, 4. We fitted the results by means of a chi-square (χ^2) test: as a matter of fact, although the distribution events within a single bin is binomial and the number of events for each bin is only 4, we could use the χ^2 test because of the large number of bins involved in the fit ($N \cdot M \geq 121$) [48]. We computed the χ^2 function of merit by comparing each entry of $R_{n,s}$ with the expected value $r_{n,s}$, obtained from the TvC model and normalized so that $\sum_{n,s} R_{n,s} = \sum_{n,s} r_{n,s}$. To minimize the χ^2 we used the Levenberg–Marquardt algorithm, suitably changed in order to take into account the modified statistics (binomial rather than Gaussian).

Results

Tab. 3.1 shows the values of k for each experimental run.

The right column reports the probability p of the null hypothesis $k = 0$, given the measured k value and its error, computed by means of the χ^2 distribution. Subjects *DT* and *AV* performed the experiment twice and three times, respectively. Results of their different experimental sessions are reported as *DT1*, *DT2*, *AV1*, *AV2*, *AV3*.

There is a single result with negative k . Other data are grouped according to whether the null hypothesis $k = 0$ is higher than $1 - 68.3\% = 31.7\%$.

*Comparison of
the results*

The fit procedure yields new values of I_{nc} , μ_0 , and σ . To compare these values with those determined during the preliminary measurement of the two psychometric functions (with and without noise), we henceforth rename the former values as I_{nc}^{pre} , μ_0^{pre} , and σ^{pre} , respectively. In order to test the reliability of the fit procedure we computed for parameters I_{nc} and μ_0 the deviation between values estimated during the preliminary measurement and during the fit procedure. The results averaged over the entire sample of experimental runs are $\langle |I_{nc} - I_{nc}^{pre}| \rangle = 4 \pm 17$ dB and $\langle |\mu_0 - \mu_0^{pre}| \rangle = 55 \pm$

3. NOISE AND ACOUSTIC PERCEPTION

Subject	k	$p(k = 0)$ %
MC	0.14(5)	0.4
DT1	0.27(1)	2.0
AV1	0.10(5)	3.2
RS	0.03(2)	16.1
AV2	0.6(5)	20.2
AV3	0.2(2)	30.3
RT	0.04(6)	57.0
DG*	0.1(2)	67.9
MF*	0.4(9)	70.2
AL*	0.2(7)	76.6
SD	0.01(5)	77.4
LN*	1(2)	82.7
DT2	0.00(6)	99.5
EZ	-0.01(2)	54.8

Table 3.1: Values of the parameter k estimated by the fit of the TvC on the histograms $R_{n,s}$ for each participant. Four experimental runs are highlighted by an asterisk: these experiments show a strong discrepancies of the values of I_{nc} , μ_0 with the corresponding values computed during the preliminary assesment, as well as a large value of σ .

15 dB. The latter result is significantly, and unexpectedly, different from zero. However, by ruling out the four worst cases, i.e. the experimental runs showing the maximum deviation of μ_0 (DG , MF , AL and LN , marked by an asterisk in Tab. 3.1.), we obtaine $\langle |I_{nc} - I_{nc}^{pre}| \rangle = 4 \pm 1.5$ dB and $\langle |\mu_0 - \mu_0^{pre}| \rangle = 1.6 \pm 1.5$ dB. Similar results were obtained with regard to σ : the average of this parameter over the entire sample is 20 ± 35 dB; however, by ruling out the four experimental runs mentioned above, $\langle \sigma \rangle$ becomes 4 ± 1 dB. The rest of the sample can be considered homogenous.

Tab. 3.2 shows the absolute and relative occurrence of the SR effect in the entire sample of experimental sessions. In 93% of the sessions, the parameter k assumes positive values; however, these are statistically significant only in the 43 % of the experimental runs. In addition, the improvement of stimuli detection is small in comparison with the shift of the perceptual threshold caused by the masking effect.

*Occurrence
of SR*

Fig. 3.6 shows three color maps of the experimentally-determined $R_{n,s}$ matrix as well as the profiles of $\mu(I_n)$ and $\mu(I_n) \pm \sigma/3$.

For the subject MC , the profile of the $\mu(I_n)$ shows a pronounced minimum

3.6. DATA ANALYSIS

condition	occurrence	occurrence rate (%)
$k > 0$, $p(k = 0) \leq 31.7$ %	6	43
$k > 0$, $p(k = 0) > 31.7$ %	7	50
$k \leq 0$, $p(k = 0) \leq 31.7$ %	0	0
$k \leq 0$, $p(k = 0) > 31.7$ %	1	7

Table 3.2: A summary of the occurrence of SR in the sample of subjects: SR effect is present if k is significantly larger than zero.

below the onset of the masking effect, that can be interpreted as evidence of SR. On the contrary, both subject *RT* and subject *EZ* show either a less detectable minimum or a flat profile. In all the three shown cases, the occurrence of the masking effect is evident.

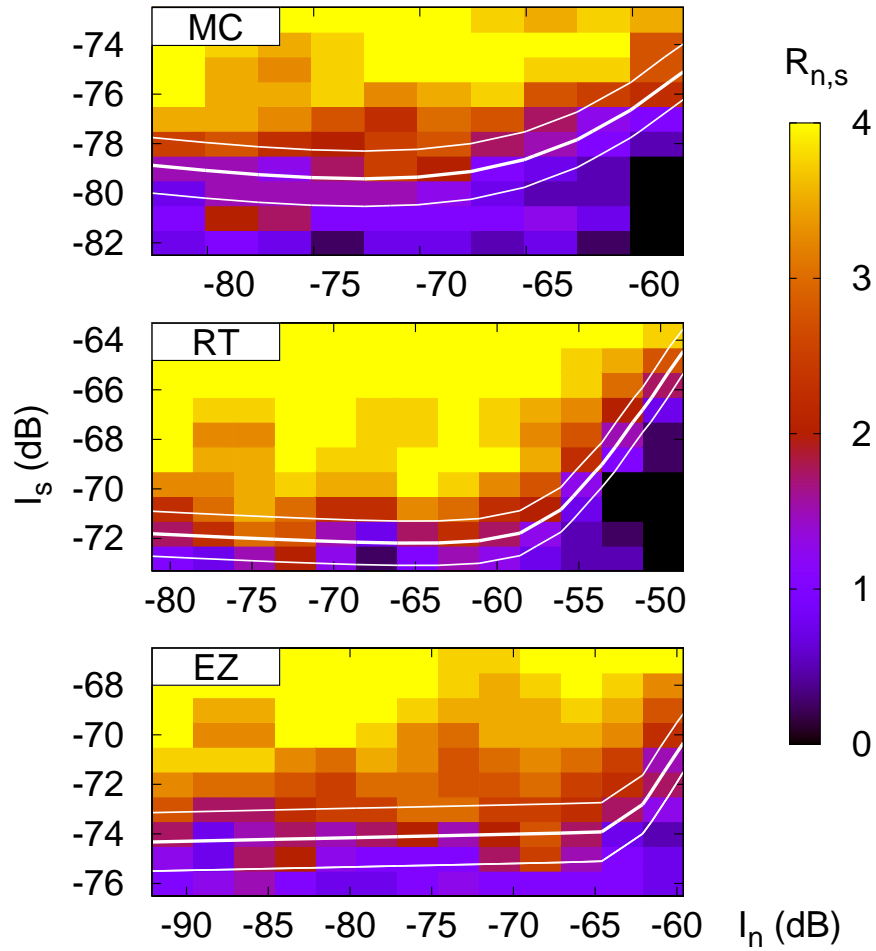


Figure 3.6: Color map of the $R_{n,s}$ matrix for three different experimental runs. On each map, the profiles corresponding to $\mu(I_n) + \sigma/3$ (top-line), $\mu(I_n)$ (middle-line) and $\mu(I_n) - \sigma/3$ (bottom-line) are shown.

3.6.2 Average procedure

In order to improve the statistical robustness of our analysis we developed a method to assess the occurrence of SR in the data collected from the entire sample of subjects. The method works as follows.

*a-posteriori
rearrangement
of the data*

Let us consider an experimental session of a particular subject. Let also I_n be a given noise level. We estimated both the parameters $\mu(I_n)$ and $\sigma(I_n)$ of the psychometric function $\psi(I_s, I_n)$ by applying a MLE procedure to the data set corresponding to I_n . To this purpose, we used the standard cumulative function:

$$\psi(I_s, I_n) = \frac{1}{2} \left[1 + \operatorname{erf} \left(\frac{I_s - \mu(I_n)}{\sigma(I_n)} \right) \right]. \quad (3.4)$$

This first step was repeated for all I_n values so as to produce a set of $(\mu(I_n), \sigma(I_n))$. Subsequently, we assumed σ to be independent from the noise intensity I_n , as for the previously reported analysis procedure. Thus we estimated $\langle \sigma \rangle$ by averaging $\sigma(I_n)$ over the I_n values. The average $\langle \sigma \rangle$ was used in a new MLE to estimate the $\mu(I_n)$ parameter of the psychometric function at each I_n :

$$\psi(I_s, I_n) = \frac{1}{2} \left[1 + \operatorname{erf} \left(\frac{I_s - \mu(I_n)}{\langle \sigma \rangle} \right) \right]. \quad (3.5)$$

Once obtained this new set of $\mu(I_n)$, the TvC given by Eq. 3.2 was fitted to the set in order to estimate the numerical value of $I_{s_0}^{th}$ and I_{n_c} .

In order to average data sets from different subjects we considered the relative distances $\Delta I_s, \Delta I_n$ of each I_s and I_n values with respect to $I_{s_0}^{th}$ and I_{n_c} .

*Lattices
of data*

We fixed the signal intensity resolution (1 dB), whereas three different noise intensity resolution were chosen to average the data from all subjects: low, middle, and high, correspond to I_n steps of 2.5 dB, 1.875 dB, and 1.25 dB, respectively. Both Fig. 3.7 and Fig. 3.8 refer to the low lattice resolution: Fig. 3.7 shows the number of subject answers (experimental data) at each $(\Delta I_n, \Delta I_s)$ value, whereas Fig. 3.8 shows the detection rates.

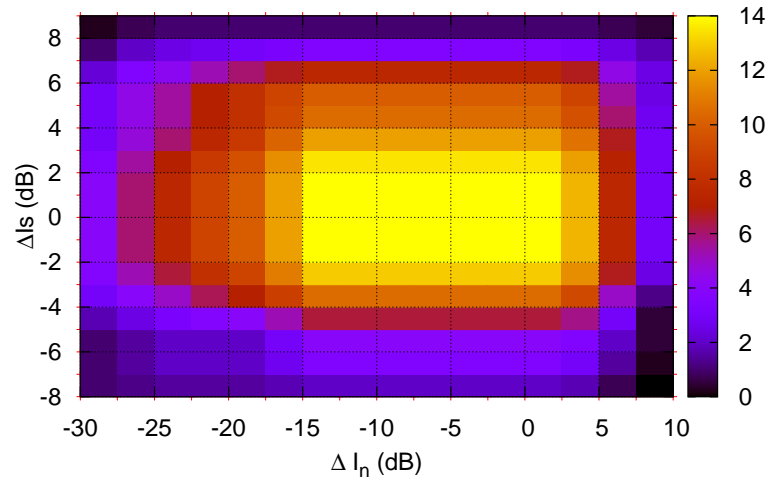


Figure 3.7: The color map shows the amount of data points for each $(\Delta I_s, \Delta I_n)$ couple of value in case of the low resolution lattice.

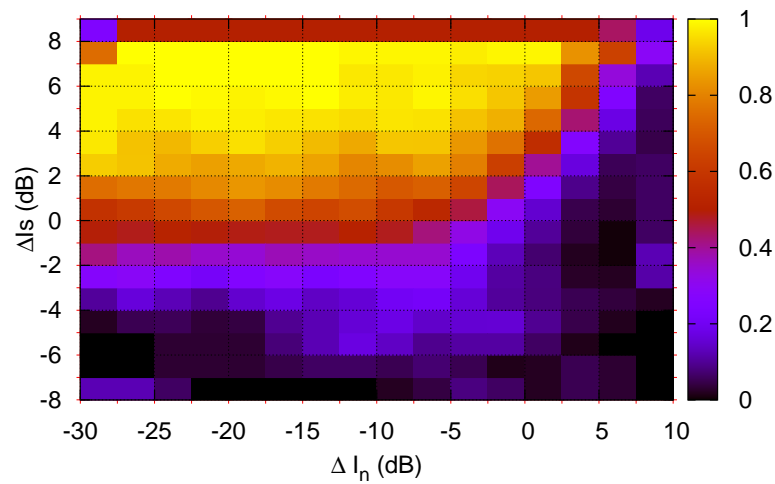


Figure 3.8: Low resolution lattice for the detection rate $P(\text{yes} | (I_s, I_n))$.

Results

Visual inspection of the data reported in Fig. 3.8 led us to hypothesize the lack of a well-marked shift of the perceptual threshold around I_{nc} ($\Delta I_n = 0$ dB). Results show that, whereas the masking effect is quite evident, the occurrence of SR is not clearly observable.

*Evidence
of SR*

However, the results of the fit reported both in Fig. 3.9 and in Tab. 3.3 show that the profile of the perceptual threshold as a function of the noise is in agreement with the occurrence of SR effects.

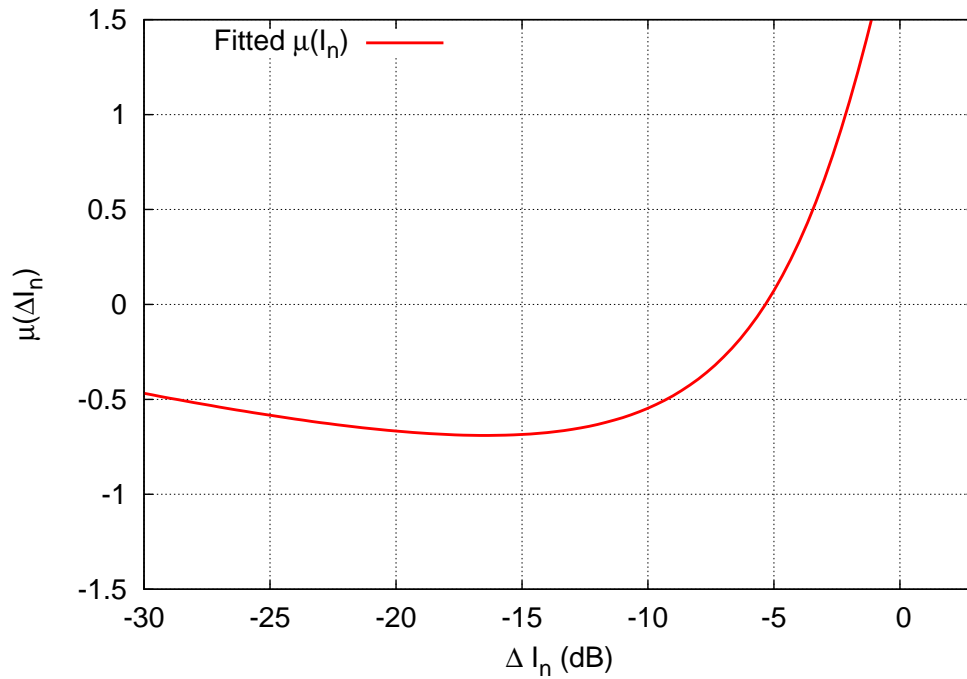


Figure 3.9: Result of the fit to low-resolution in case of the average lattice: the perceptual threshold μ reaches a minimum at a noise intensity value $I_n = -16(1)$ dB. The SR effect is 0.7 dB.

I_n resolution	1.25dB	1.875dB	2.5dB
k	0.03(2)	0.04(2)	0.04(2)
D	5.4(9)	5.8(9)	6(1)
σ	4.0(1)	3.9(1)	3.9(1)
I_{s_0}	-1.4(5)	-1.7(5)	-1.8(5)
I_{n_c}	-1.0(3)	-1.2(3)	-1.7(3)
χ^2	0.42	0.23	0.14

Table 3.3: Numerical values of the fit parameters of the fit: the positive values of the parameter k is considered as an evidence of SR.

In Tab. 3.3, the numerical values of the fit parameters k , D , σ , I_{s_0} and I_{n_c} are presented. Positive values of the parameter k for each of the selected resolutions confirm the occurrence of SR.

3.7 Conclusions

Our data show that SR produces a weak, though significant improvement in sound detection driven by an optimal, non-vanishing level of noise. As asserted in previous works [106, 109, 111], our results highlight that the effect of stimuli detection improvement is tiny in comparison with the dynamical range of the perceptual threshold. In order to quantify the effect of SR in this experimental context, it is also crucial to reduce as much as possible fluctuations of the threshold.

Both the methods we proposed and tested are statistically robust and have an additional advantage with respect to the results available in the literature: they offer the possibility to investigate the change of the entire psychometric curve as a function of the exogenous noise intensity. The choice of 50% of the correct detection as the value for the threshold is arbitrary.

In conclusion, the problem of whether and possibly which part of the human auditory system uses the effect of SR to improve the overall ability to detect stimuli remains unclear. Nevertheless, the methodological approach described in the present work can provide a starting point for further investigation, especially in relation with specific characteristics of the subjects (e.g. age, deficits such as deafness).

Our findings have two main implications: first, they reveal that SR in the auditory modality is a small effect, easily masked by fluctuations of the perceptual threshold. This conclusion poses some serious constraints to the suggested applications of auditory SR for hearing-aid devices or prosthesis

3.7. CONCLUSIONS

(such as cochlear implants [107, 108]). Second, it calls for a re-examination of the SR effect in vision and somatosensation using our statistically-robust methodology. This could help disentangle whether the difference in SR size between audition and the other sensory modalities reflects different methodological approaches or, rather, some fundamental difference between the various perceptual systems.

Part II

Criterion Setting Dynamics

Chapter 4

Signal Detection Theory

Abstract Aim of the present chapter is to introduce the reader to the Signal Detection Theory (SDT), representing a widely diffused model used to interpret “Yes/No” experiments with only two possible classes of stimuli. After a brief introduction regarding the historical evolution over the last two centuries of psychophysics, SDT quantities are presented in detail. Special attention is devoted to the role of the criterion; this part can be considered introductory for the next chapter, focused on criterion setting dynamics in human brain.

4.1 Introduction

In this section we present a brief overview of the historical development of psychophysics.

Fechner's work

Starting point of psychophysics is usually considered the work carried out by the German experimental psychologist Gustav Theodor Fechner (April 19, 1801 – November 28, 1887). The main goal of his investigation was to connect the experience occurring within the human brain at a stimulus presentation with the physical feature of the stimulus itself. Fechner's most important contribution to this aim is the introduction of the concept of *difference threshold* or *just noticeable difference (JND)*. From a methodological point of view, his approach represents an effort to apply an atomistic view in the field of perception. Fechner's main question can be formulated as follows: how does the human brain implement a fundamental unit for perception?

In Fechner's view, if stimuli are physical identical, there is no way for an observer to notice any difference. On the other hand, if the experimenter slightly change one of the two stimuli, there is a minimal difference that leads to a change in experience. This difference is defined as *JND*.

Problems with *JND*

In the decades after Fechner's formulation, the concept of *JND* was reconsidered on the basis of new experimental evidence of perception. Investigations focused on measuring *JND* in different experimental conditions led to two main problematic results:

1. *JND* measured by using different experimental procedures assumes different numerical values,
2. perception of difference between stimuli, measured as an increase in correct discrimination's rate, does not increase linearly with the physical difference.

With regard to the second point, a solution was proposed by the joint effort of Ernst Heinrich Weber (Wittenberg, June 24, 1795 – Leipzig, January 26, 1878) and Gustav Fechner himself. They founded that minimal variations of the perceived intensity ΔI linearly depend on the stimulus intensity I . In other words, $\Delta I/I$ is a constant, independent from I . This relation allowed the two scientists to formulate the logarithmic relation, known as *Weber–Fechner law* [15].

*Weber–Fechner
law*

However, the variability of JND in different experimental situations revealed that the assumption of a fixed brain response evoked by a constant stimulus presentation was wrong.

Noise and criterion

A step further, in direction to SDT , was carried out by Louis Leon Thurstone (Chicago, May 29, 1887 – Chapel Hill, September 30, 1955). His work was focused on the high variability intrinsic in the JND measurement. In 1927 [112, 113] he suggested that multiple repetitions of the same stimulus are encoded by different internal representations. In particular, this noisy neural response can be considered to vary into a continuous range and to be normally distributed. This assumption is now considered fundamental for the subsequent development of SDT .

*normally
distributed
neural response*

In addition to the work of Thurstone, the definitive formulation of SDT received an important impulse during the 40's and the early 50's, mainly due to develop military applications. Scientists focused their attention to the problem of disentangle the subjective ability of a radarists to detect a danger from the strategy adopted. In this context the concept of criterion was introduced and, as a consequence, the subject's tendency to be more liberal or conservative, independently from his/her own sensitivity.

The first application of SDT to a psychophysical investigation dates back to 1953. In that year, Wilson P. Tanner and John A. Swets performed a set of visual discrimination experiments [114, 115, 116] interpreted by using SDT .

SDT

Signal Detection Theory (SDT) is presently the most successful theory used to interpret psychophysical experiments on human [14, 15] and animal [123] perception. SDT is applied in a wide range of situations, from the interpretation of perceptual tasks involving the discrimination of a single stimulus feature [124] to more complex cognitive tasks [125].

The present chapter is organized as follows: the two main assumption of SDT are presented in Sec. 4.2. Then, we introduce the *Stimulus/Response matrix* in Sec. 4.3, whereas definition of d' and criterion are reported in Sec. 4.4. Receiver Operating Characteristics are the topic of Sec. 4.5. Finally, the central role of criterion is pointed in evidence in Sec. 4.6.

4.2 SDT assumptions

SDT , similarly to the model presented in Ch. 2, is mainly based on two fundamental assumptions: first, the neural response evoked by a stimulus presentation is noisy. Second, the choice between two possible responses is

the result of a comparison between the neural activity and a threshold set within the subject's brain.

4.2.1 Noise

Upon the presentation of a stimulus to a subject, many areas of the cerebral cortex are activated. On the other hand, SDT parametrize only an average value of this activation, without taking into account its spatial and temporal distribution, by means of a single quantity called *evoked neural activity*. In the present dissertation this activity is labelled with the letter x . Evoked neural activity is assumed to be influenced by noise which, as mentioned in Sec. 2.2.1, is normally distributed. In the following, its standard deviation σ is assumed to be stimulus independent, whereas the mean μ is proportional to the stimulus intensity¹.

4.2.2 Criterion

The possibility to discriminate between two mutually exclusive responses is modelled by a comparison between the evoked neural activity and a threshold, also called criterion in *SDT* language. If the neural activity x does (does not) overcome the threshold, then the subject will provide a certain response (the opposite one).

*Criterion
encoding*

While many works in the literature report important results relative to the encoding of neural activity evoked by a stimulus presentation [119, 120, 121, 122], very few works address the topic of how the SDT criterion is encoded within the brain. In the next chapter we will tackle this issue providing a model, also tested by ad-hoc experiments, for the criterion setting dynamics under feedback-controlled conditions.

4.3 Stimulus/Response matrix and probability of correct answer

The experimental situation described by SDT is slightly different from that one described in Ch. 2 and Ch. 3. In that case, an unspecified number of classes of stimuli were included in the experimental design. In the example of Sec. 3.4, the psychometric function was investigated by providing to the

¹With intensity we mean the value assumed by the physical feature that characterizes the stimulus. For example, in case of visual stimuli of different inclinations, the tilting angle is the feature linked with the value of μ .

subject 13 different acoustic intensities of the stimulus. In the rest of our work, if not differently reported, we will take into account the situation in which only two possible stimuli, s_1 and s_2 , are presented at each trial. As in the previous case, the possible responses r_1 and r_2 are again mutually exclusive.

The starting point for further considerations to this type of experiments is the Stimulus/Response matrix of Tab. 4.1.

	r_2	r_1
s_2	hit $H \equiv p(r_2 s_2)$	miss $M \equiv p(r_1 s_2)$
s_1	false alarm $F \equiv p(r_2 s_1)$	correct rejection $CR \equiv p(r_1 s_1)$

Table 4.1: Stimulus–Response matrix in a “Yes–No” experiment. A motor response of the type r_2 (r_1) after the presentation of a stimulus s_2 corresponds to a *hit* (*miss*); on the contrary, the same response to a stimulus s_1 is defined as *false alarm* (*correct rejection*).

If the subject provides a response r_2 (r_1) to a stimulus s_2 (s_1), this is considered as a correct one and defined as *hit* (*correct rejection*); on the contrary, a response r_2 (r_1) to a stimulus s_1 (s_2) is an error defined as *false alarm* (*miss*).

*Hit
&
false alarm*

From Tab. 4.1, we can write the relation between H (F) and M (CR) as follows:

$$\begin{aligned} M &= 1 - H \\ CR &= 1 - F \end{aligned}$$

Another important quantity, widely used in psychophysical experiments, is the percentage of correct answer $p(c)$, defined as:

$p(c)$

$$p(c) = \begin{cases} p(s_2) H + p(s_1) (1 - F) \\ p(s_1) + p(s_2) = 1 \end{cases}, \quad (4.1)$$

4.4. DEFINITION OF D' AND χ

where $p(s_k)$ is the *a priori* presentation probability of stimuli s_k , $k = 1, 2$. The quantity $p(c)$ is often used to measure the subject performance at the end of an experimental session. In the following section, two additional quantities will be introduced, sensitivity (d') and criterion (χ), both related with the subject's performance.

4.4 Definition of d' and χ

The two main assumptions of the SDT described in Sec. 4.2 allow us to interpret *hit rate* and *false alarm rate* as a function of the neural activity evoked by the stimuli presentation, $p(x|s_2)$ and $p(x|s_1)$, and of the criterion c_r . More in detail, H and F correspond to:

$$H = p(r_2|s_2) = \int_{c_r}^{\infty} p(x|s_2) dx = \Phi \left[\frac{\mu_2 - c_r}{\sigma} \right] \quad (4.2)$$

$$F = p(r_2|s_1) = \int_{c_r}^{\infty} p(x|s_1) dx = \Phi \left[\frac{\mu_1 - c_r}{\sigma} \right] \quad , \quad (4.3)$$

where the standard normal cumulative distribution Φ is defined as

$$\Phi(x) \equiv \frac{1 + \operatorname{erf}(x)}{2} = \int_{-\infty}^x \frac{e^{-\frac{y^2}{2}}}{\sqrt{2\pi}} dy \quad . \quad (4.4)$$

Fig. 4.1 shows the area corresponding to H and F underlying s_2 and s_1 distributions.

H and F depend on the relative position on the x-axis of the mean of the two distributions associated with the stimuli. The measure of the relative distance between the two distribution is d' , defined as

$$d' \equiv \frac{\mu_2 - \mu_1}{\sigma} \quad . \quad (4.5)$$

The parameter χ is defined, in term of the parameters of the distributions, as

$$\chi \equiv \frac{1}{\sigma} \left[c_r - \frac{\mu_2 + \mu_1}{2} \right] \quad . \quad (4.6)$$

By linking together Eqq. (4.2) and (4.3) with Eqq. (4.5) and (4.6), we obtain the operative definition of d' and χ :

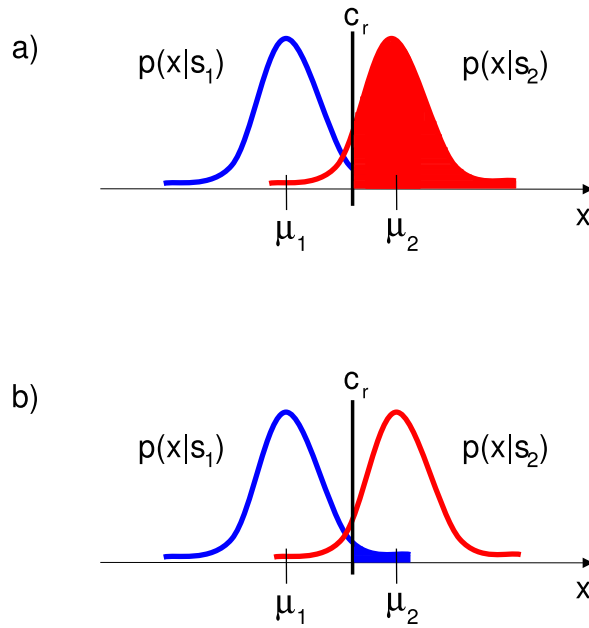


Figure 4.1: Hit rate and False alarm rate: in (a) the red area corresponds to the hit rate given by Eq.(4.2), whereas the blue area in (b) corresponds to the false alarm rate given by Eq.(4.3).

$$d' = z(H) - z(F) \quad (4.7)$$

$$\chi = -\frac{1}{2} [z(H) + z(F)] \quad , \quad (4.8)$$

where $z(x)$ is the inverse of the standard normal cumulative distribution: $z[\Phi(x)] = x$.

Optimal criterion position

Although the sensitivity d' does not depend on the criterion, both H and F depend on χ . As a consequence, it can be shown that $p(c)$ varies as a function of χ .

$$p(c) = [1 - p(s_1)] \cdot \Phi\left(\frac{d'}{2} - \chi\right) + p(s_1) \cdot \Phi\left(\frac{d'}{2} + \chi\right) \quad . \quad (4.9)$$

Prior
presentation
probabilities

Considerations relative to the symmetry of the system allow us to assume a non monotonical profile for $p(c)$ as a function of χ . By letting $\frac{dp(c)}{d\chi} = 0$, we found a maximum for $p(c)$ for $\chi = \chi_0$ at the value for $\chi = \chi_0$

$$\chi_0 = \frac{1}{d'} \ln \left[\frac{p(s_1)}{1 - p(s_1)} \right] . \quad (4.10)$$

Pay-off / loss
matrix

It is interesting to note that, if $p(s_1) = p(s_2) = 0.5$, then the optimal criterion position is to the midpoint of the two Gaussian distributions ($\chi_0 = 0$). Eq. (4.10) shows a possibility to modify the optimal criterion position by simply acting on the prior presentation probabilities of the two classes of stimuli. An additional possibility to shift χ_0 is related with the introduction of a *pay-off/loss* matrix in the experimental paradigm. Being V_{ij} coefficients of pay-off (or, if negative, loss), the criterion position that maximizes reward can be shown to be given by

$$\chi_0 = \frac{1}{d'} \ln \left[\frac{V_{11} - V_{12}}{V_{22} - V_{21}} \cdot \frac{p(s_1)}{1 - p(s_1)} \right] . \quad (4.11)$$

Both the two results of Eqq. (4.10) and (4.11) are applied to induce a criterion shift by simply acting on $p(s_i)$ or V_{ij} [14, 15].

4.5 H-F space

As shown in Sec. 4.3, given two classes of stimuli and a discrimination task, the result of each experimental session is completely described by the rates of *hit* and *false alarm*. A possible way to link together the information relative to this quantities is the assessment of $p(c)$, d' and χ , as reported in Sec. 4.4. On the other side, each couple of numerical values of H and F can be represented by a point in the bidimensional (H, F) – space, bounded by the conditions $H \in [0 : 1]$ and $F \in [0 : 1]$.

4.5.1 Receiver Operating Characteristics (ROC)

Given the definition of $p(c)$, d' and χ as functions of H and F , the loci of points in the (H, F) -space corresponding to constant values of these quantities are defined as *iso-p(c)*, *iso-d'* and *iso-bias* curves, respectively. These curves are referred to in the literature as *Receiver Operating Characteristics*, or *ROC* - curves [14, 15].

ROC curves

If $p(s_1) = p(s_2) = 0.5$ (balanced *a-priori* presentations), Eq. (4.1), (4.7) and (4.8) can be rewritten as follow:

$$H(F, p(c)) = 2p(c) - (1 - F) \quad (4.12)$$

$$H(F, \chi) = \Phi[-z(F) - 2\chi] \quad (4.13)$$

$$H(F, d') = \Phi[z(F) + d'] \quad (4.14)$$

Fig. 4.2 shows the graphical representations of the ROC - curves of Eqq. (4.12), (4.13) and (4.14), respectively.

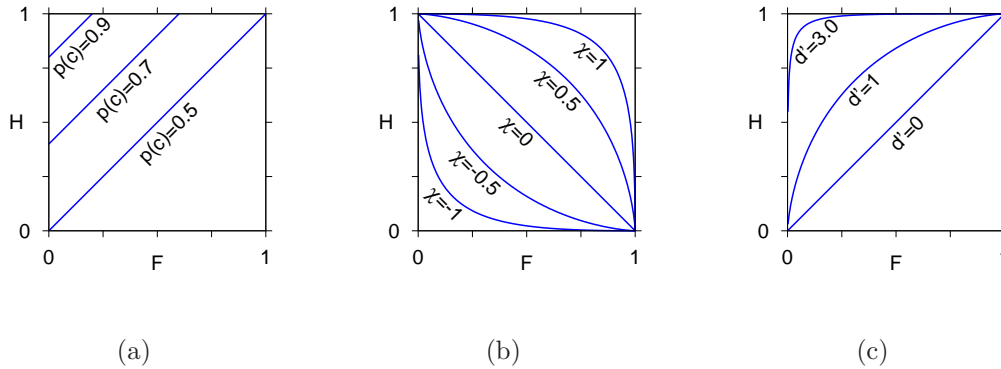


Figure 4.2: Receiver Operating Characteristics curves in (H, F) -space: (a) *iso-p(c)* curves; (b) *iso-bias* curves; (c) *iso-d'* curves.

Of particular interest for our investigation are the plots of Fig. 4.2(c); here we observe the effect of different strategies (or criteria, in SDT terms), that maintain the sensitivity of the observer constant. If a more liberal strategy is adopted, both the Hit and the False alarm rate increase: then the

iso-d' curves

subject performance, in terms of numerical value of the H–F couple, will be represented by a point on the iso- d' curve closed to the upper right angle of the H–F space. On the contrary, if the subject is more conservative, the point on the same iso- d' will be more closed to the lower left angle.

A ROC iso- d' curve can be measured by keeping d' fixed and inducing the subject to adopt different strategies. The implementation of the rating procedure represents a different way to measure iso- d' curves. In this type of experiments the subject is asked to provide not only a response to the task, but also to select a degree of confidence on a scale². The original experiments testing this hypothesis has been performed in the first half of the 60's [117, 118]

4.6 The role of Criterion

We report a summary of the work by Gong *et al.* [126], providing a model based on SDT for stochastic resonance in perception. Particular attention is devoted to the role of criterion.

4.6.1 A model for stochastic resonance in perception

The model by Gong *et al.* [126] uses SDT to interpret the phenomenon of *SR* in “Yes/No” experiments. An important difference with our experimental setup (see Ch. 3) is that only two possible classes of stimuli are given. The main hypothesis underlying the model is that noise does not act to the mean of the distribution relative to the evoked neural activity, but only to their standard deviation: an increase of the level of noise superimposed to the signal causes a broadening of the relative distribution of the evoked neural activity.

The increase of σ , proportionally to the noise intensity I_n , acts both on H and on F , as shown in Eqq. (4.2) and (4.3). The trend predicted for d' as a function of σ by Eq. (4.5) is a monotonical decrease. Thus, Gong *et al.* [126] describe a SR-like effect in terms of percent of correct answer. In particular

$$P(c) = 50 \int_{c_r}^{\infty} p(x|s_2) dx + 50 \int_{-\infty}^{c_r} p(x|s_1) dx \quad (4.15)$$

or

$$P(c) = 50 + 25 \left[\operatorname{erf} \left(\frac{c_r - \mu_1}{\sigma \cdot \sqrt{2}} \right) - \operatorname{erf} \left(\frac{c_r - \mu_2}{\sigma \cdot \sqrt{2}} \right) \right]. \quad (4.16)$$

²Often discrete scales are adopted, for example from “1” (*I have randomly chosen*) to “10” (*I am completely sure*).

Fig.4.3 shows the profile of $P(c)$ as a function of both σ and the criterion c_r . For each c_r value, a maximum of $P(c)$ as a function of noise (expressed in terms of σ) is considered evidence of SR.

Evidence of SR

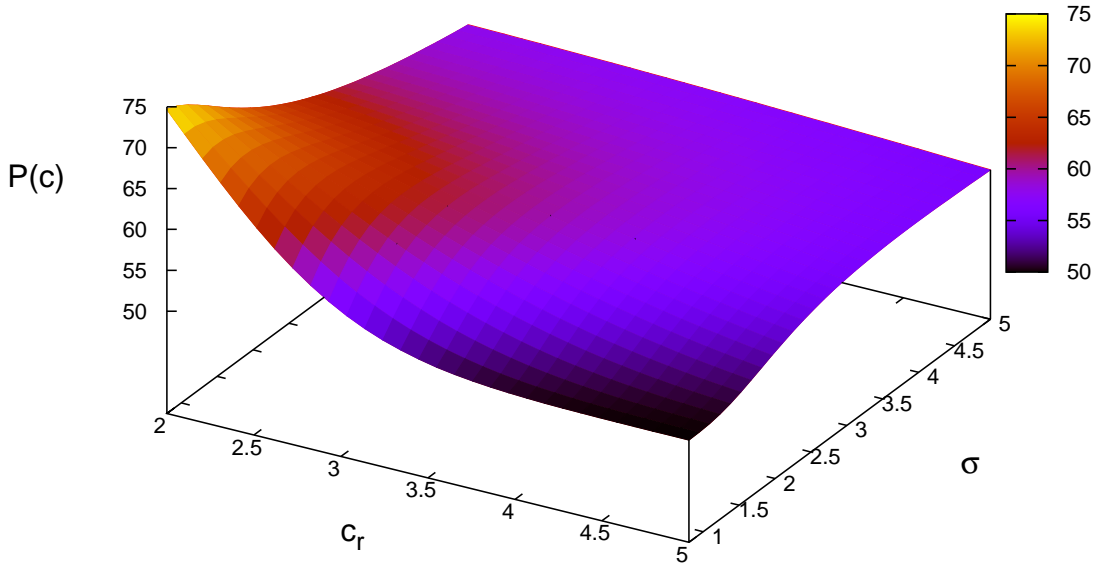


Figure 4.3: Profile of $P(c)$ as a function of both σ and c_r . Numerical values of the parameters of Eq.(4.16) are $\mu_1 = 0$ and $\mu_2 = 2$. $P(c)$ is computed for $\sigma \in [0.5, 5]$ and $c_r \in [2, 5]$.

By letting $\frac{dP(c)}{d\sigma} = 0$, they find that the percent of correct answer has a maximum in correspondence to

Conditions posed to the criterion

$$\sigma_{max} = \sqrt{\frac{(2c_r - \mu_1 - \mu_2)(\mu_2 - \mu_1)}{2 \ln \left[\frac{c_r - \mu_1}{c_r - \mu_2} \right]}} \quad (4.17)$$

that, as shown in Fig. 4.4, has real positive solutions only in the case

$$c_r > \mu_2. \quad (4.18)$$

The condition posed to the criterion position, far from the optimality defined in Eq.(4.10), and the demand of stability represent two important limitations to test experimentally the prediction by Gong et al. [126]. Small

4.7. CONCLUSIONS

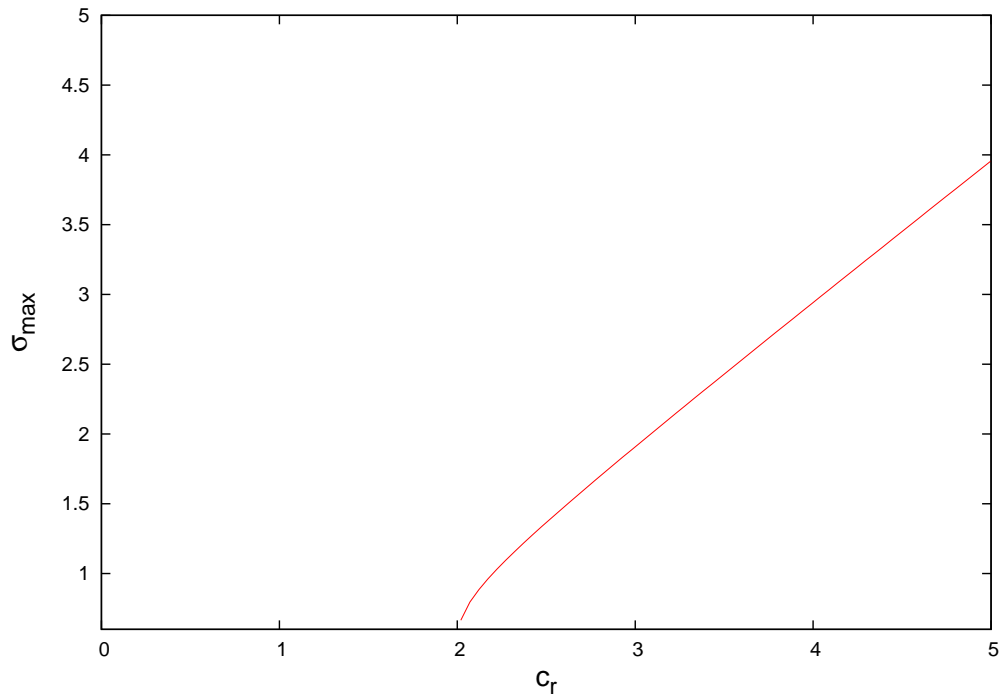


Figure 4.4: For each c_r value, SR is reported as a maximum of percent of correct response at a specific value of $\sigma = \sigma_{max}$. Values of σ_{max} exist only if $c_r > \mu_2$.

fluctuations of c_r dramatically reduce the effect and consequently the possibility to measure it. Fluctuations are here meant on the time scale of the same order of magnitude of the trial time-line.

4.7 Conclusions

Signal Detection Theory (SDT) represents a robust model usually adopted to interpret results of discrimination experiments. If only two mutually exclusive classes of response are provided, SDT allows to interpret the *Stimulus-Response* matrix in terms of sensitivity and criterion.

Sensitivity, or d' in SDT language, is considered as a measure of the subject ability to solve the task: it is also independent from the strategy adopted to respond. In the present chapter particular attention was devoted to the central role of criterion in discrimination. The definition of *optimal criterion position*, related to the possibility to maximize the rate of correct answer, was introduced in Sec. 4.4.

Finally, a model based on SDT for stochastic resonance in perception was presented in Sec. 4.6. An important condition to test this model in real experimental situations is the demand of criterion stability: thus, we focused our attention to an extensive investigation on criterion dynamics. Results of our investigation are reported in the following chapter.

4.7. CONCLUSIONS

Chapter 5

Feedback Control over Criterion Setting

Abstract Signal detection theory (SDT) provides a reliable model for experiments on discrimination, perhaps the most basic implementation of decision making. However, the knowledge of how SDT parameters are encoded in brains is still poor. Given a discrimination task, SDT assumes the existence of an internal criterion: responses provided by the observer are the result of a comparison between this criterion and the neural response evoked by the stimulus. Despite its important role, it is still largely unknown how this criterion is set and maintained. To gain insight on this crucial, but yet unresolved, issue, we focused our attention to dynamical aspects of criterion setting. We used an experimental phase-detection technique and modelled feedback-induced criterion shifts by means of a linear response system.

5.1 Introduction

*Criterion
shifts*

In the previous chapter, the fundamental role of criterion in decisional processes [14, 15] was highlighted. The existence of a criterion represents one of the two fundamental assumptions of SDT: its position, with respect to the neural activity evoked by the stimulus presentation, determines the subject's response in "Yes/No" experiments. Shifts of the criterion from its optimal position are related to a more liberal or conservative attitude of the subject. During a measurement session, this attitude, and consequently the rate of responses "Yes" or "No", can change depending on several factors external or internal to the subject. For example, a change of the presentation probabilities of the two classes of stimuli induces a shift of the optimal criterion position; in this case, the subject should readjust his/her response strategy, with respect to the case of equal prior presentation probabilities, in order to improve his/her performance.

This chapter concerns experiments we carried out, in which dynamical aspects of criterion setting were investigated.

Our experiments on the stochastic resonance in perception has revealed how the topic of criterion dynamics is crucial to the psychophysical investigation of the role of the noise in the brain.

*Criterion
dynamics*

In this thesis, the word experiment is used according to its common meaning in *physics*: an experiment coincides with an experimental setup rather than with a variation of a given experimental design. These experiments were expected to shed a new light on the problem of how a criterion is set, maintained and, in some circumstances, modified within the brain. More in general, the problem we were interested in was related to the encoding of the criterion in the human brain. To tackle this issue, we induced a well-known shift of the optimal criterion position at each single trial and reconstructed the criterion dynamics on the basis of a physical model.

Experimental data consisted in a set of of a stimulus $s[i]$, each belonging to one of two distinct classes, and a dichotomic response $r[i]$ (i represents the trial number). They were analyzed by means of a maximum likelihood estimation (MLE) procedure and interpreted by assuming a single-pole, feedback-loop model [17] characterized by a time constant and a gain term. The experimental approach was essentially a standard phase-detection technique [127].

The chapter is organized as follows: two works representing, to our knowledge, the main contributions relative to the problem under examination are presented in Sec. 5.2. Then, we present in detail our model for the criterion dynamics in Sec. 5.3, reporting both the technique used to induce a criterion shift and some physical considerations about the model. Details of the two

experiments we carried out are reported in the two following sections: in the first experiment, presented in Sec. 5.4, we monitored the criterion dynamics entailed by a shift imposed through the techniques presented in Sec. 5.3. In a second experiment, described in Sec. 5.5, an additional control over the subject's head motion was introduced. In addition, we present a merging of the results relative to the two experimental procedures in Sec. 5.6. Finally, a test used to evaluate the goodness of our linear model for criterion setting is presented in Sec. 5.7. Final remarks and conclusions are presented in Sec. 5.8.

5.2 State of the art

Perhaps for the sake of simplicity in interpreting results, criterion is assumed to be constant in almost every psychophysical experiment. However, as shown in Sec. 4.4, it is well-known that it can be modified also during an experimental session by changing, for example, prior presentation probabilities and/or the payoff/loss matrix [14, 15].

Remarkably, very few studies have thoroughly addressed this topic, and furthermore a satisfactory theory accounting for how these criterion changes may take place was not yet devised.

In one of these studies [128], a model using correlations between the response to a new stimulus and a set of previous responses (sequential effects) was proposed to explain how observers optimally adjust their criterion. The model proposed by Treisman [128], based on correlations between consecutive responses, has important caveats: for example, this model does not provide a robust prediction on how a certain response influences the following one. Different mechanisms, based, for example, on a linear or exponential adaptation, are proposed to describe the shift of the criterion position induced after a trial, but the authors do not provide a definitive argument supporting one of the different options, as well as a robust definition of "optimality" for the criterion position. An additional problem related with the proposed model [128] is the absence of any physically-based interpretation.

*Sequential
effects*

In a more recent work [129], the so-called "block paradigm" was used to induce criterion shifts and to investigate the corresponding dynamics. Trials were grouped in blocks; task difficulty (and thus the sensitivity parameter d') was kept constant within a block and stepwise changed at each block transition. At the end of each block, the observer received a feedback on his/her performance. In this way, a shift of the decision criterion was induced as a *mirror effect* of the change in task difficulty. The criterion shift was assumed to occur after a time lag with respect to the d' modification

*Stepwise
criterion
variations*

and observed data were fitted using SDT. However, the authors do not provide any physical interpretation of this model. The stepwise, time-lagged criterion modification model was explicitly chosen only by virtue of its computational simplicity. Moreover, the chosen paradigm did not allow for a criterion control independent from d' .

These two works [128, 129] exhibit unresolved problems in the attempt of gaining insight into the topic of measurement and modelling criterion dynamics. The main problem regards the lack of a reliable model, based on physical considerations: for example, the idea that the brain stepwise changes the criterion position after a certain time-lag [129] was applied only by reason of the lack of a model for the trial-by-trial dynamics. In the next section, we will focus our attention to this problem: the feedback system analysis will be applied to the mechanism of criterion setting.

5.3 Model for criterion dynamics

Criterion shift

Aim of the present section is to provide an explanation of how feedback acts on criterion position in order to induce a controlled shift. Fig. 5.1 shows two examples of criterion shifts, represented by arrows, from position “A” to “B” and, in the opposite direction, from “B” to “C”.

Criterion shifts occur, either because of internal fluctuations, independently from the external conditions, or as a consequence of the external action by the experimenter. In the present chapter we are interested to induce a well-defined criterion shift by changing the physical features of the stimuli. Different strategies are usually adopted to this purpose: one of the most frequently applied [14] is the change of the prior presentation probability relative to the two classes of stimuli. As reported in Sec. 4.4, the optimal criterion position is given by

*Optimal
criterion
position*

$$\chi_0 = \frac{1}{d'} \ln \left[\frac{p(s_1)}{1 - p(s_1)} \right], \quad (5.1)$$

where $p(s_1)$ is the prior presentation probability of type 1 stimuli. By changing $p(s_1)$, and consequently $p(s_2)$, the optimal criterion position χ_0 is shifted away from the midpoint of the two distributions underlying the response evoked by the stimuli.

Although it is always possible a definition of optimal criterion position, this does not directly imply that during an experimental session the strategy adopted by the subject performing the task corresponds to the optimal one.

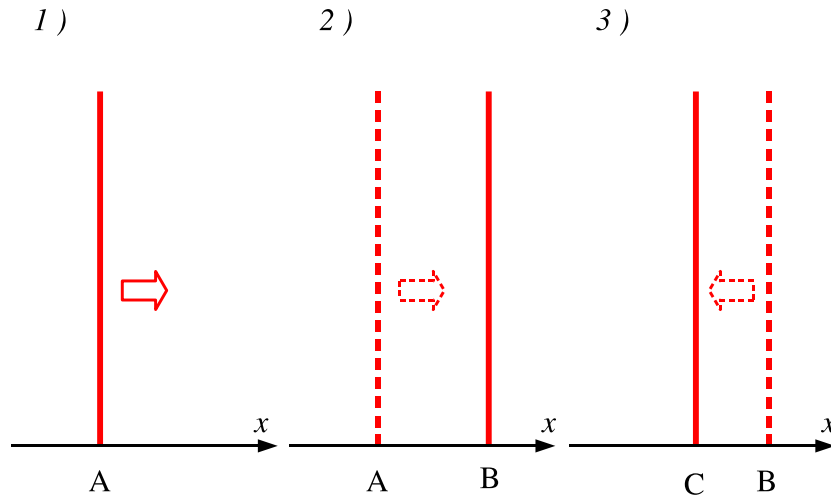


Figure 5.1: Time evolution of criterion position. In “1” the criterion (red line) is fixed in “A”. If a shift of the criterion position (red arrow) is somehow induced to the subject, after a certain amount of time, the criterion moves to its new position “B” (2). Similarly, if the subject is forced to shift the criterion back to the initial position the new criterion position moves closer to the original one.

In particular, if the subject does not maximize the rate of correct responses, the criterion probably turns out to be different from its optimal position. However, if the criterion is not optimally positioned, the request of performance improvement may induce the subject to use a criterion closer to the optimal one. The strategy is then to explicitly formulate this request at the beginning of the experimental session and regularly inform the subject about his/her performance. This additional information can not be set *a priori* by the experimenter, because it depends on the subject’s trial-by-trial performance.

The implementation of such a procedure, where the subject is informed on the correctness of his/her responses, inevitably yields a feedback loop. Fig. 5.2 shows a very general scheme of feedback loop: part of information contained in the output of the system V_{out} is fed back to the input. This is usually called *error signal*, labelled with e in Fig. 5.2. After the processing by the block F , the correction signal c is subtracted from the input V_{in} ¹.

*Feedback
loop*

¹The type of feedback shown in Fig. 5.2 is defined as *negative feedback*.

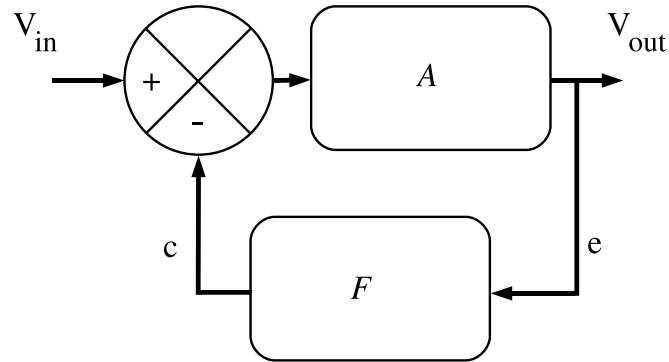


Figure 5.2: Graphical representation of a feedback loop. From left to right, V_{in} represents the input signal for the system A . Part of the output signal V_{out} is redirected to the input of the system. The block labelled with F processes the information contained within the so-called error signal e . Output of the block F , also called “correction” c , is subtracted, in case of negative feedback, to V_{in} .

Given a certain input signal V_{in} , the output of the system V_{out} depends on the behaviour of both the two blocks A and F . In our view, they represent two distinct phenomena occurring within the human brain. If the feedback loop is open, i.e. the block F does not play any role in the dynamics, the scheme of Fig. 5.2 is very similar to Fig. 2.1. In that case, the input is the stimulus presented to the subject, the intermediate block represents the set processes allowing the subject to provide a response to the task, and V_{out} is the response itself.

To sum up, besides the existence of a criterion, we assume that a different mechanism for the criterion setting works within the human brain. This mechanism acquires the feedback information, processes the error signal and coherently changes the criterion position.

Physical model for feedback loops

In the rest of the chapter, where not differently reported, we assume the feedback loop to be described by the simplest model used for this type of systems. The main characteristic of this model is linearity. This means that if the input sinusoidally oscillates at a specific frequency ω_0 with unitary

amplitude, the output $V_{out}(t)$ is given by

$$V_{out}(t) = \frac{G}{\sqrt{1 + (\omega_0\tau)^2}} \sin[\omega_0(t - \tau)] \quad (5.2)$$

where G is the amplitude (or "gain factor") and τ the phase of the output oscillation. In other words, no additional frequency components ($\omega \neq \omega_0$) are superimposed to the output².

A more precise definition of the feedback loop investigated in the present chapter is depicted in Fig. 5.3.

The blue area in Fig. 5.3 shows the elements under the experimenter's control: the stimulus and the evaluation about the correctness of the subject's response. Conversely, the decisional block, labeled with "SDT element", and the mechanism acting on the criterion position, labeled with Γ , are internal to the subject's brain.

*Feedback
on criterion*

After the presentation of the stimulus s , evoking a noisy ($s + n$) neural activity x , the subject's brain produces a response r by comparing x with the internal criterion c_r . Then, the experimenter evaluates subject's response r and provides a feedback (error signal labeled with e) about the correctness of the response. The subject's brain uses this information, by processing it in the block Γ and setting a new criterion position through a negative feedback-like mechanism. The output of the Γ -block is a correction for the criterion position c_c that, subtracted from the original criterion c_0 , yields the final criterion c_r used for the discrimination at the next trial.

The model described in Fig. 5.3 joints two components for the criterion: c_0 is independent from the feedback loop and allows the observer to produce a response also in the case in which the error signal e is not provided to the subject; if this is the case, then $c_r = c_0$ at each trial. This does not necessary means that c_r remains fixed at its initial position during the experiment: internal fluctuation of c_r , independent from the feedback loop, are possible, though not considered in our model.

In the model presented above, there is no way for the experimenter to act on c_0 . On the other hand the correction c_c on criterion position plays an important role in inducing shifts of c_r .

In the following sections we describe the two experiments carried out to test the model.

²See Appendix B for mathematical details.

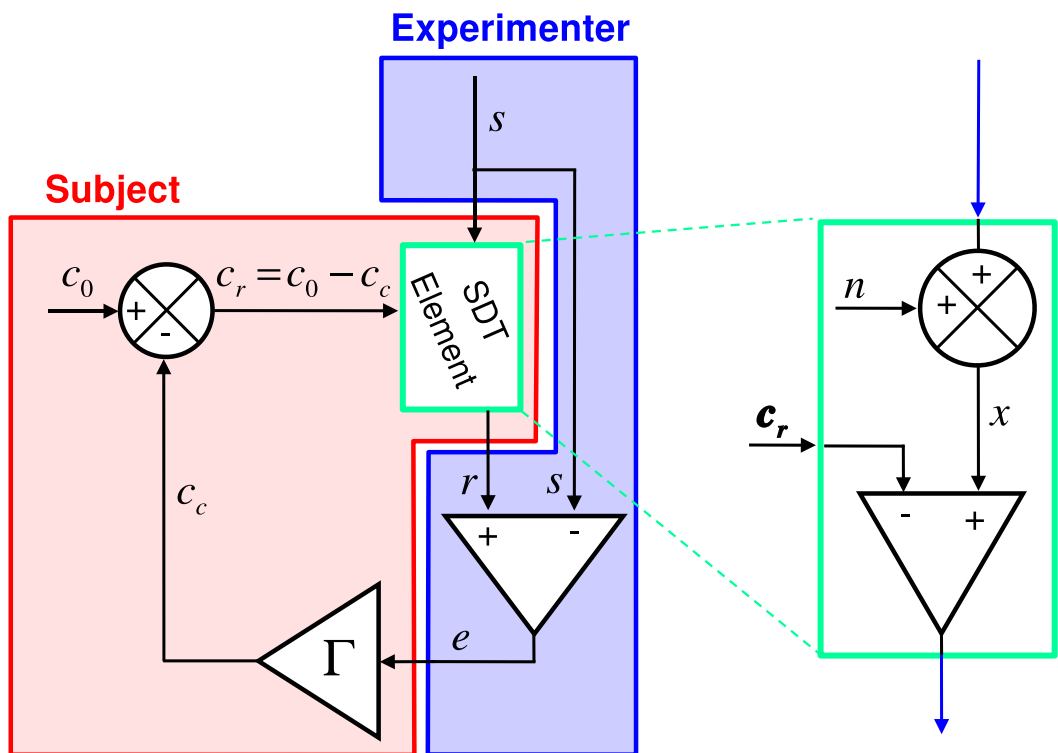


Figure 5.3: Feedback loop for criterion setting.

5.4 Experiment 1

Aim of this experiment was to tackle the problem of criterion dynamics in a simple visual discrimination task. We induced feedback-controlled criterion shifts and assessed how the observer's response changed over time. The discrimination task addressed a single feature, namely the orientation of a Gabor patch.

5.4.1 Stimuli

The stimuli presented to the subjects were Gabor patches. An example of this type of stimuli is presented in Fig. 5.4.

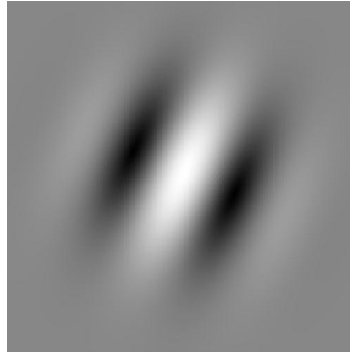


Figure 5.4: Example of right-oriented Gabor patch.

A Gabor patch is a monochromatic visual stimulus: the gray intensity is spatially modulated by a sinusoidal grating convolved with a bidimensional Gaussian function:

*Gabor
patch*

$$G(x, y) = G_0 + G_1 \cos \left[\frac{2\pi}{\Xi} (x \cos \phi - y \sin \phi) + \alpha \right] \times \exp \left[-\frac{(x \cos \phi - y \sin \phi)^2}{2\sigma_x^2} - \frac{(x \sin \phi + y \cos \phi)^2}{2\sigma_y^2} \right]. \quad (5.3)$$

In this expression, G_0 is the background gray level and G_1 the average gray intensity of the stimulus. Conventionally, $G(x, y) = 0$ for black and $G(x, y) = 1$ for white. In addition, x and y correspond to the pixel's position with respect

5.4. EXPERIMENT 1

to the center of the stimulus, whereas Ξ and α are the wavelength and the phase, respectively. The standard deviations σ_x e σ_y are proportional to the width of the stimulus along the two axes. Finally, ϕ is the tilting angle with respect to the vertical orientation.

G_0	0.625
G_1	0.078
Ξ	$1.5(1)^\circ$
σ_x	$0.7(1)^\circ$
σ_y	$0.7(1)^\circ$
α	0

Table 5.1: Numerical values used in Eq. 5.3 for the stimuli generation. The values of parameters Ξ , σ_x and σ_y are expressed in degrees relative to the visual angle.

*Orientation
of the stimulus*

At each trial, a single Gabor patch was presented at the center of the screen and subjects were requested to evaluate if the stimulus was oriented to the left or to the right of a reference line titled by λ with respect to the vertical axis. Fig. 5.5 shows two example of left – or right – oriented Gabor patches.

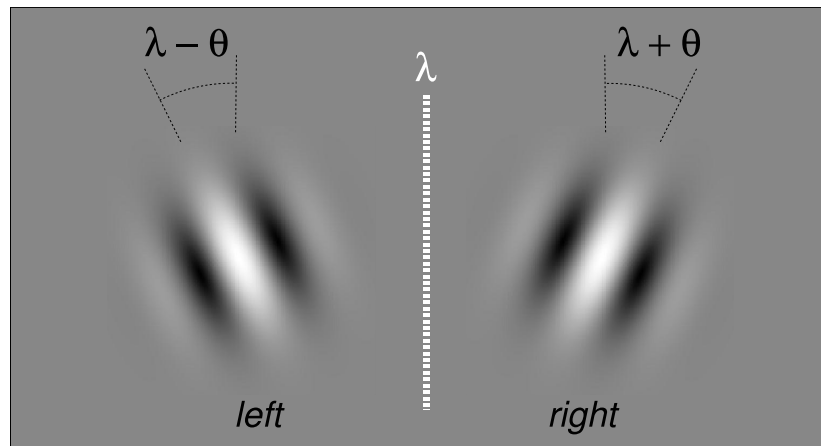


Figure 5.5: Left/right oriented Gabor patches. The tilting angle ϕ is given by $\lambda - \theta$ (left) or $\lambda + \theta$ (right). Here $\lambda = 0$.

So, the two classes of stimuli were symmetric with respect to λ , that in

general could be different from the vertical orientation. Angles are assumed to be positive if they produce tilting to the right (*clockwise* direction).

The separation between the two classes of stimuli was defined only by the parameter θ ; in particular, this separation was equal to 2θ .

Generation and presentation of stimuli was controlled by a home-made program written in C++, using OpenGL libraries and running under Linux on a Pentium IV PC. The program defined a 121×121 matrix of pixels, with a resolution of 32 bits, on the basis of Eq. 5.3 and the numerical values of Tab. 5.1. The stimuli were presented over a grey background (luminosity density of 39.6 cd/m^2).

5.4.2 Criterion shift

According to *SDT*, a stimulus evokes a neural response whose occurrence probability is Gaussian-distributed. In Fig. 5.6 left (right) stimuli are associated to a green (blue) distribution. The response is “right” or “left” according to whether the neural response does or does not overcome a criterion c_r encoded within the observer’s brain. Criterion shifts were induced by changing the orientation of both the two classes of stimuli while leaving the sensitivity d' unchanged. In addition, observers were informed about the correctness of their response after each trial; in this way the feedback loop was established.

Fig. 5.6 shows the effect of the rotation on the evoked neural activity and the related SDT-quantities. The upper part shows the evoked neural activity relative to the two Gabors. Given an equal prior presentation probabilities of left and right stimuli, the percentage of correct answers $p(c)$ was maximized if the criterion c_r coincided with the center of mass of the two distributions. This corresponded to the axis of symmetry coincident with λ . In the lower part, a change of λ , corresponding to a rigid rotation of both the classes of stimuli, induced a shift of the means of the two distributions. During the shift, d' remained unchanged³, while the optimal criterion position was shifted to the midpoint of the two new distributions. In order to increase the rate of correct answer, subjects were therefore implicitly requested to shift (red arrow) their criterion c_r towards the new optimal position.

*Maximize
p(c)*

The mechanism shown in Fig. 5.6 is restricted to only two value of the tilting angle λ ($\lambda = 0^\circ$ – vertical – and $\lambda \neq 0^\circ$). In general the time evolution of $\lambda(t)$ can be more complex. Fig. 5.7 shows the case of a sinusoidal modulation of $\lambda(t)$. At the beginning of the experiment, the Gabor patch was oriented to the left ($-\theta$) or to the right ($+\theta$) with respect to the observer’s subjective vertical orientation (in the figure $\lambda = 0^\circ$). The criterion was as-

*Sinusoidal
modulation*

³ d' is proportional to the separation $\Delta\phi$ between the two tilting angles ($\Delta\phi = 2\theta$).

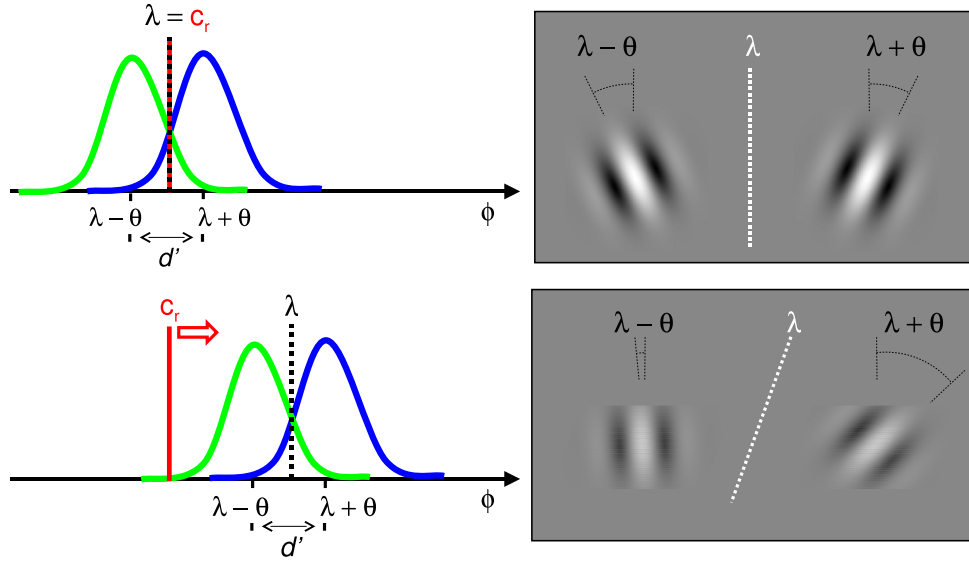


Figure 5.6: Effect of a rigid rotation. The upper part shows the experimental situation referred to the standard vertical orientation ($\lambda = 0^\circ$). The lower part shows the effect of a rigid rotation ($\lambda \neq 0^\circ$) applied to both the stimuli.

sumed to be placed as the optimal position ($\chi = \chi_{opt}$, given by Eq. (5.1)). The two classes of stimuli oscillated around the initial tilting angle at a constant frequency. The amplitude of the modulation was given by the angle η_{max} (see right side). In the left side, the shifts of the relative distributions are plotted for four possible time steps. In the bottom plot, the red solid line represents a possible time evolution of the criterion χ as predicted by a linear model in response to a harmonic χ_{opt} modulation (black dashed line): the oscillation was damped ($A < 1$ in Eq. (5.2)), the criterion moved with a non-vanishing delay ($\tau \neq 0$ in Eq. (5.2)); moreover, only the component having the same frequency of the stimuli modulation is shown, according to the linear assumption.

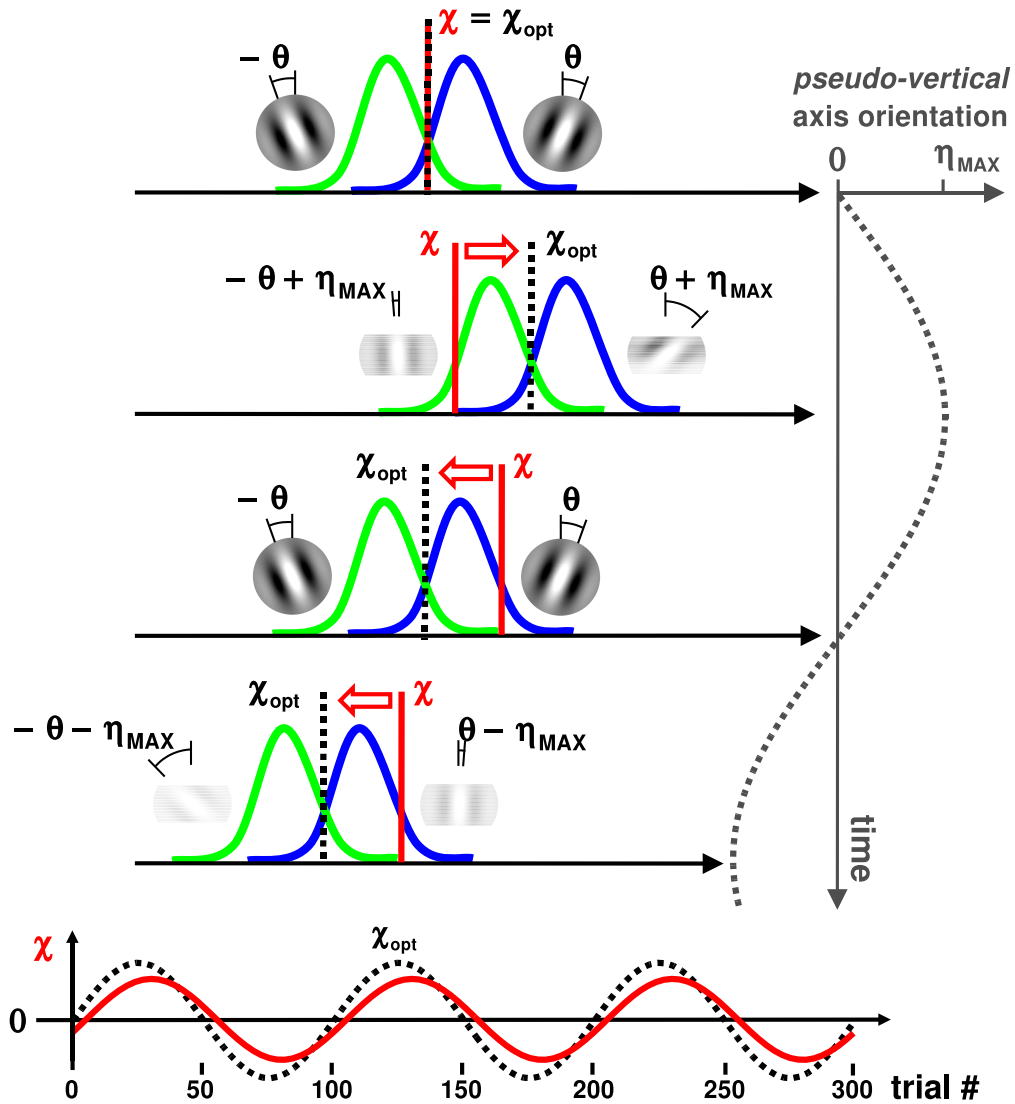


Figure 5.7: Stimulus modulation and criterion evolution. A sinusoidal modulation of the two classes of stimuli induces a shift of the neural activity distributions. In order to maximize the rate of correct answers, criterion χ tends to its optimal position χ_{opt} . Bottom: χ oscillates at the same frequency of χ_{opt} .

5.4.3 Experimental apparatus

Observers sat 46.5 cm in front of a 2070SB Mitsubishi CRT monitor (20", 1280 x 1024, vertical and horizontal refresh rate of 87.5 Hz and 93.3 kHz, respectively); head position and orientation with respect to the monitor was constrained by a chin rest. Fig. 5.8 shows a scheme of the experimental setup.

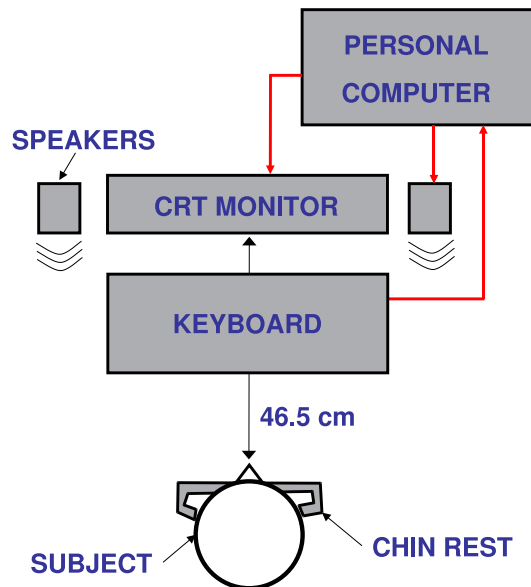


Figure 5.8: Experimental setup: subject's head, resting on a chin rest, was set at 46.5 cm from the screen. The response was given by pressing the keys *S* (left) or *D* (right) on the keyboard.

A personal computer recorded the responses and generated the feedback signal presented to the subject through the speakers.

5.4.4 Trial time-flow

The trial time-flow is schematically shown in Fig. 5.9.

At the beginning of each trial, a fixation point (black square, 0.1° visual angle) appeared at the centre of the screen for 300 ms. 100 ms later, the Gabor patch (Michelson contrast of 20 %) was presented for 100 ms. The observer was asked to maintain his/her gaze at fixation throughout the trial. Once the Gabor disappeared, the observer reported whether the Gabor was tilted to the left or to the right by pressing the letter "S" (*sinistra*) or "D" (*dextra*), respectively. In the "feedback session" the recorded voice informed the subject about the correctness of his/her response. The correctness was

The task

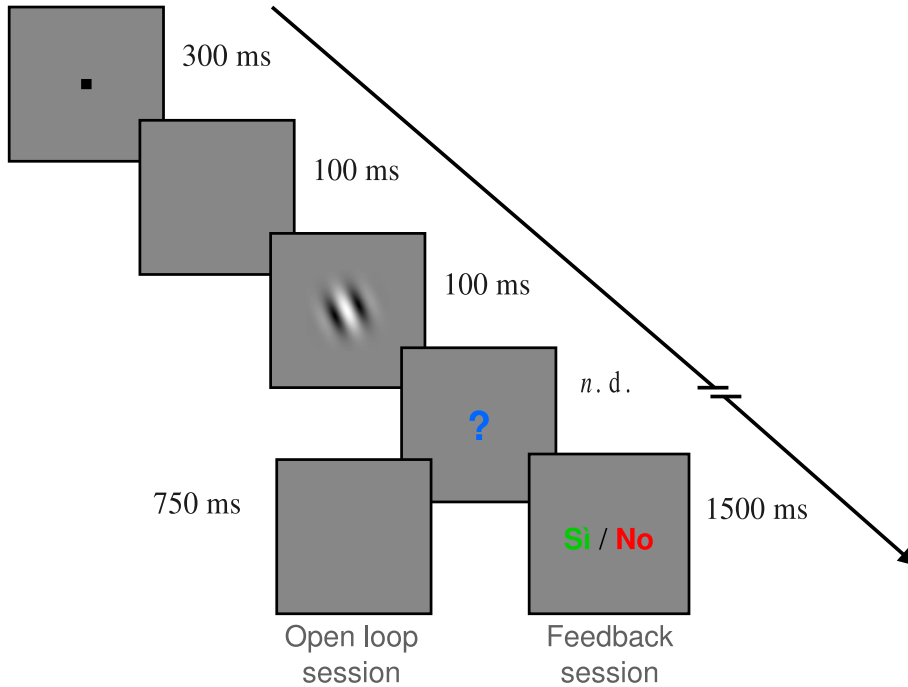


Figure 5.9: Time-flow of a single trial. After the presentation of a fixation point at the center of the screen, the stimulus is shown for 100 msec. Subsequently, without any constraints on reaction time, the subject provides his/her response and, if the feedback is activated, a recorded voice informs about the correctness of the answer.

expressed by the experimenter on the basis of the reference orientation λ . A new trial started 1500 ms after the observer's response.

5.4.5 Subjects

A set of 35 observers (15 males and 20 females) participated. All were students or staff members of the University of Trento, aged 19 to 45 (mean 26, standard deviation 6), and reported normal or corrected-to-normal visual acuity. Prior to the experiment, each observer declared to know nothing about the experimental procedure and aim. Preliminary and final declarations were collected by filling two distinct, *ad-hoc* made forms, reported in App. A.

5.4.6 Time–line of the experimental session

As shown in Fig. 5.10, the experimental session was divided in three phases, named with *training*, *psychometric assessment* and *main experimental phase*, respectively. Instructions were provided separately for each phase (see App. A).

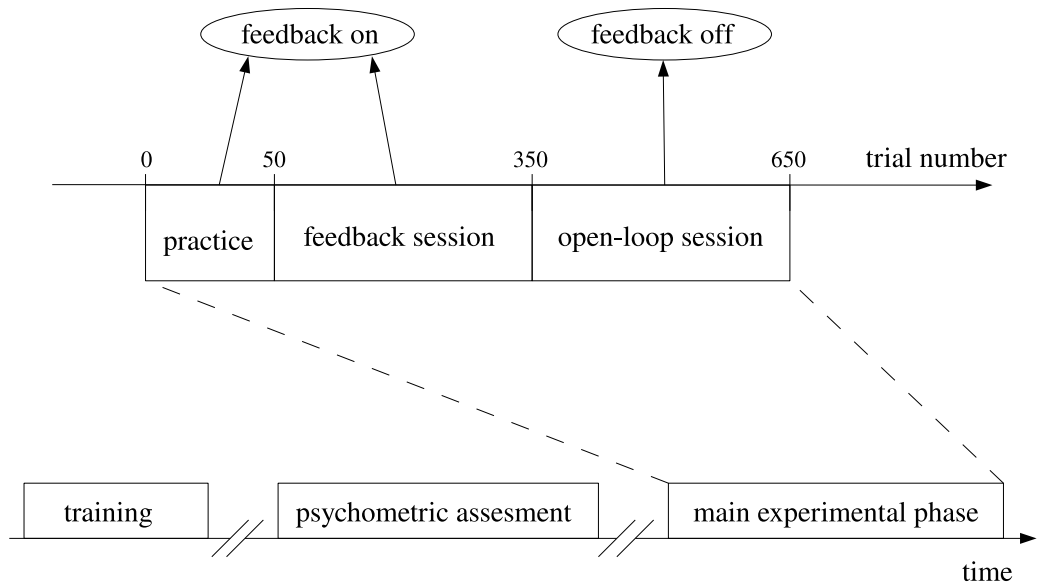


Figure 5.10: Scheme of the experimental time–line. At the end of each phase the subject took a break and received instructions for the next step. Details of the main experimental session are shematized above. Feedback was active only during the **practice** and the **feedback session**.

Sequence of stimuli

During the training phase, a sequence of 130 stimuli was presented to the subject. Each stimulus was characterized by one of 13 possible angles ϕ_i ,

$$\phi_i = \Delta\theta \cdot i \quad (5.4)$$

where $i \in [-6 : 6]$ and $\Delta\theta = 0.3^\circ$; each angle was used 10 times. The entire sequence was randomized.

Training

At the end of the *training* part, the parameters of the corresponding psy-

chometric function, assumed to be modelled by a cumulative normal distribution function, were assessed by means of the data analysis procedure described in Sec. 2.3. Evaluation of parameters μ and σ allowed the experimenter to set $\Delta\theta$ for the following session. The strategy adopted to possibly increase $\Delta\theta$ for the *psychometric assessment* phase was based on qualitative considerations: if the \mathcal{L} -surface (see Eq. (2.8)) did not show a pronounced peak in correspondence to its maximum (as in the upper part of Fig. 5.11), then $\Delta\theta$ of Eq. 5.4 was increased to 0.6° . In Fig. 5.11 two examples of \mathcal{L} -surfaces are shown: Likelihood is here defined as *joint probability*, P_{joint} . A well-defined peak is present only in the bottom plot.

*Task
difficulty*

5.4. EXPERIMENT 1

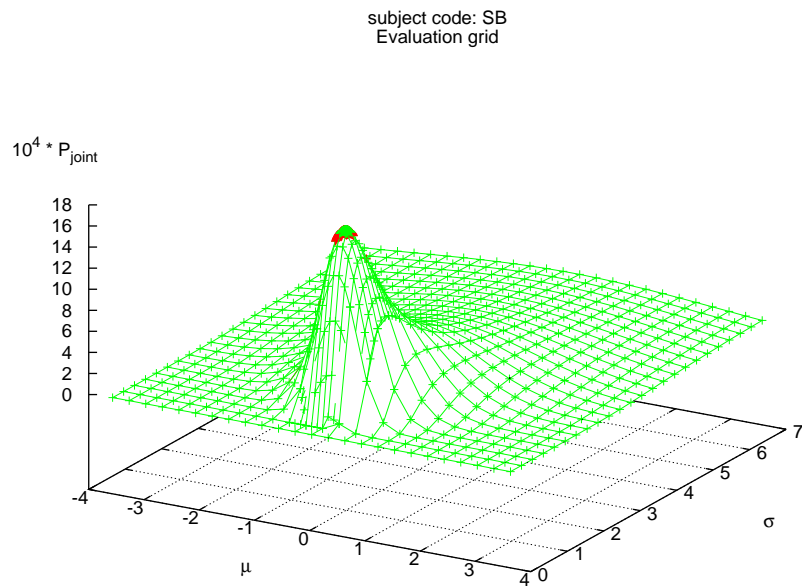
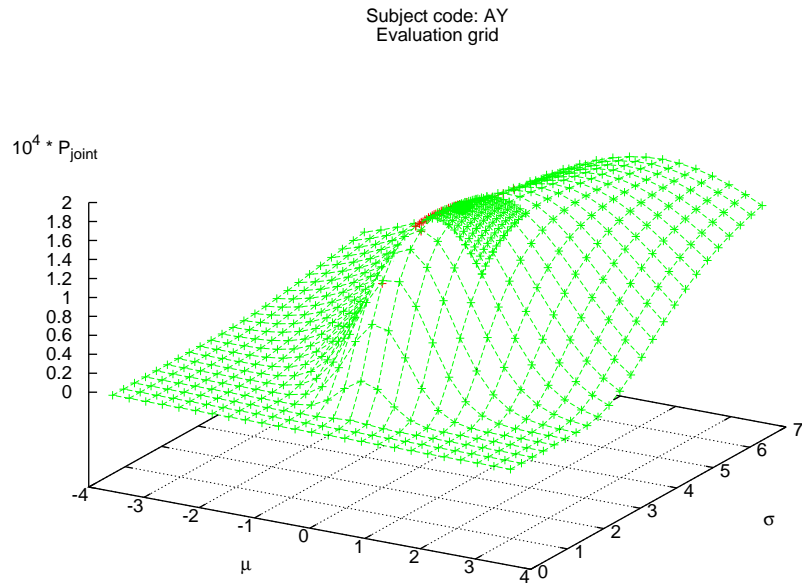


Figure 5.11: Two examples of grid of numerical values for the parameter P_{joint} as a function of both μ ($-4^\circ \leq \mu \leq 4^\circ$, step 0.4°) and σ ($0^\circ \leq \sigma \leq 7^\circ$, step 0.4°). Unlike the lower plot (subject SB), P_{joint} does not show any pronounced maximum in the upper plot. Consequently, the task difficulty in the next part (*psychometric assessment*) was reduced by increasing $\Delta\theta$ to 0.6° .

Psychometric assessment

The *psychometric assessment* phase differed from the previous one in the repetition number of each stimulus, which, in order to improve the statistical power, was presented 40 times. Also in this case, the entire sequence of stimuli was randomized before presentation. Fig. 5.12 shows an example of psychometric function: red dots correspond to the measured values for each ϕ_i , whereas the blue curve corresponds to the fit on the data, obtained by using the procedure reported in Sec. 2.3.

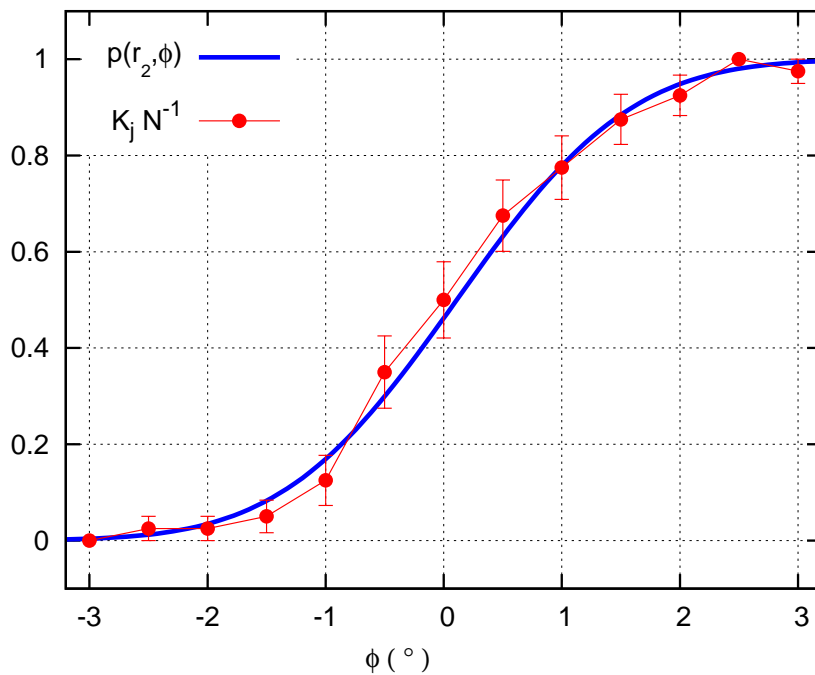


Figure 5.12: Example of psychometric function: the rate of response “right” is measured as a function of the tilting angle ϕ . In this case, the numerical values for the psychometric function parameters are $\mu = 0.1(2)^\circ$ and $\sigma = 2.2(2)^\circ$.

The mean μ – that corresponds to the perceived vertical orientation – and the standard deviation σ of the psychometric function assessed in this phase of the experimental session are used in the following, main one.

Main experimental phase

The main phase of the experimental session consisted of 650 trials divided in three sessions, named *practice*, *feedback*, and *open-loop session*, and containing 50, 300, and 300 trials, respectively. Results of the practice session

*Recorded
voice*

were not included in data analysis. Both in the practice and feedback sessions the observer was provided with a feedback relative to his/her response: during the 1500 ms blank period, a recorded voice reported whether the response was correct (*si*)“ or incorrect (*no*). The feedback was absent in the open-loop session. The average duration of the main experiment was 28(2) min, corresponding to an average time interval between two consecutive trials of 2.6(2) s.

5.4.7 Instructions

The set of slides presented to the subject, in order to provide to him/her instructions for each part of the experimental session, is reported in App. A. Subjects were carefully instructed to maximize the number of correct responses, and thus $p(c)$. In the “training” and “psychometric assessment” phases they performed a simple *left/right* discrimination task, and were preliminary instructed only about the type of stimuli (Gabor patch) and responses (“S” and “D” keys on the keyboard).

*Reference system
in
deep space*

Otherwise, an additional set of instruction was presented preliminarily to the “main experimental phase”. During this phase stimuli were modulated so as shown in Sec. 5.4.2. Then, **subjects correctly perform the task if they do not discriminate the orientation of the stimuli on the basis of their own vertical**. Aim of the additional set of instructions was to suggest the idea of rotating reference system. Subjects were requested to imagine to sit on a space ship, that is travelling in the deep space. In this situation, different “vertical orientations” are possible: the direction defined by the hearth gravitational field is not perceived by the subject. If two distinct space ships are differently oriented, their idea of verticality is consequently different.

Then, the subject is informed that his/her ship is in contact with a freely rotating space station: a recorded voice will help him/her to perceive the relative tilting angle between the ship and the station. In particular, the feedback about the correctness of the response will be based on the vertical orientation perceived by the station. His/her task is also to take in mind the orientation of the station with respect to his/her ship, and coherently respond assuming that reference system as the natural one.

In the final form subjects declared if they were able to perform the task, inclusive the use of the acoustic feedback, to rotate the axis of symmetry coherently with the imaginary space station. After the experiment completion, a set of 30 observers declared to have used the feedback. Data analysis refers to this set only.

5.4.8 Criterion modulation

During the main experimental phase, the Gabor patch of the i -th trial was tilted by an angle

$$\phi_i = \eta_i + (2s_i - 1) \cdot \theta \quad (5.5)$$

around the observer's subjective vertical orientation given by μ where s_i is randomly set to 0 (left) or 1 (right) with equal prior probability. The angle η_i corresponded to the orientation of a "pseudo-vertical" axis that harmonically oscillated with period $T = 100$ trials and amplitude $A_0 = 0.5 \sigma$:

$$\eta_i = A_0 \sin\left(\frac{2\pi i}{T}\right). \quad (5.6)$$

The angle θ was set to 0.8σ ; consequently, the parameter d' for the discrimination task was expected to remain constant at 1.6 throughout the experiment. *A posteriori*, averaging the measured d' over the entire sample of subjects provided 1.4(5) for feedback sessions and 1.4(4) for open-loop sessions.

d' is constant

The maximal excursion of the overall angle with respect to the subjective vertical orientation was $\pm 1.3 \sigma$. At this value, a linear approximation of the psychometric function yields a maximum error of 11%. Consequently, a linear relationship between the orientation of the stimulus and the corresponding neural response could be assumed.

5.4.9 Data analysis

A given experimental session was represented by the two sets $\{s_i\}$, $\{r_i\}$, representing the stimuli and response sequences, respectively. Similarly to s_i , the elements r_i were binary: an outcome 0 (1) for r_i corresponded to a left (right) observer's choice. According to SDT, an observer was modelled by a single-bit quantizer with noisy input [130]. At any given time — trial number i —, the probability H of answering right to a right-oriented Gabor patch was given by $N[(+\theta + \eta_i - \chi_i)/2\sigma]$, where $N(x) \equiv [1 + \operatorname{erf}(x)]/2$ and χ_i was the criterion used by the observer at the i -th trial. Similarly, the probability F of answering right to a left-oriented Gabor patch was given by $N[-\theta + \eta_i - \chi_i)/2\sigma]$.

Considering the feedback sessions, the maximum performance (in terms of $p(c)$) was achieved when the observer optimally set his/her criterion to η_i for each trial i . This would have required, however, an infinite bandwidth (vanishing response time) and/or infinite gain of the feedback loop. As introduced in Sec. 5.3, we assumed the simplest possible dynamics for a stable

*Model for
criterion dynamics*

Gain
&
phase

feedback system, i.e. a linear response described in the frequency domain by a single-pole, closed-loop gain function [17]. Since discrete-time events were processed, the model could be implemented within the brain as a standard low-pass digital filter [131] of the kind $y[i] = gy[i - 1] + x[i]$, where g was a gain factor and the sequences $x[i]$, $y[i]$ were proportional to a suitable error feedback variable and the difference $\chi_i - \eta_i$, respectively. Given these assumptions and the harmonic input, the expected time evolution of the criterion was $\chi_i = G \eta_{i-\tau} + C \sigma$, where τ is a delay, expressed in trials, G an amplitude gain and C an offset (normalized to σ) accounting for a possible discrepancy between the subjective vertical orientation occurring during the assessment of the psychometric function and that one occurring in the main experimental phase. An ideal observer would yield $\tau = 0$, $G = 1$, and $C = 0$.

In order to determine the three parameters τ , G and C , we used a MLE procedure acting on the two sets $\{s_i\}$, $\{r_i\}$. For a given trial i , the likelihood factor \mathcal{L}_i was given by $H^{s_i r_i} F^{(1-s_i)r_i} (1-H)^{s_i(1-r_i)} (1-F)^{(1-s_i)(1-r_i)}$, where the probabilities H and F depended on the difference $\chi_i - \eta_i$ between the instantaneous criterion and the vertical axis orientation. The three parameters were estimated by maximizing the whole likelihood $\mathcal{L} = \prod_i \mathcal{L}_i$ on a three-dimensional lattice. The error on each parameter was determined by evaluating the range on which the maximum likelihood value dropped by 5%.

5.4.10 Results

Scatter plot

The results of both the *feedback* and the *open-loop* sessions are reported in Tab. 5.2. The likelihood \mathcal{L} is reported in terms of $\mathcal{L}' \equiv \log_{10} \mathcal{L} / \mathcal{L}_r$, where $\log_{10} \mathcal{L}_r = -90.3$ is the likelihood of an ideal observer providing random responses; it can be easily shown that $\mathcal{L}_r = 2^{-N}$, where N is the number of trials; in the present case, $N = 300$. At the end of the experiment, the observer reported, separately for the two sessions, if he/she did or did not become aware of the stimuli modulation; a filled (empty) circle in each of the columns a corresponds to a positive (negative) answer.

5. FEEDBACK CONTROL OVER CRITERION SETTING

observer	feedback session				open-loop session			
	τ	G	\mathcal{L}'	a	τ	G	\mathcal{L}'	a
NM	43(6)	0.19(8)	30.7	●	23(4)	0.30(7)	26.5	○
MR	30(25)	0.06(7)	42.9	○	-2(2)	0.78(7)	28.2	○
BT	17(2)	0.66(7)	25.7	●	-17(4)	0.35(8)	26.7	○
GC	17(1)	0.98(8)	33.4	●	-47(2)	0.58(9)	39.3	○
FB	17(5)	0.26(8)	42.7	●	-45(5)	0.25(8)	26.3	●
SS	16(2)	0.51(8)	32.5	●	14(3)	0.44(8)	42.9	○
PZ	15(2)	0.57(8)	24.4	●	-36(25)	0.06(8)	23.4	○
CP	12(2)	0.49(7)	27.9	●	26(9)	0.15(8)	29.4	○
FP	7(1)	0.89(7)	13.7	●	40(3)	0.44(8)	25.9	○
CV	7(2)	0.72(7)	18.0	●	-38(6)	0.20(8)	31.3	○
DP	6(2)	0.72(7)	11.1	●	11(3)	0.38(7)	3.2	●
MP	6(2)	0.51(7)	15.7	○	-12(2)	0.66(7)	7.2	○
MA	6(2)	0.60(7)	30.2	●	-31(2)	0.62(8)	26.0	○
GF	5(4)	0.32(7)	27.7	●	43(1)	1.18(8)	32.6	○
AG	4(2)	0.55(7)	15.3	●	-25(6)	0.20(8)	34.3	○
SC	3(1)	0.85(7)	5.0	●	27(2)	0.78(7)	15.2	○
CD	3(2)	0.74(7)	21.2	●	29(3)	0.49(8)	35.6	○
IB	1(2)	0.69(7)	-1.0	●	8(1)	1.07(7)	3.9	●
EF	0(1)	0.92(7)	19.8	●	22(1)	0.87(8)	30.9	○
SB	0(3)	0.33(7)	4.6	●	-5(3)	0.42(7)	4.2	○
FD	-1(1)	1.00(7)	18.9	●	-7(3)	0.35(8)	26.9	○
ND	-1(1)	1.18(7)	20.9	●	-23(1)	0.90(7)	8.9	○
MG	-1(2)	0.62(7)	19.0	●	16(2)	0.77(7)	14.7	○
SF	-2(1)	1.24(7)	-1.4	●	38(2)	0.51(8)	11.7	○
DJ	-2(3)	0.38(7)	16.6	●	-48(2)	0.75(8)	21.3	○
FR	-3(1)	0.80(7)	20.2	●	-49(1)	0.87(8)	28.6	○
LI	-4(2)	0.66(7)	16.6	●	37(3)	0.45(8)	35.2	●
MV	-4(2)	0.64(7)	6.0	●	13(2)	0.64(7)	5.8	●
LK	-15(5)	0.24(7)	19.8	●	45(1)	0.83(8)	32.1	○
RT	-35(2)	0.60(8)	14.5	●	-17(6)	0.20(7)	23.0	●

Table 5.2: Values of the parameters τ and G estimated via MLE on the time series produced both in the feedback and the open-loop session.

5.4. EXPERIMENT 1

The measured values of τ and G are also plotted in Fig. 5.13, where red points correspond to the values obtained in the feedback session and blue points are relative to the open-loop session.

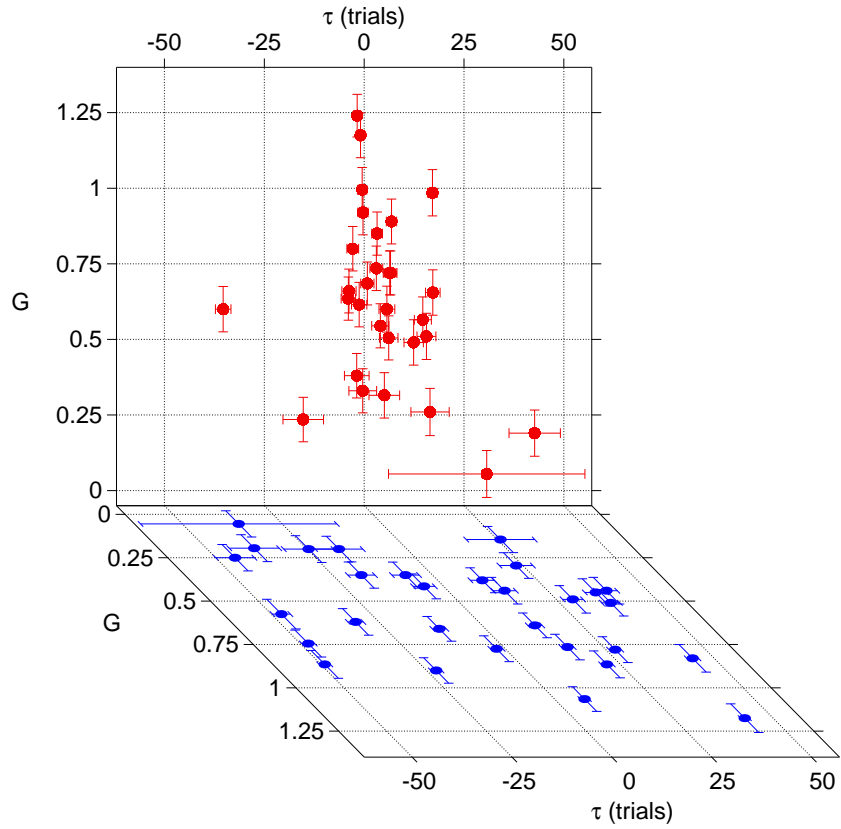


Figure 5.13: Scatter plot of parameters τ and G , plotted for each subject. The data points correspond to the data contained in Tab. 5.2.

For feedback sessions, data points lie within a well-defined region of the diagram; averaging phasors of the kind $Ge^{2\pi i\tau/T}$, each built on an observer's τ and G pair, yields the average values $\langle\tau\rangle = 4(8)$ trials and $\langle G\rangle = 0.5(4)$. On the contrary, results corresponding to open-loop sessions are decidedly scattered, showing that, on average, observers do not adapt their criteria; in this case, $\langle\tau\rangle = 30(70)$ trials and $\langle G\rangle = 0.1(4)$. Finally, the average value of offset C is equal to 0.0(1) and 0.0(3) for feedback and open-loop sessions, respectively. Negative values of τ can be accounted for as statistical fluctuations intrinsic to the MLE fitting procedure. This was verified by simulating 200 observers with $\tau = 4$ trials, $G = 0.5$, $C = 0$ and reconstructing the three parameters via a MLE procedure. Average results are $\langle G\rangle = 0.5(3)$, $C = 0.0(1)$ and, more importantly, $\tau = 4(7)$ trials.

*Effect of
feedback*

Grand-average

The grand-average of the evolution of the data relative to the entire sample of subjects shows the time-course of criterion position. In Fig. 5.24, blue lines correspond to the criterion shift predicted by the model. Red dots correspond to the criterion position determined as $-[z(H) + z(F)]/2$, where H and F were computed by averaging the responses of all observers within blocks of 5 consecutive trials. Errors are estimated by assuming binomial distributions for H and F .

The difference $\xi_i \equiv \chi_i - \eta_i$ corresponds to the instantaneous position of the criterion relative to the center of mass of the two Gaussian distributions. Thus, if the observers do not adapt their criteria, ξ is expected to oscillate with the same amplitude of η . This is confirmed by the open-loop data, where the observed oscillation amplitude for ξ , i.e. 0.52σ is consistent with the amplitude A_0 set for η , i.e. 0.5σ . Conversely, in the feedback sessions, as the observers' criterion χ tends to lock to η , we observe a reduction by a factor $\xi_{ol}/\xi_{feed} \cong 2$ in the ξ oscillation amplitude; ξ_{feed} would vanish in case of an ideal observer.

*Reduction
of ξ*

Our results show that, when the external feedback loop is closed, the brain uses the feedback information to maintain the criterion in the optimal position. On the other hand, when the external loop is open, the observer criterion χ_i is no more locked to the oscillating pseudo-vertical orientation η_i .

5.4. EXPERIMENT 1

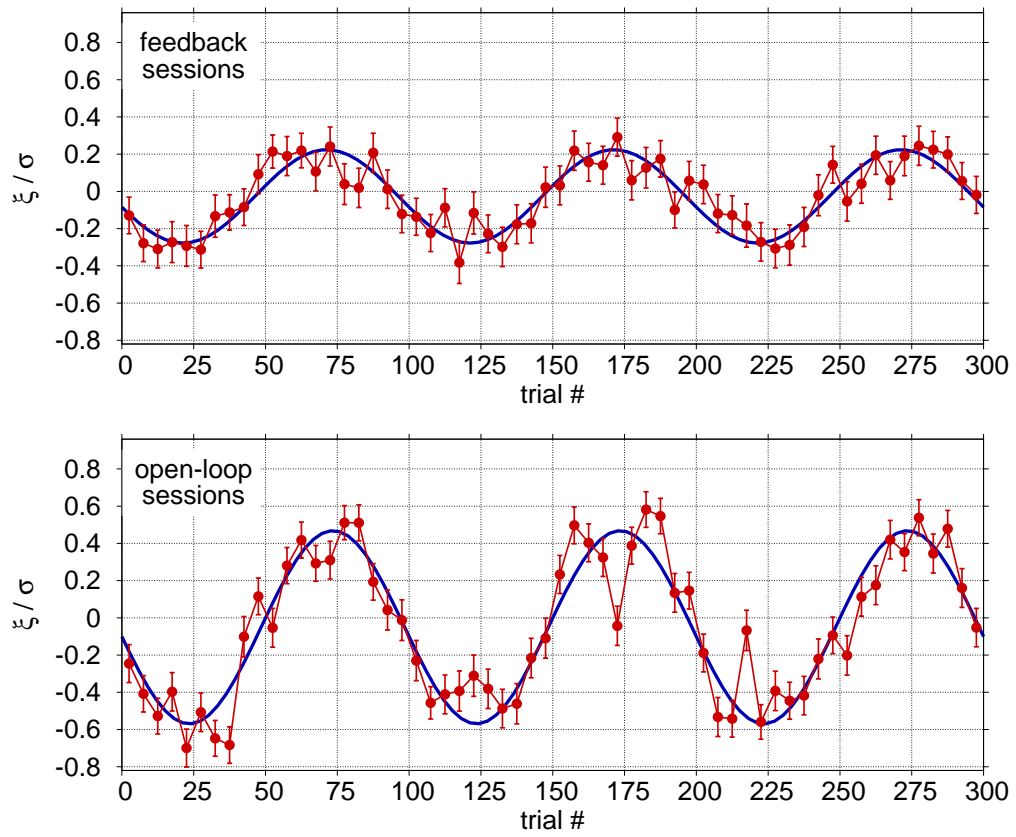


Figure 5.14: Grand-average over the entire data set. The criterion dynamics with respect to the center of mass of the stimulus-evoked distributions is shown.

5.5 Experiment 2

5.5.1 Motivations

In the previous experiment, we showed the expected behaviour for the criterion setting: subjects were able to modify their decisional strategy, and follow with a certain delay (τ) and gain factor (G), the optimal criterion position. In particular we monitored criterion oscillations induced by external modulation of the axis of symmetry relative to the two classes of stimuli.

On the other hand, the previous experimental setup did not allow the experimenter to rule out the **possibility that observed criterion shifts were caused, at least in part, by a tilting of the subject's head**. This would contradict our model, according to which the criterion position is controlled by the mechanism of Fig. 5.3, that takes place within the subject's brain. Given the experimental apparatus of Fig. 5.8 and the type of stimuli presented to the subjects, a tilting of the head, though small, could strongly influence the perceived orientation. For example, if the head is tilted to the right, the rate of response "left" would increase, and *vice versa*. Small oscillations of head position naturally occur during an experimental session.

Aim of the present experiment is to rule out the possibility that perceived vertical orientation could be accounted for by head tilting.

*Role of
the head*

We are interested in replying the previous results relative to criterion dynamics, while monitoring the head position. Head motion is analyzed in terms of frequency components and related amplitude synchronous with the oscillation of the stimuli.

5.5.2 Experimental setup

First goal of Experiment 2 is to reply the results relative to criterion dynamics presented in case of Experiment 1. Thus, many part of the experimental setup of Sec. 5.4 (in particular, the parts described in Sec. 5.4.1, Sec. 5.4.2, Sec 5.4.4, Sec. 5.4.7, Sec. 5.4.6, Sec. 5.4.8 and Sec. 5.4.9) remained unchanged.

The average duration of the main experiment was 28(3) min, corresponding to an average time interval between two consecutive trials of 2.6(2) s.

The control of head position needed some modifications of the experimental apparatus, as shown in Fig. 5.15. The main difference in comparison with the setup described in Fig. 5.8 was the presence of a system of four cameras pointing to the subject's head. Picture of Fig. 5.16 shows the placement of the cameras.

The orientation of the head was monitored by using a *Qualisys Motion Capture System* (QMCS), consisting in a set of *ProReflex MCU1000* cameras

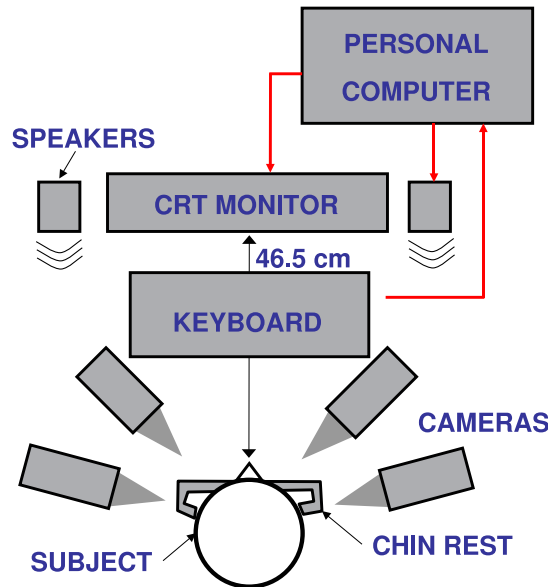


Figure 5.15: Experimental setup for Experiment 2: four cameras were added, with respect to the setup shown in Fig. 5.8, in order to monitor the head position.

*Qualisys
Motion Capture
System (QMCS)*

(maximal measurement frequency: 1000 Hz) based on low-noise, high-speed CCD sensors. Each camera was equipped with an infrared light source. Part of the light emitted by these sources was reflected back to the cameras by low-mass, retro-reflective targets, or *markers*, (see Fig. 5.17).

The effective number of pixels for each camera was 20,000 x 15,000, which corresponded to a spatial resolution as small as 50 μm . Sampling frequency was set to 20 Hz (20 sample/sec).

*Position
of the markers*

The system used the reflected light to calculate the position in space of each single target. Two markers were placed on the subject's head at eyebrow height and fixed with adhesive tape. The system monitored the position of both the two targets during the three phase (practice, psychometric assessment and main session – see Sec. 5.4.6 –) of each experimental session. We monitored the position along the x , y and z axes for both markers. The position of each marker was evaluated with respect to a well-known reference system, that was set through a preliminary calibration step [132].

The QMC system was controlled by a home-made C++ program: the program triggered the acquisition of the marker position at the start of the first trial of each session; moreover, the program stored the time at which the response was given by the subject with a millisecond resolution. In this

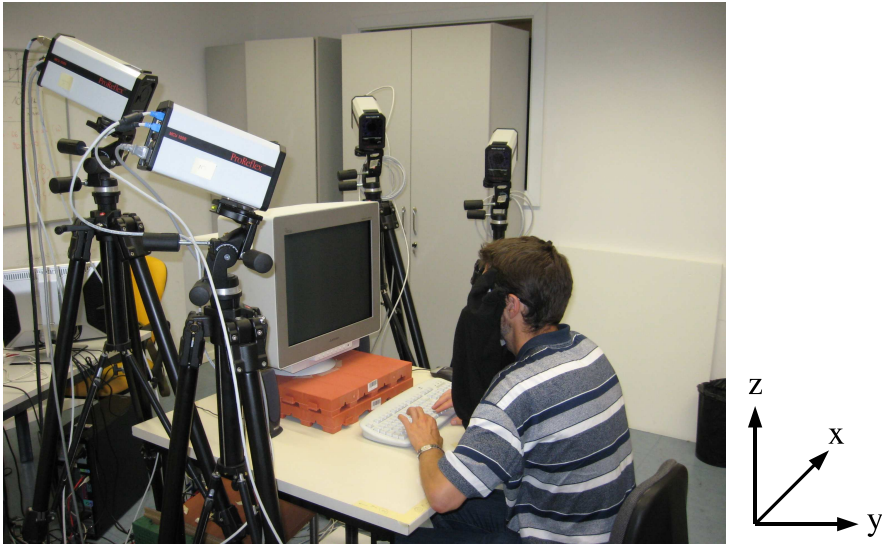


Figure 5.16: Experimental apparatus. Orientation of the axes are reported in the bottom-right corner.

way, the file on which the QMC system wrote the marker position and the file produced by the C++ program and containing the responses, and the related timing are synchronized.

Then, for each trial, an home-made Tcl script computed the tilting angle of the head with respect to the vertical orientation as follows:

*Tilting angle
of the head*

$$\phi_i = \text{atan} \left(\frac{|\langle z_1 \rangle_i - \langle z_2 \rangle_i|}{\sqrt{(\langle x_1 \rangle_i - \langle x_2 \rangle_i)^2 + (\langle y_1 \rangle_i - \langle y_2 \rangle_i)^2}} \right) \quad (5.7)$$

where “1” and “2” corresponded to the two markers, and $\langle x \rangle_i$, $\langle y \rangle_i$, $\langle z \rangle_i$ are the component of the marker position averaged over the time window relative to the duration⁴ of each i-th trial.

5.5.3 Subjects

A set of 32 observers (18 males and 14 females) participated. All were students or staff members of the University of Trento, aged 19 to 40 (mean 26, standard deviation 6), and reported normal or corrected-to-normal visual acuity. Prior to the experiment, each observer declared to know nothing about the experimental procedure and aim. As in Experiment 1, preliminary

⁴With duration of a single trial we mean the interval of time between two subsequent stimuli presentations



Figure 5.17: Marker used to monitor head position.

and final declarations were collected by filling two distinct, *ad-hoc* made forms. Finally, after the experiment completion, a set of 30 observers declared to have used the feedback. The ensuing analysis refers to this set only.

5.5.4 Results

Data analysis was divided in two parts: in the first part we focused our attention to head motion, performing a spectral analysis. Then, we analyzed the data relative to the criterion dynamics with the same procedures described in Sec. 5.4.9.

Head motion

Aim of the analysis relative to the sequences of the tilting angle, ϕ_i , computed according to Eq. (5.7), was to rule out the possibility that an oscillation of the subject's head occurred coherently with the stimuli modulation and thus masked the internal criterion shift.

At the beginning of the measurement session, subjects were explicitly requested to not move the head and, in particular to not tilt it with respect to the vertical. Nevertheless, small oscillations occurred, typically within a range of few degrees: an example of plot of the tilting angle (subject DD) as a function of the trial number is shown in Fig. 5.18.

A *FFT* (*Fast Fourier Transform*) analysis was carried out for each subject. As an example, the frequency spectrum for each of the three phases for subject DD is reported in Fig. 5.19.

No significant peak is – on average – present at the crucial frequency of 3 periods per session, corresponding to the stimuli modulation: in fact the total number of trials presented to the subject during both the *feedback* and the *open-loop* is 300 whereas the period T is equal to 100 trials.

*Fast Fourier
Transform (FFT)*

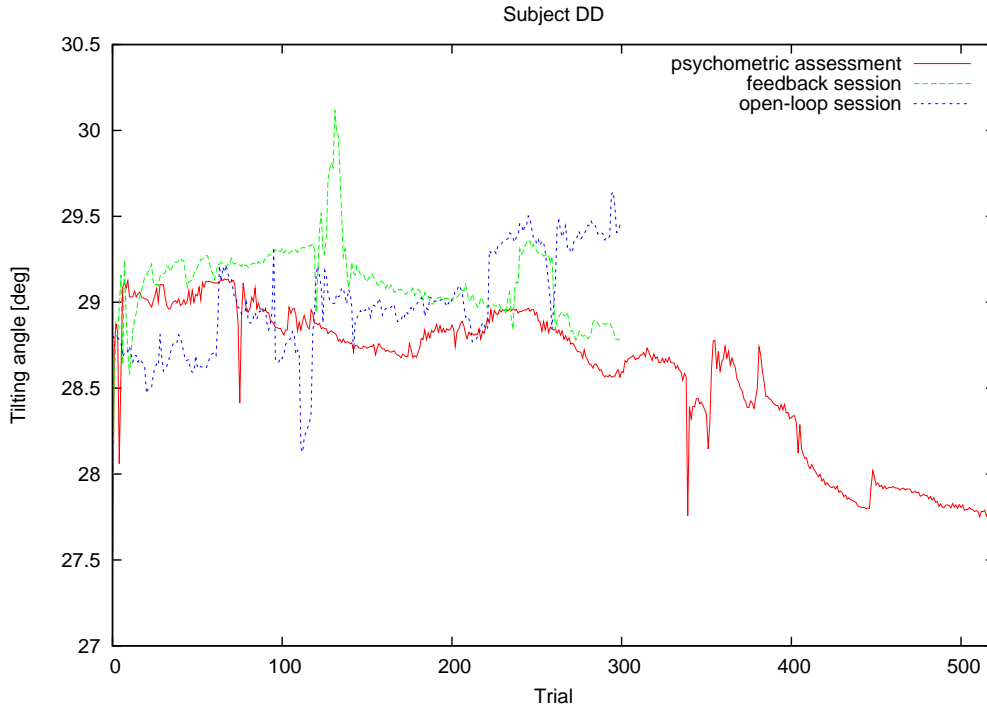


Figure 5.18: Head's tilting angle, expressed in degrees, as a function of trial number for subject *DD*.

In order to reduce the fluctuations, we averaged the results of the entire set of subjects. The resulting frequency spectra are shown in Fig. 5.20. Again, the frequency spectrum did not show any peak for the amplitude at the component at 3 period/session.

We modelled the profiles reported in Fig. 5.20 by means of a superimposition of white noise (i.e. with uniform frequency spectrum), and $1/f$ noise:

*Fit of
the noise*

$$A(f) = \frac{K}{f} + c \quad (5.8)$$

where A is the amplitude of the component at the frequency f , whereas K and c represent the magnitude of the $1/f$ and white noise component, respectively. Numerical value of the fits for the three experimental phases are reported in Tab. 5.3.

Further investigations on head motion, aimed to provide a model for the observed noise spectral behaviour are out of the scope of this work.

In conclusion we can assert that the head motion does not influence the observed dynamics of the criterion, and that this occurs **within** the subject's brain.

5.5. EXPERIMENT 2

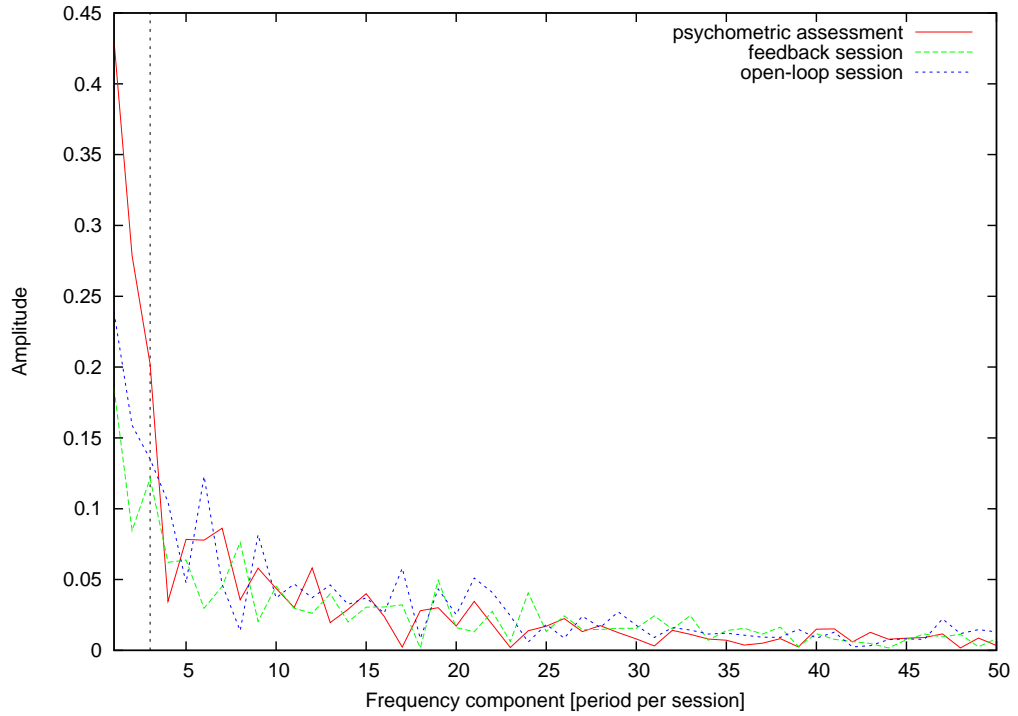


Figure 5.19: Frequency spectrum of the data shown in Fig. 5.18: for the sake of clarity, we report only the amplitude of the components within the range [1:50] (periods per session). The dashed line corresponds to the frequency of 3 periods per session, used in the stimuli modulation.

phase	K	c	χ^2
psychometric assessment	0.209(3)	-0.003(3)	$9.9 \cdot 10^{-6}$
feedback	0.54(2)	-0.012(2)	$4.9 \cdot 10^{-4}$
open-loop	0.100(3)	-0.0020(3)	$1.3 \cdot 10^{-5}$

Table 5.3: Values of the parameters K and c of Eq. (5.8).

5. FEEDBACK CONTROL OVER CRITERION SETTING

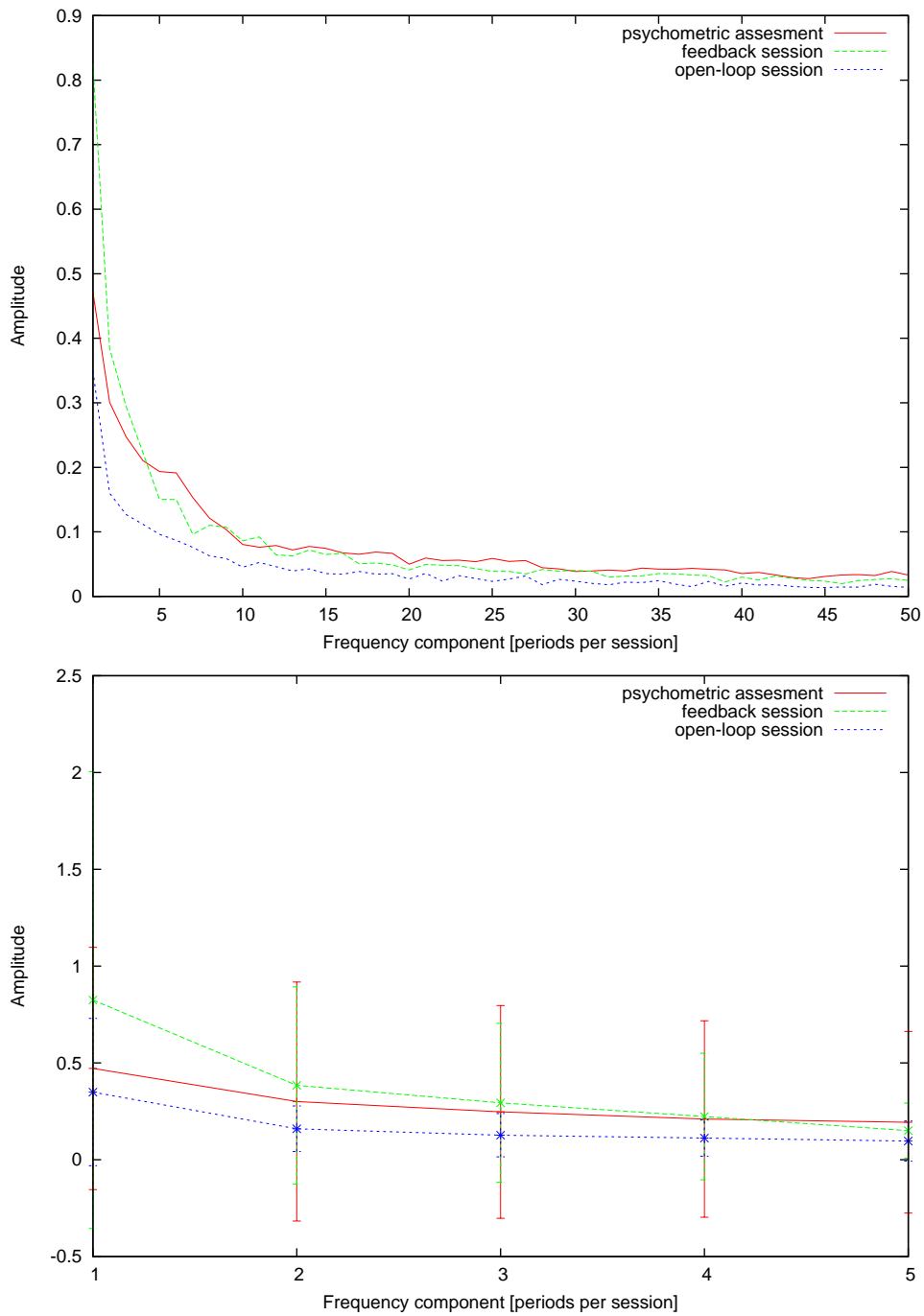


Figure 5.20: FFT spectrum of head motion averaged over the entire sample of subjects: in the upper plot, the range considered for the number of *periods per session* is [1:50]; whereas, in the lower plot the range is reduced to [1:5]. For the sake of clarity, error bars, computed as standard deviation of the results relative to the 30 subjects, were reported only in the lower plot.

Criterion dynamics

Similarly to the previous experiment, we report the numerical values of the parameters τ and G resulting by the fits on the data of Experiment 2 in Tab. 5.4 and in Fig. 5.21. The shown data refer to the 30 subjects that reported to have used the feedback information at the end of the experimental session are considered.

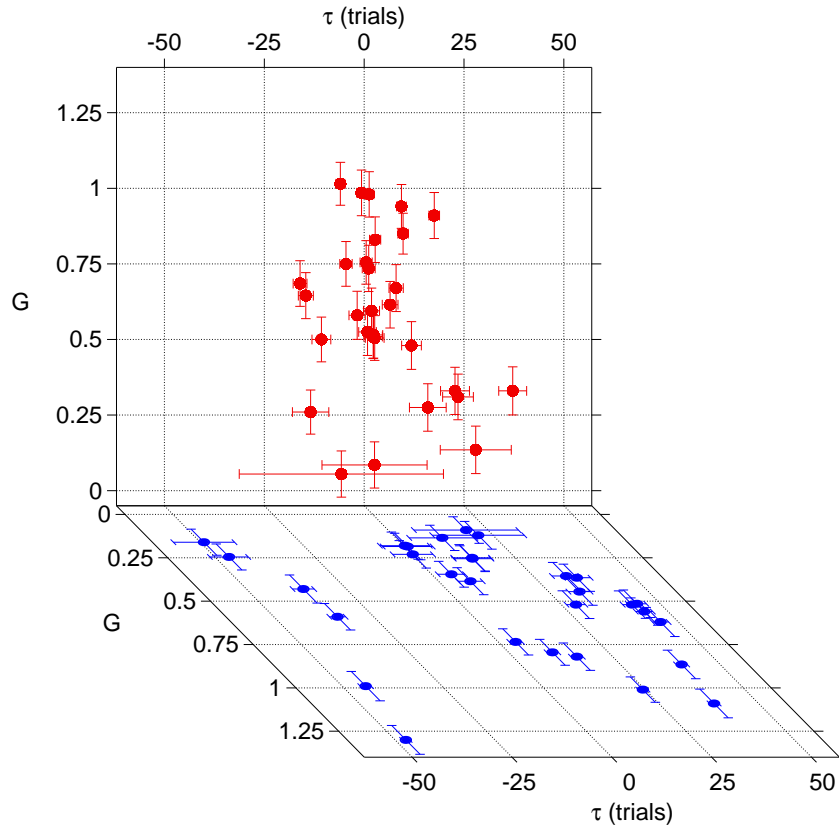


Figure 5.21: Scatter plot of the parameters τ and G , both for the feedback (upper diagram, red circles) and open-loop (lower diagram, blue circles) sessions.

*Effect of
the feedback*

As in Experiment 1, data show a cluster in a restricted range of values for the parameter τ in case of feedback session (red points); results of open-loop sessions show a more scattered behaviour. From a quantita-

5. FEEDBACK CONTROL OVER CRITERION SETTING

tive point of view, the angular mean on the phasors (computed as in Experiment 1) provides $\tau_{feedback} = 3(10)$ and $G_{feedback} = 0.5(3)$, as well as $\tau_{open-loop} = 33(26)$ and $G_{open-loop} = 0.2(4)$. With regard to the offset parameter, $C_{feedback} = C_{open-loop} = -0.1(2)$.

The damping effect for the parameter ξ , was observed also for this new set of data. Fig. 5.22 shows the average of the criterion shift dynamics over the entire sample of subjects. As in Fig. 5.14, the blue lines represent the time evolution of ξ predicted via the model; the red dots represent the criterion positions measured, according to SDT, as $-[z(H) + z(F)]/2$; the rates H and F are computed by averaging the responses of all observers within 60 blocks of 5 consecutive trials.

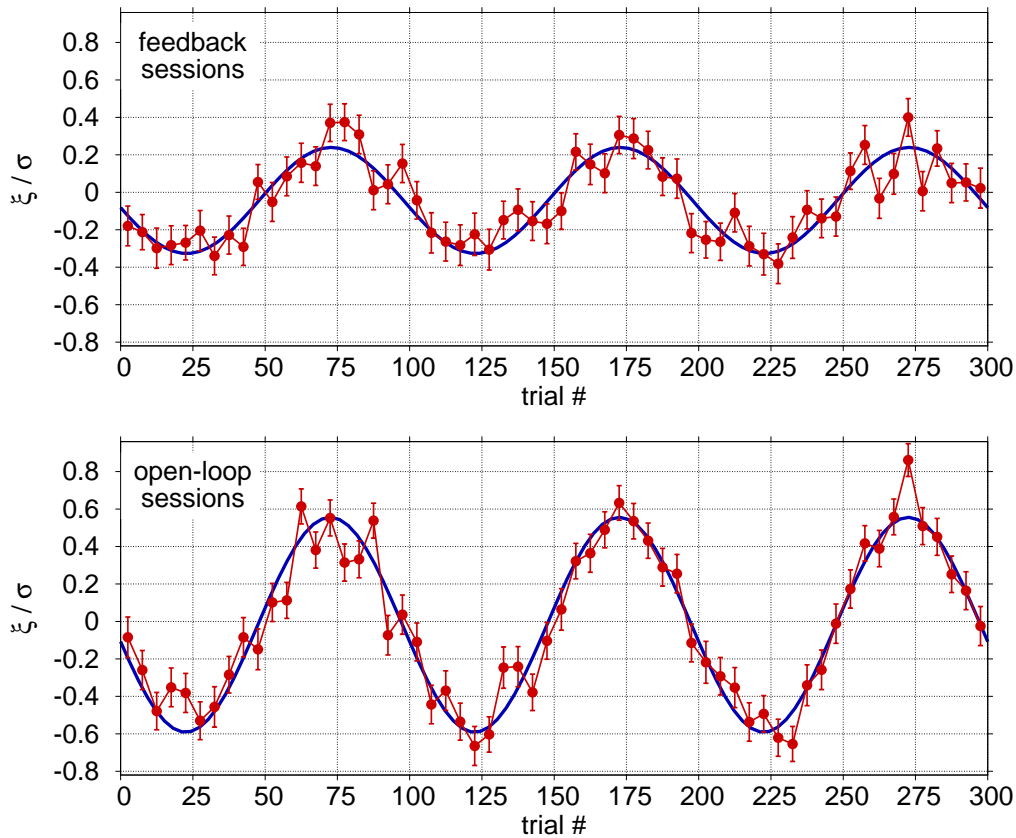


Figure 5.22: Grand-average of the set of data of Experiment 2.

Similarly to the results of Sec. 5.4.10, it is $\xi_{ol}/\xi_{feed} \cong 2$.

5.5. EXPERIMENT 2

observer	feedback session				open-loop session			
	τ	G	\mathcal{L}'	a	τ	G	\mathcal{L}'	a
FD	37(3)	0.33(8)	28.7	●	29(2)	0.52(8)	30.9	●
AD	28(9)	0.14(8)	36.2	●	0(6)	0.18(8)	22.3	○
AS	24(4)	0.31(8)	18.6	○	1(6)	0.19(8)	22.6	○
BG	23(4)	0.33(8)	32.5	●	40(1)	0.87(8)	28.8	●
DB	18(1)	0.91(8)	24.3	●	12(8)	0.14(7)	4.3	●
AD	16(5)	0.28(8)	28.2	○	43(2)	0.52(8)	23.6	○
MG	12(2)	0.48(8)	33.4	●	8(3)	0.39(8)	37.3	●
AB	10(1)	0.85(7)	-26.3	●	5(3)	0.35(7)	24.4	○
GL	9(1)	0.94(7)	4.7	●	-44(1)	0.99(8)	39.1	○
DD	8(2)	0.67(8)	22.9	●	-36(3)	0.43(8)	24.3	○
AY	7(2)	0.62(8)	28.9	●	20(13)	0.09(8)	30.1	●
MF	3(13)	0.09(8)	21.4	●	14(5)	0.25(8)	24.1	○
ST	3(1)	0.83(8)	14.5	●	4(2)	0.74(8)	22.4	○
FO	3(2)	0.51(7)	18.1	●	39(1)	1.09(8)	36.1	●
GG	2(2)	0.52(8)	20.3	●	46(2)	0.62(8)	28.6	○
SB	2(2)	0.60(8)	28.7	●	33(3)	0.45(8)	33.9	●
FF	2(2)	0.51(7)	11.5	●	14(5)	0.26(7)	21.4	●
LF	1(2)	0.53(8)	26.9	●	11(1)	0.80(7)	19.8	●
EV	1(2)	0.74(8)	30.1	●	36(3)	0.37(8)	31.2	○
KR	1(2)	0.76(7)	4.7	●	44(2)	0.56(8)	23.4	○
FD	1(1)	0.98(8)	11.6	●	36(1)	1.15(8)	24.3	○
CP	-1(1)	0.99(8)	17.5	●	16(1)	0.82(8)	24.8	●
NS	-2(2)	0.58(8)	36.2	●	21(12)	0.12(8)	38.5	○
AP	-5(2)	0.75(7)	17.9	●	-49(8)	0.16(8)	17.8	○
AK	-6(26)	0.06(8)	32.6	●	0(5)	0.23(8)	35.8	●
PR	-6(1)	1.02(7)	-8	●	24(1)	1.01(7)	-4.0	●
AV	-11(2)	0.50(7)	19.7	●	-34(2)	0.59(8)	26.4	○
SB	-13(5)	0.26(7)	5.8	●	-46(5)	0.25(8)	15.9	●
SS	-15(2)	0.65(8)	34.9	○	33(4)	0.36(8)	41.4	○
MT	-16(2)	0.69(8)	20.6	●	44(2)	0.52(8)	22.3	○

Table 5.4: Values of the parameters τ and G for each single subject. As in Tab. 5.2, filled (empty) circle in each of the columns a corresponds to the subject's awareness (unawareness) of the stimuli modulation.

5.6 Merging of the Experiments 1 and 2

In the present section we merge the data of Experiment 1 with those of Experiment 2. Experiment 2, described in Sec. 5.5 differed from Experiment 1 of Sec. 5.4 because of the additional control on head motion. With except to the head motion tracking system, the two experimental setups were equal. In particular, the time evolution of the optimal criterion position was imposed to be sinusoidal with a period $T = 100$ trials in both experiments. As for each of the two experiments, we collect the results of all the 60 data sets. All the (τ, G) pairs are plotted in Fig. 5.23.

As in Fig 5.13 and Fig 5.21, the effect of the feedback on criterion dynamics is clearly visible in the clustering of the data (red dots) in a restricted area, unlike the open-loop sessions, where they show a completely scattered behaviour.

*Effect of
the feedback*

Similarly to the analysis presented in the previous cases, a *grand average* with time resolution of 5 trials was computed for the entire set of 60 subjects. The result is shown in Fig. 5.24.

As expected, the amplitude of the oscillation in the open-loop session is higher than in the feedback session. Again, $\xi_{ol}/\xi_{feed} \cong 2$.

5.6. MERGING OF THE TWO EXPERIMENTS

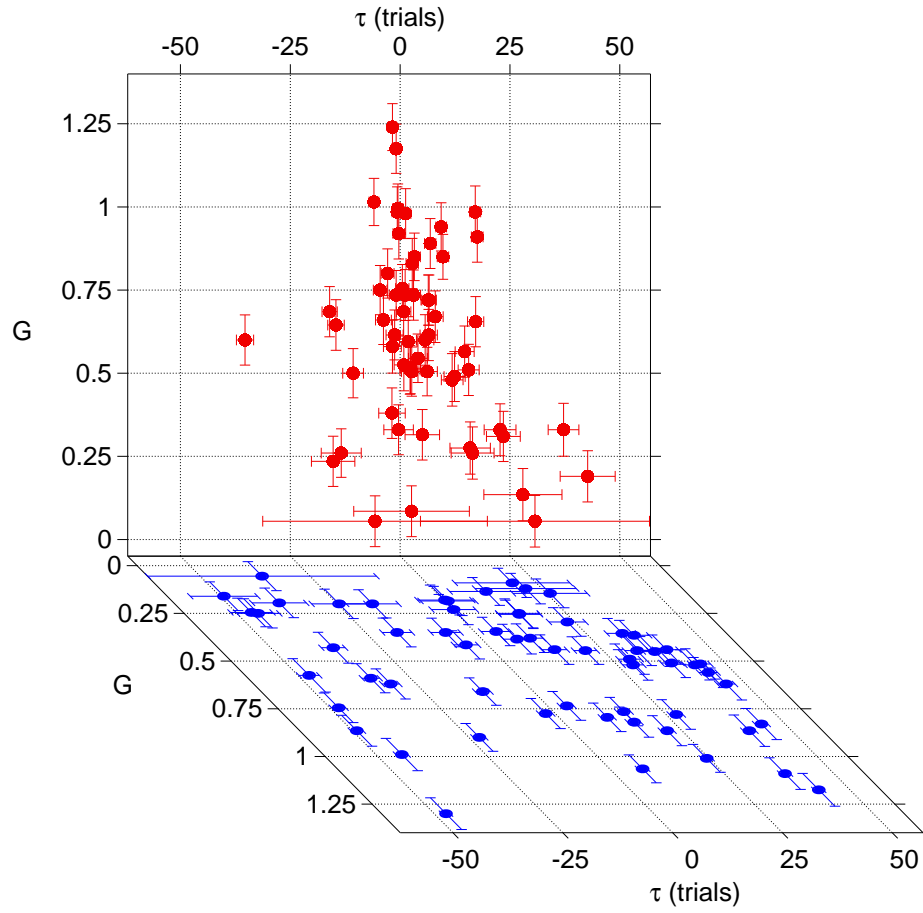


Figure 5.23: Scatter plot of the parameters τ and G , both for the feedback (upper diagram, red circles) and the open-loop (lower diagram, blue circles) sessions. Data are collected from both Experiments 1 and 2.

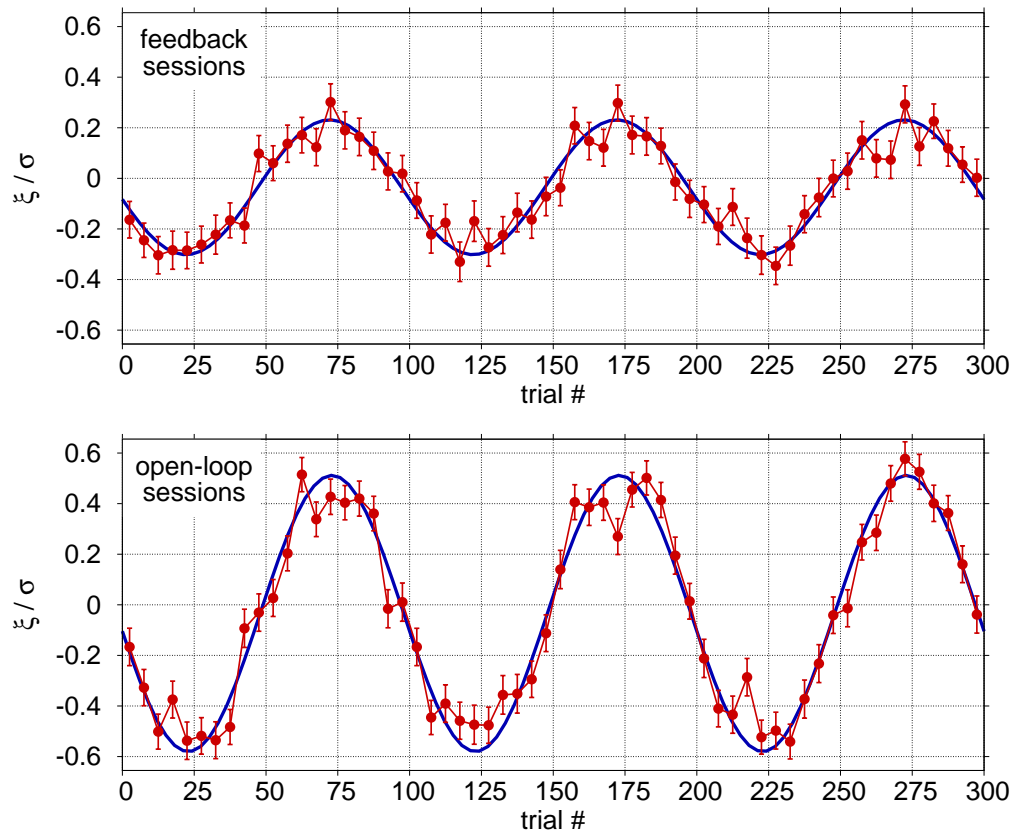


Figure 5.24: Criterion dynamics averaged over the entire sample of 60 subjects in the feedback and the open-loop case.

5.7 Non-linear components of criterion dynamics

In this section, we introduce an additional analysis on the data of each subject evaluated in Experiment 1 (Sec. 5.4) and Experiment 2 (Sec. 5.5). The aim is to evaluate the goodness of the model formulated in Eq. 5.2.

A single-pole, closed-loop gain function is mathematically expressed by an output of the system (the criterion position, in our case) that oscillates at the same frequency as the input modulation ω_0 ($= \frac{2\pi}{T}$), though with different amplitude G and phase τ . Additional frequency components of period $T^* \neq T$ were then excluded from the analysis described so far.

*Additional
frequency
components*

On the other hand, it is also possible that the model of Eq. 5.2 does not properly describe the mechanism of criterion setting: additional components of its dynamics like, for example, a slow drift of criterion position or fluctuations independent from the feedback loop, could play a role. Moreover, non-linear contributions to the dynamics could result in frequency components, i.e. periods different from those characterizing the stimuli modulation.

To explore this possibility, each data set was analyzed with the same analysis technique described in Sec. 5.4.9, by letting, however, the parameter T^* vary from $T_{min} = 80$ trials to $T_{max} = 120$ trials with a resolution of $\delta T = 2$ trials. $\mathcal{L}(T^*)$ values were computed for each of the 60 subjects; if our model robustly interpret the data, a maximum of $\mathcal{L}(T)$ should occur at $T = 100$ trials.

Fig. 5.25 show, for two subjects (MT and EF), a maximum of \mathcal{L} in correspondence to $T = 100$. In Fig. 5.26, the maximum is shifted by $\Delta T = +2$ trials for subject GB and $\Delta T = -8$ trials for subject AB. Two examples of critical results, representing the case in which $\mathcal{L}(T)$ spectra do not show a well-defined peak in the range of possible T value are reported in Fig. 5.27.

5. FEEDBACK CONTROL OVER CRITERION SETTING

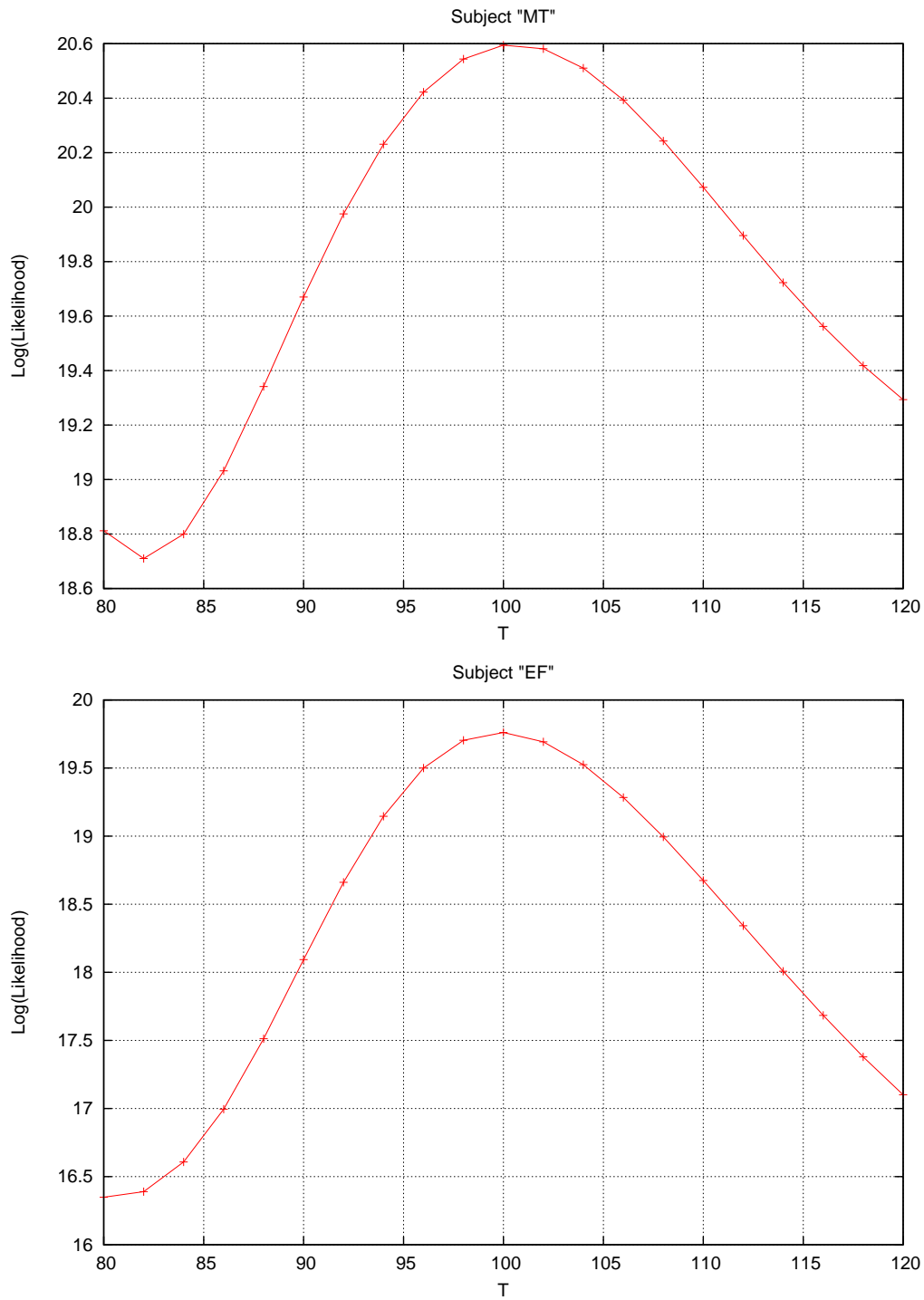


Figure 5.25: $\mathcal{L}(T)$ spectra, relative to two different subjects, showing a maximum in correspondence of a period $T_{max} = 100$ trials.

5.7. NON-LINEAR COMPONENTS OF CRITERION DYNAMICS

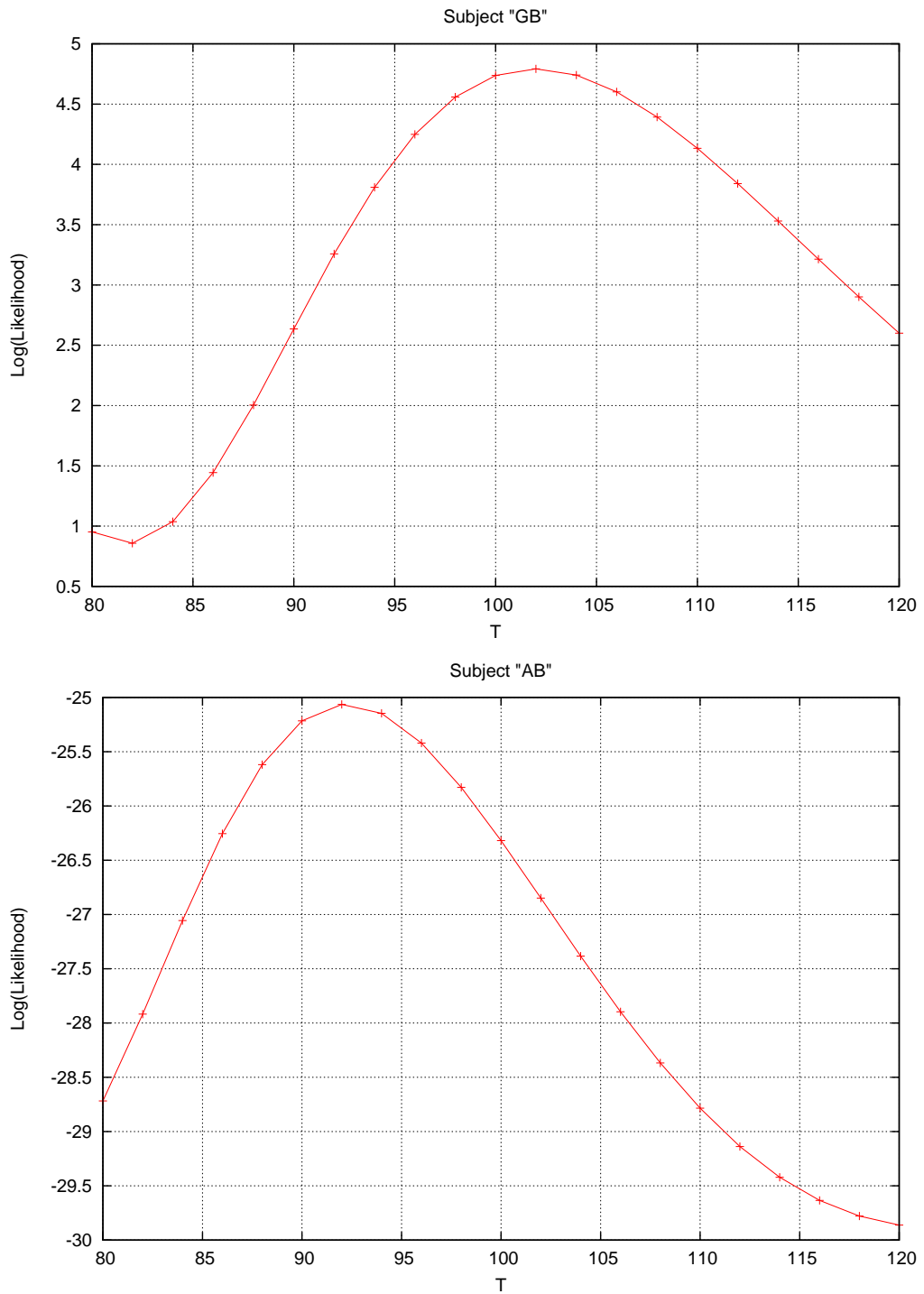


Figure 5.26: The upper $\mathcal{L}(T)$ profile (subject GB) shows a maximum in correspondence of $T_{max} = 102$ trials, whereas, for subject AB, $\mathcal{L}_{max}(T)$ is in correspondence of $T_{max} = 92$ trials.

5. FEEDBACK CONTROL OVER CRITERION SETTING

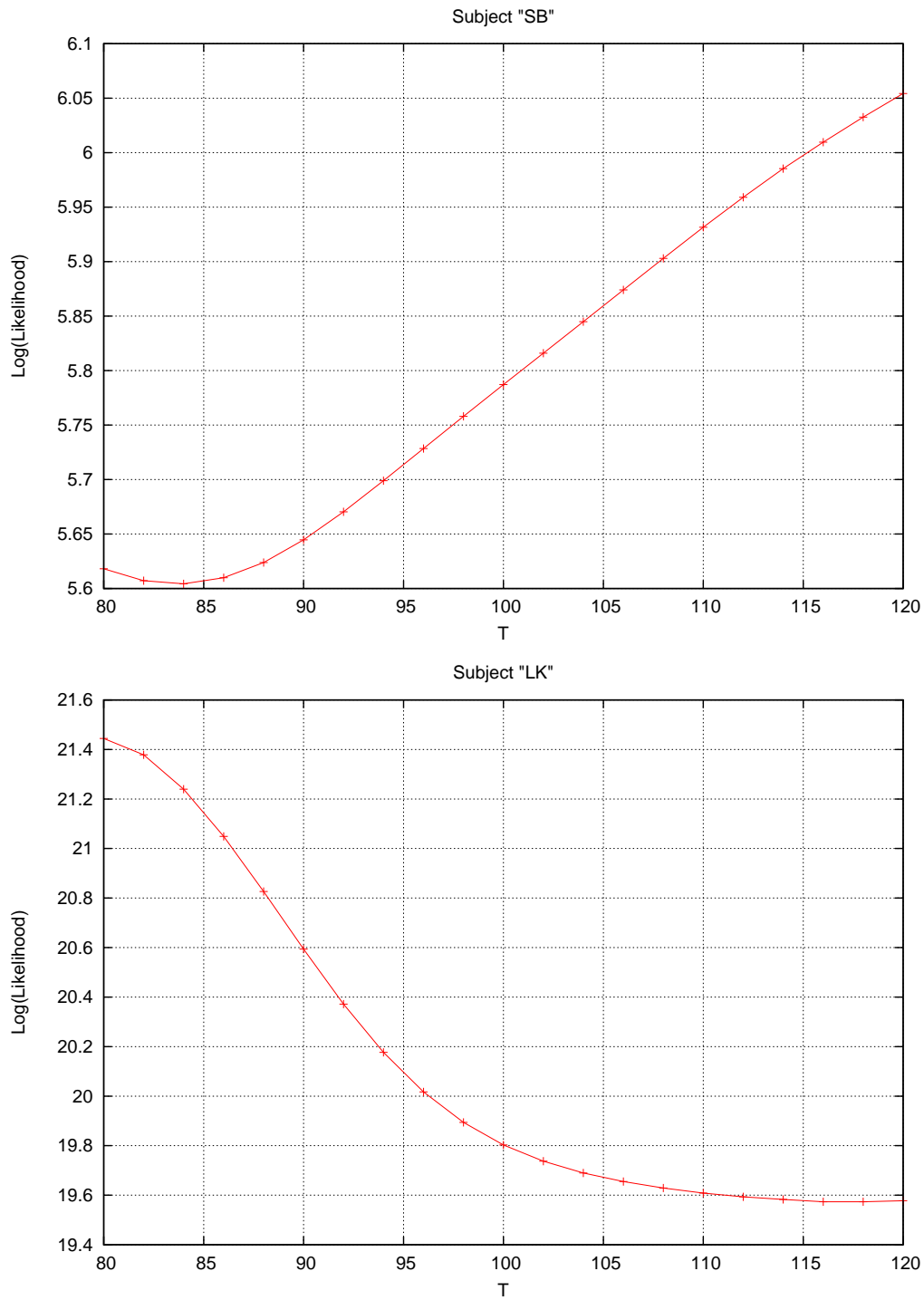


Figure 5.27: $\mathcal{L}(T)$ profiles for subjects SB and LK. No well-defined maxima, in the range of T-values considered in our analysis, are present.

In addition, we computed $\mathcal{L}(T)$ spectra also for the *open-loop session* of each subject. Then, we focussed our attention to the spectra of the types of Figg. 5.25 and 5.26. Subjects that showed a behaviour similar to Fig. 5.27, i.e. without a pronounced peak in the range $T_{min} \leq T \leq T_{max}$, were not considered for the rest of the analysis procedure. For this reason, the number of experimental sessions was reduced from 60 to 51.

5.7.1 Results

Thus, we averaged T^* values over data set of the resting 51 elements. Results for $\langle T^* \rangle$ are 99(9) and 100(18) trials, for feedback and open-loop sessions, respectively. These results induced two possible considerations: because both $\langle T^* \rangle_{feedback}$ and $\langle T^* \rangle_{open-loop}$ were compatible with the expected value $T^* = 100$ trials, then the model of Eq. 5.2 robustly describe the criterion dynamics so as imposed in our experiment.

*Our model
is robust*

In addition to that, error values on $\langle T_{max} \rangle$, computed as standard deviation over the entire data set, confirm the effect of feedback. An increased standard deviation in open-loop sessions ($\sigma_{feedback} \cong 0.5 \cdot \sigma_{open-loop}$) is expected: the model expressed by Eq. 5.2 correctly represent the criterion dynamics only if the feedback loop is active.

Scatter plot

The effect of feedback on criterion dynamics can be observed in Fig. 5.28: as usual, data represent (τ, G) couples. Fig. 5.28 shows τ and G values, for feedback (red dots) and open-loop (blue dots) sessions, obtained from a MLE procedure (so as in Sec. 5.4.9) with $T = T^*$.

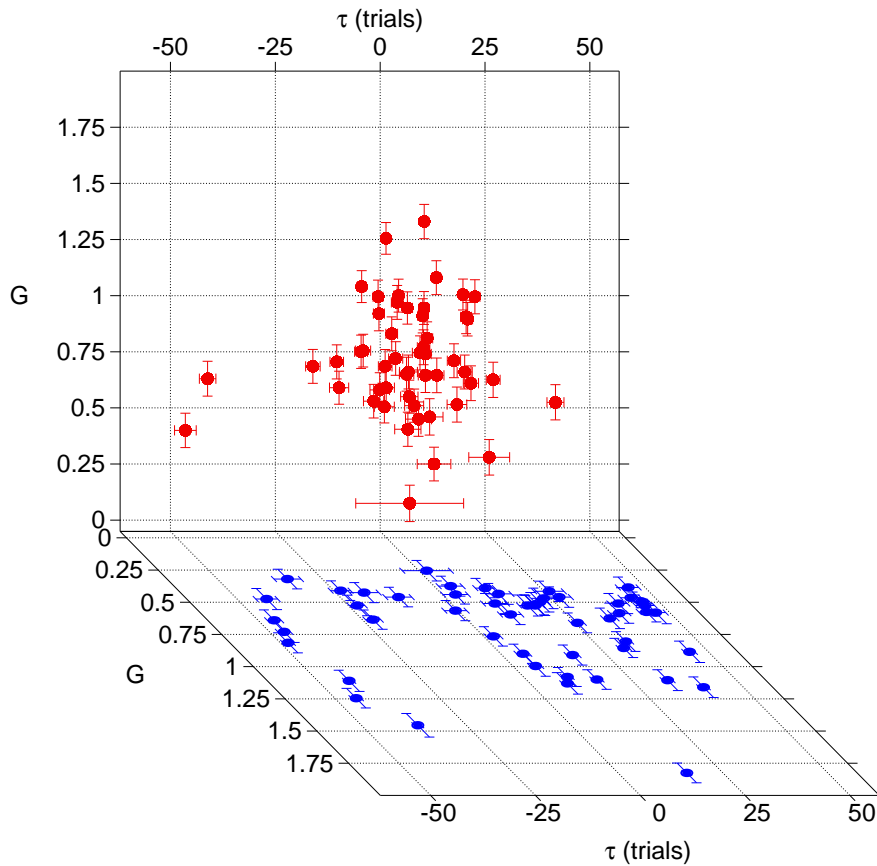


Figure 5.28: Scatter plot of the G and τ values obtained by maximizing the likelihood \mathcal{L} also with respect to the parameter T .

As in the previous similar plot of Fig. 5.23, data of feedback sessions show a clustered behaviour, whereas blue dots result more scattered. Average values for parameters G and τ are $G = 0.6(4)$ and $\tau = 8(10)$ trials for

*Effect of
feedback*

feedback sessions and $G = 0.2(5)$ and $\tau = 28(40)$ trials for open-loop sessions. Offset parameter results $C_{feedback} = -0.1(2)$ and $C_{open-loop} = -0.1(6)$. These values confirm the effect of feedback on criterion dynamics.

5.8 Final discussion

We reported a model for dynamics of criterion setting relying on strong physical bases and a method to test it with the highest possible time-resolution. Predictions of the model can be summarized as follows: when the optimal criterion position is shifted and forced to oscillate at a well-known frequency, set a-priori by the experimenter, subjects are able to follow this oscillation, though with a certain phase-delay. They change their criterion at each trial, if motivated to increase the rate of correct responses.

The proposed model reliably accounts for the criterion setting dynamics, at least for the visual feature (orientation) tested here: single-pole, closed-loop gain function is the simplest choice to achieve stable control.

A possible interpretation for the subject ability to shift the criterion, adapting his/her behaviour strategy to the new external conditions, is learning. With learning we mean an improvement of subject performance driven by information about his/her previous responses. Thus, it involves the subject's motivation to improve his/her ability and the possibility to store information from previous experience. In terms of *SDT*, an improvement of subject's ability to perform specific tasks, is usually referred to in the literature as an increase of sensitivity (d') [133].

Results presented in this chapter are d' independent, i.e. the subject sensitivity to the task remains constant during each experimental session. Only criterion evolve in time, on the basis of a mechanisms involving both memory of previous trials and the subject's willing of increase the rate of correct answer and also the performance. In this way, subjects continuously learn to set their criterion to the optimal position.

Our results provide a starting point for further investigation on the encoding of criterion within the brain, for example addressing the dependence of the closed-loop gain function parameters on quantities such as d' or the amplitude or frequency of the external modulation.

Part III
General Discussion

Chapter 6

Conclusions

In the emerging field of neuroscience many topics are characterized by strong crossdisciplinarity. It frequently occurs that, contributes and approaches from different research areas converge to tackle specific issues of actual interest, sometimes providing novel investigation tools. An important example of interdisciplinary topic, representing the *trait d'union* of our investigations, is noise. Whatever the physical system under investigation, noise is present as a stochastic fluctuation of the measured signal. Theoretical considerations, as well as a robust experimental evidence, substantiate its ubiquitous nature.

The occurrence of noisy processes, although not yet exhaustively investigated, has been also observed in many brain mechanisms. For example, stochastic fluctuations of the spike's rate make impossible to predict the exact neuronal behaviour.

*Noise in
human brain*

Our work was devoted to gain insight into the problem of noise in perceptual processes in humans by using psychophysical methods. We developed two types of behavioural experiments in order to shed light on two distinct aspects of the issue: the first part of our work was focused on the question whether **exogenous noise superimposed to a stimulus changes perception of the stimulus itself**. In particular, we focused our attention to the occurrence, in the acoustic perceptual modality, of an effect referred to in the literature as *stochastic resonance*. Depending on noise intensity three different effects were observed. For low intensities, the signal perception is not affected by the presence of superimposed noise. Conversely, if noise intensity overcomes a critical value, the subjective perceptual threshold is shifted progressively to higher values. This is the so-called masking effect, that is widely experienced also in real life.

In an intermediate range of intensities, closed to the noise critical value, it has been observed the opposite effect. **Detection ability is improved by**

*Noise improves
acoustic
perception*

the presence of noise. This was interpreted as an evidence of stochastic resonance in human acoustic perceptual system.

Although this effect was previously observed – as described in several works – we obtained results that, from the statistical point of view, are more robust. Our new data analysis procedure, opens the possibility to investigate the effect also with other kinds of experiments like, for example, cochlear implant recipients or subjects with deafness problems. In these particular cases, a gain in acoustic perception would be of coarse significant.

Our second field of investigation concerns the encoding of *Signal Detection Theory*'s quantities in human brain. In particular, we developed a model for **decisional criterion dynamics**. In SDT, discrimination ability is based on two main elements: the stimulus encoding into neuronal electrical activity and the definition of a decisional strategy, related to the *criterion*. While, on the one hand, electrical activity is affected by noise and consequently to trial-by-trial variations, on the other hand, criterion is traditionally assumed to be constant, at least during blocks of subsequent trials. We investigated the trial-by-trial criterion dynamics aiming to tackle the issue of its stability.

*Time – evolution
of SDT criterion*

So, in the second part of the present dissertation we tested a model for criterion dynamics based on the theory of feedback. Subjects were requested to discriminate between two possible responses (*left* or *right*) while the tilting angle characterizing the stimuli, was changing periodically over time. The optimal criterion position is induced to oscillate at a well-defined frequency; we observed that subjects were able to follow this dynamics and set their decisional criterion closed to the optimal position, though with a certain phase-delay.

The possibility to induce a well-defined criterion dynamics can be interpreted as an unusual form of learning. In the literature, learning is often associated with an improvement of subject's ability to perform specific tasks. In terms of *SDT* this is usually thought as an increase of sensitivity (d').

We showed that, by fixing d' , the **criterion can evolve in time if a mechanisms involving both memory of previous trials and the subject's willing of improving performance acts on decisional strategy**. The disentanglement of sensitivity and criterion offers the possibility to shape each subject's response, during an experimental session, independently from his/her ability in performing the task.

Future possible developments of this result concern investigations on criterion dynamics in different perceptual modalities. In addition, the problem of criterion stability, with regard to possible internal stochastic fluctuations, could be coped with by using the experimental techniques presented in the dissertation.

Appendix A

Preliminar statement, instruction and final questions

DICHIARAZIONE PRELIMINARE:

Io sottoscritto/a _____ dichiaro di non essere in possesso di alcuna informazione relativa alla modalità o ai contenuti dell'esperimento che mi accingo a svolgere.

In fede,

Figure A.1: Preliminar statement of naiveness to the aim of the experiment.



<p>1.</p> <p>Durante questo esperimento ti verranno presentati degli stimoli visivi (Gabor) e ti verrà chiesto di dichiararne l'orientazione.</p> <p>Gli stimoli potranno avere differenti orientazioni: il tuo compito consiste nel dire se sono orientati a destra o a sinistra.</p> <div style="display: flex; justify-content: space-around; align-items: center;">   </div> <p>Esempio di stimolo orientato a sinistra Esempio di stimolo orientato a destra</p>	<p>2.</p> <p>Ogni stimolo è preceduto da un punto di fissazione: gli stimoli compariranno sempre nello stesso punto, al centro dello schermo.</p> <p>Dopo la scomparsa dello stimolo dovrai dare la tua risposta. Premi il tasto 'D' per rispondere "DESTRA" o il tasto 'S' per rispondere "SINISTRA".</p>
<p>3.</p> <p>Non cercare di rispondere il più velocemente possibile; cerca piuttosto di essere IL PIÙ ACCURATO POSSIBILE.</p> <p>Infatti non c'è fretta: lo stimolo successivo ti verrà presentato solo dopo che avrai fornito la risposta.</p>	<p>4.</p> <p>L'esperimento è diviso in tre parti:</p> <p>una prima di familiarizzazione con il compito e gli stimoli, una seconda, definita "psicometrica", del tutto analoga alla precedente ed una terza per la quale ti verranno successivamente fornite altre istruzioni.</p> <p>Quando sei pronto FAI ATTENZIONE e, dopo esserti comodamente posizionato sulla mentoniera, premi la barra spaziatrice per cominciare l'esperimento.</p>

Figure A.2: Instruction provided to the participant preliminarily to training session.

A. PRELIMINAR STATEMENT, INSTRUCTION AND FINAL QUESTIONS

<p>1</p> <p>Nello spazio, in assenza di gravità, non esiste una definizione univoca di verticalità, visto che manca un riferimento per definire l'orientazione degli oggetti.</p> <p>Immagina di essere il pilota di una navicella spaziale che deve agganciarsi ad una stazione spaziale.</p> <p>Per effettuare correttamente la manovra è necessario allineare la navicella alla stazione.</p>	<p>2</p> <p>Purtroppo, l'orientazione della stazione rispetto alla tua navicella può cambiare nel tempo in maniera a te sconosciuta.</p> <p>Per ovviare a tale problema, la stazione ti fornirà alcune informazioni per consentirti di conoscere l'orientazione reciproca e la sua evoluzione nel tempo.</p>
<p>3</p> <p>La stazione invierà sullo schermo del tuo computer di bordo degli stimoli visivi (Gabor); per ogni stimolo la stazione sceglierà in maniera casuale un'orientazione sinistra o destra rispetto al SUO asse di riferimento.</p> <div style="display: flex; justify-content: space-around; align-items: center;"><div style="text-align: center;"><p>Esempio di stimolo orientato a sinistra</p></div><div style="text-align: center;"><p>Esempio di stimolo orientato a destra</p></div></div>	<p>4</p> <p>Per ogni stimolo dovrai dichiarare se esso è orientato a destra (tasto 'D') o sinistra (tasto 'S').</p> <p>Ricevuta la risposta, la stazione spaziale ti informerà, tramite una voce registrata, se l'orientazione da te percepita coincide ('SI') o non coincide ('NO') con l'orientazione da lei stabilita per quello stimolo.</p> <p>Sarai un ottimo pilota se riuscirai ad immaginare via via l'orientazione della stazione ed a massimizzare quindi il numero di coincidenze ('SI').</p>
<p>5</p> <p>Supponiamo ora che ti venga presentato il seguente stimolo</p> <div style="text-align: center;"></div> <p>e che la tua risposta sia</p> <p style="text-align: center;">SINISTRA!</p> <p>Supponiamo inoltre che la successiva informazione proveniente dalla stazione sia</p> <p style="text-align: center;">SÌ</p> <p>Questo significa che anche per la stazione lo stimolo era orientato a sinistra.</p>	<p>6</p> <p>Supponiamo ora che ti venga presentato questo secondo stimolo</p> <div style="text-align: center;"></div> <p>e che la tua risposta sia</p> <p style="text-align: center;">DESTRA!</p> <p>... e supponiamo anche che la successiva informazione proveniente dalla stazione sia</p> <p style="text-align: center;">SÌ</p> <p>Questo significa che anche per la stazione lo stimolo era orientato a destra.</p>

<p>7</p> <p>E' quindi probabile che l'orientazione della stazione spaziale sia quella indicata dalla barra rossa nella figura sottostante.</p> 	<p>8</p> <p>Un altro stimolo che ti potrebbe essere presentato è il seguente</p>  <p>supponiamo ora che la tua risposta sia</p> <p>DESTRA!</p> <p>mentre l'informazione proveniente dalla stazione sia</p> <p>NO</p> <p>Questo vorrà dire che per la stazione lo stimolo era orientato a sinistra.</p>
<p>9</p> <p>E' quindi probabile che l'orientazione della stazione spaziale sia quella indicata dalla barra rossa nella figura sottostante.</p> 	<p>10</p> <p>Analogamente, se per il seguente stimolo</p>  <p>dichiarando SINISTRA, avrai ricevuto un NO! da parte della stazione,</p> <p>potrai immaginare che l'orientazione della stazione spaziale sia quella indicata dalla barra rossa nella figura sottostante</p> 
<p>11</p> <p>Ricorda allora: dovrai immaginare come cambia nel tempo l'orientazione della stazione;</p> <p>lo farai bene solo se MASSIMIZZERAI IL NUMERO DI COINCIDENZE,</p> <p>ossia il numero di informazioni SI che riceverai dalla stazione in seguito ad ogni tua risposta.</p>	<p>12</p> <p>Ad un certo punto nel corso dell'esperimento, la voce registrata verrà disattivata. Da quel momento in poi non riceverai più alcuna informazione dalla stazione spaziale.</p> <p>Dovrai comunque CONTINUARE A RISPONDERE NEL MODO CHE RITIENI PIU' ACCURATO.</p>

A. PRELIMINAR STATEMENT, INSTRUCTION AND FINAL QUESTIONS

QUESTIONARIO DI FINE ESPERIMENTO:

Hai concluso con successo l'esperimento, ti chiediamo ancora pochi minuti per compilare il seguente questionario.

Domanda 1

Nel corso dell'esperimento l'orientazione della stazione spaziale rispetto alla tua navicella poteva essere soggetta a cambiamenti: hai notato eventuali variazioni?

sì
no

in caso affermativo, le variazioni erano:

lente rapide

sempre in caso affermativo, le variazioni erano:

regolari casuali

Domanda 2

Ti è stata utile l'informazione vocale fornita dalla stazione spaziale?

sì
no

Domanda 3

Quando l'informazione vocale era assente, hai notato variazioni dell'orientazione della stazione spaziale?

sì
no

in caso affermativo, le variazioni erano:

lente rapide

sempre in caso affermativo, le variazioni erano:

regolari casuali

Domanda 4

Nella fase dell'esperimento in cui ti veniva fornita l'informazione vocale, quante volte hai percepito un cambiamento dell'orientazione?

Quante volte hai percepito un cambiamento dell'orientazione nella fase senza l'informazione vocale?

In conclusione ti preghiamo di non divulgare informazioni sull'esperimento che hai appena effettuato. Questo al fine di non influenzare l'esecuzione dell'esperimento da parte di futuri candidati.

Grazie mille per la tua collaborazione.

Rovereto, _____

Appendix B

Linear model for feedback loops

In control system, feedback consists in comparing the output of the system with the desired output and making a correction accordingly. In particular, with negative feedback we mean the process of coupling the output back in such a way as to cancel some of the input. We will start our mathematical description of the issue with the study of the open-loop system such as in Fig. B.

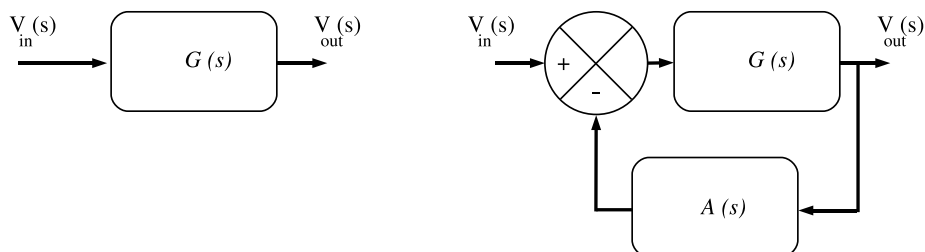


Figure B.1: On the left side is shown a circuit-like scheme of open-loop system. The right the feedback loop is added to the system.

Open-loop circuit

Being s a complex number of the form $s = \sigma + i\omega$, then, if ω is intended as the frequency

$$V_{out}(s) = V_{in}(s) \cdot G(s), \quad (\text{B.1})$$

that in the time domain, by applying the Laplace anti-transform, becomes

$$v_{out}(t) = v_{in}(t) * g(t) = \int_{-\infty}^{\infty} g(\tau) \cdot v_{in}(t - \tau) d\tau \quad (\text{B.2})$$

where, as usual t is time.

Feedback circuit

As shown in Ch. 5, feedback loop can be schematized as in Fig. 5.2. Then, similarly to Eq. B.1,

$$V_{out}(s) = V_{in}(s) G(s) - V_{out}(s) A(s) G(s), \quad (\text{B.3})$$

or alternatively

$$V_{out}(s) = \frac{V_{in}(s) G(s)}{1 + A(s) G(s)}. \quad (\text{B.4})$$

Being $H(s) = \frac{V_{out}(s)}{V_{in}(s)}$, then

$$H(s) = \frac{G(s)}{1 + A(s) G(s)}. \quad (\text{B.5})$$

In our investigation we are interested to a particular class of input signals, mathematically expressed by the form $v_{in}(t) = e^{st}$. This type of signals show a particular behaviour if processed as in Eq. B.2:

$$v_{out}(t) = \int_{-\infty}^{\infty} h(\tau) \cdot e^{s(t-\tau)} d\tau = e^{st} \int_{-\infty}^{\infty} h(\tau) \cdot e^{-s\tau} d\tau = v_{in}(t) H(s) \quad (\text{B.6})$$

where $H(s) = \int_{-\infty}^{\infty} h(\tau) \cdot e^{-s\tau} d\tau$ is the laplace transform of $h(t)$.

By taking into account the case $s = i\omega$ ($\sigma = 0$), where $i = \sqrt{-1}$, we can focus our attention to the real part of the signals under investigation: in particular, $Re[e^{i\omega\tau}] = \cos(\omega\tau)$. In this case, Eq. B.6 that can be written in the form

$$v_{out}(t) = e^{i\omega t} \cdot H(i\omega) \quad (\text{B.7})$$

becomes

$$Re[v_{out}(t)] = Re[e^{i\omega t} \cdot H(i\omega)] \quad (\text{B.8})$$

In polar coordinates, $H(i\omega) = |H(i\omega)|e^{i\phi}$, where ϕ is a generic phase parameter. It follows that

$$Re[v_{out}(t)] = |H(i\omega)| \cdot \cos(\omega t + \phi), \quad (\text{B.9})$$

or, in other words, the amplitude of the output is proportional to the input shifted of a phase ϕ and multiplied by a factor $|H(i\omega)|$. The single pole,

B. LINEAR MODEL FOR FEEDBACK LOOPS

closed-loop gain function¹ is expressed by the gain function $H(s) = \frac{G_0}{1+s\tau}$, or, similarly as before,

$$H(i\omega) = \frac{G_0}{1+i\omega\tau}. \quad (\text{B.10})$$

If considering only the real part

$$|H(i\omega)| = \frac{|G_0|}{\sqrt{(1+i\omega\tau)(1-i\omega\tau)}} = \frac{G_0}{\sqrt{1+(\omega\tau)^2}}. \quad (\text{B.11})$$

By linking together Eq. B.7 with Eqq. B.9 and B.11 we obtain

$$v_{out}(t) = \frac{G_0}{\sqrt{1+(\omega\tau)^2}} \cos[(\omega t) + \phi] \quad (\text{B.12})$$

that is of the same form of Eq. 5.2.

¹In Ch. 5 we used this model to interpret the phenomenon and the experimental data.

List of Tables

3.1	Single subject analysis: values of k of each subject	39
3.2	Single subject analysis: statistics relative to k	40
3.3	Values of the fit parameters	45
4.1	Stimulus–Response matrix in “Yes–No” experiments	53
5.1	Experimental setup parameters	72
5.2	Values of the parameters phase and gain: Experiment 1	85
5.3	Head position: fit parameters	94
5.4	Values of the parameters τ and G : Experiment 2	98

List of Figures

2.1	Schematic view of behavioural experiments	9
2.2	Stimulus-evoked neural activity	12
2.3	Stimulus evoked neural activity in multidimensional case	13
2.4	Threshold models decision	14
2.5	standard “Yes/No” trial time-line	15
2.6	Link between stimuli and psychometric function	17
3.1	Discrimination process with and without exogenous noise	24
3.2	Masking profile	25
3.3	SR: experimental setup	32
3.4	TvC profile with and without SR	35
3.5	Number of experimental sessions in which a particular value of I_n was presented	37
3.6	SR experiment: three data set	41
3.7	Number of data points for each $(\Delta I_s, \Delta I_n)$ couple	43
3.8	Lattice of detection rate averaged over the entire data set	43
3.9	Fit at low resolution	44
4.1	Hit rate and False alarm rate	55
4.2	ROC – curves in (H, F) -space	57
4.3	<i>Stochastic resonance</i> and <i>signal detection theory</i>	59
4.4	For each c_r value, SR is reported as a maximum of percent of correct response at a specific value of $\sigma = \sigma_{max}$. Values of σ_{max} exist only if $c_r > \mu_2$	60
5.1	Time evolution of criterion position	67
5.2	Graphical representation of a feedback loop	68
5.3	Feedback loop acting on criterion setting	70
5.4	Example of Gabor patch	71
5.5	Left/right oriented Gabor patches	72
5.6	Effect of a rigid rotation	74

LIST OF FIGURES

5.7	Stimulus modulation and criterion evolution	75
5.8	Criterion Setting Dynamics: experimental setup	76
5.9	Trial time–line	77
5.10	Experimental time–line	78
5.11	Grids of likelihood	80
5.12	Example of Psychometric function	81
5.13	Scatter plot: data Experiment 1	86
5.14	Grand–average: data Experiment 1	88
5.15	Experimental setup: Experiment 2	90
5.16	Picture of the apparatus Experiment 2	91
5.17	Picture of a marker	92
5.18	Head’s tilting angle for subject <i>DD</i>	93
5.19	Frequency spectrum of the head position for subject <i>DD</i>	94
5.20	FFT spectrum of head motion	95
5.21	Scatter plot: data Experiment 2	96
5.22	Grand–average: data Experiment 2	97
5.23	Scatter plot: data from both the experiments	100
5.24	Grand–average: data from both the experiments	101
5.25	Likelihood spectra: $T_{max} = 100$	103
5.26	Likelihood spectra: $T_{max} \neq 100$	104
5.27	Likelihood spectra: T_{max} out of range	105
5.28	Scatter plot: data at T_{max}	107
A.1	Preliminar statement of naiveness to the aim of the experiment.	115
A.2	Instruction provided to the participant preliminarily to training session.	116
A.3	Instruction provided preliminarily to main session.	118
A.4	Questions asked at the end of the experimental session.	119
B.1	Schemes of open–loop and feedback circuits	121

Bibliography

- [1] *Spatiotemporal order out of noise*
F. Sagues, J. M. Sancho and Jordi Garcia-Ojalvo
Rev. Mod. Phys. **79**, (2007) 829
- [2] *Stochastic resonance: a remarkable idea that changed our perception of noise*
L. Gammaitoni, P. Haenggi, P. Jung and F. Marchesoni
Eur. Phys. J. B **69** (2009) 1
- [3] *Stochastic resonance*
L. Gammaitoni, P. Haenggi, P. Jung and F. Marchesoni
Rev. Mod. Phys. **70/1**, (1998) 223
- [4] *Noise in the neural system*
A. A. Faisal, L. P. J. Selen and D. M. Wolpert
Nature Review Neuroscience **9**, (2008) 292–303
- [5] *Effects of Synaptic Noise and Filtering on the Frequency Response of Spiking Neurons*
N. Brunel, F. S. Chance, N. Fourcaud, and L. F. Abbott
Phys. Rev. Lett. **86**, (2001) 2186–2189
- [6] *Noisy neurons can certainly compute*
E. Salinas
Nature Neuroscience **9**, (2006) 1349–1350
- [7] *Dynamic Brain Sources of Visual Evoked Responses*
S. Makeig, M. Westerfield, T.-P. Jung, S. Enghoff, J. Townsend, E. Courchesne and T. J. Sejnowski
Science **295**, (2002) 690–694
- [8] *Magnetoencephalography—theory, instrumentation, and applications to noninvasive studies of the working human brain*
M. Haemaelaenen, R. Hari, R. J. Ilmoniemi, J. Knuutila, and O. V.

BIBLIOGRAPHY

- Lounasmaa
Rev. Mod. Phys. **65**, (1993) 413–497
- [9] *Analysis of fMRI Time-Series Revisited*
K. J. Friston, A. P. Holmes, J.-B. Poline, P. J. Grasby, S. C. R. Williams,
R. S. J. Frackowiak and R. Turner
NeuroImage **2**, (1995) 45–53
- [10] *Reliability, synchrony and noise*
G. B. Ermentrout, R. F. Galan and N. N. Urban
Trends in Neurosciences **31**, (2008) 428–434
- [11] *Stochastic resonance without tuning*
J. J. Collins Carson C. Chow and Thomas T. Imhoff
Nature **376**, (1995) 236–238
- [12] *Functional stochastic resonance in the human brain: noise induced sensitization of baroreflex system*
I. Hidaka, D. Nozaki and Y. Yamamoto
Phys. Rev. Lett. **85/17**, (2000) 3740
- [13] *The Neural Basis of Decision Making*
J. I. Gold and M. N. Shadlen
Annu. Rev. Neurosci. **30**, (2007) 535–74
- [14] *Signal Detection Theory and Psychophysics*
D. M. Green and J. A. Swets
Wiley (1966) New York
- [15] *Detection Theory: A User's Guide*
N. A. MacMillan and C. D. Creelman
Lawrence Erlbaum Associates (2005) Mahwah, NJ
- [16] *Statistically robust evidence of stochastic resonance in human auditory perceptual system*
D. Tabarelli, A. Vilardi, C. Begliomini, F. Pavani, M. Turatto and L. Ricci
Eur. Phys. J. B **69** (2009) 155
- [17] *Feedback Networks: Theory and Circuit Applications*
J. Choma and W. K. Chen
World Scientific (2007)
- [18] *Receptive fields of single neurones in the cat's striate cortex*
D. H. Hubel and T. N. Wiesel
J. Physiol. **148**, (1959) 574–591

- [19] *Receptive field, binocular interaction and functional architecture in the cat's visual cortex*
D. H. Hubel and T. N. Wiesel
J. Physiol. **160**, (1962) 106–154
- [20] *Receptive field and functional architecture of monkey striate cortex*
D. H. Hubel and T. N. Wiesel
J. Physiol. **192**, (1968) 215–243
- [21] *Dynamics of orientation coding in area V1 of the awake primate*
S. Celebrini, S. Thorpe, Y. Trotter and M. Imbert
Visual Neuroscience **10**, (1993) 811–825
- [22] *Dynamics of orientation tuning in macaque primary visual cortex*
D. L. Ringach, M. J. Hawken and R. Shapley
Nature **387**, (1997) 281–284
- [23] *How MT cells analyze the motion of visual patterns*
N. C. Rust, V. Mante, E. P. Simoncelli and J. A. Movshon
Nature Neuroscience **9**, (2006) 1421–1431
- [24] *Coding of stimulus sequences by population responses in visual cortex*
A. Benucci, D. L. Ringach and M. Carandini
Nature Neuroscience **12**, (2009) 1317–1324
- [25] *Implanted neural electrodes cause chronic, local inflammation that is correlated with local neurodegeneration*
G. C. McConnell, H. D. Rees, A. I. Levey, C. A. Gutekunst, R. E. Gross and R. V. Bellamkonda
J. Neural Eng. **6**, (2006) 056003
- [26] *Multiple neural spike train data analysis: state-of-the-art and future challenges*
E. N. Brown, R. E. Kass and P. P. Mitra
Nature Neuroscience **7**, (2004) 456–461
- [27] *The Cognitive Neurosciences (4th Edition)*
M. S. Gazzaniga
MIT Press (2010) Cambridge
- [28] *Timing of human cortical functions during cognition: role of MEG*
R. Hari, S. Levänen and T. Raij
Trends in Cognitive Sciences **4** (2000) 455–462

BIBLIOGRAPHY

- [29] *What does fMRI tell us about neuronal activity?*
D. J. Heeger and D. Ress
Nature Reviews Neuroscience **3**, (2002) 142–151
- [30] *Spikes versus BOLD: what does neuroimaging tell us about neuronal activity?*
D. J. Heeger, A. C. Huk, W. S. Geisler and D. G. Albrecht
Nature Neuroscience **3**, (2000) 631–633
- [31] *Interpreting functional imaging studies in terms of neurotransmitter cycling*
R. G. Shulman and D. L. Rothman
Proc. Natl. Acad. Sci. USA **95**, (1998) 11993–11998
- [32] *Dynamics of blood flow and oxygenation changes during brain activation: the Balloon model*
R. B. Buxton, E. C. Wong and L. R. Frank
Magn. Reson. Med. **39**, (1998) 855–864
- [33] *Increased cortical oxidative metabolism due to sensory stimulation: implications for functional brain imaging.*
I. Vanzetta and A. Grinvald
Science **286**, (1999) 1555–1558
- [34] *Neurophysiological investigation of the basis of the fMRI signal*
N. K. Logothetis, J. Pauls, M. Augath, T. Trinath and A. Oeltermann
Nature **412**, (2001) 150–157
- [35] *Stochastic resonance in psychophysics and in animal behavior*
L. M. Ward, A. Neiman, F. Moss
Biol. Cybern. **87**, (2002) 91–101
- [36] *Optimal decision rule for some common psychophysical paradigms*
D. L. Norren
in Mathematical Psychology and Psychophysiology, SIAM--AMS Proceedings **13** (1981)
- [37] *Regional response differences within the human auditory cortex when listening to words*
C. Price, R. Wise, S. Ramsay, K. Friston, D. Howard, K. Patterson and R. Frackowiak
Neuroscience Letters **146**, (1992) 179–182

- [38] *Speed and cerebral correlates of syllable discrimination in infants*
G. Dehaene-Lambertz and S. Dehaene
Nature **370**, (1994) 292–295
- [39] *Multidimensional perceptual scaling of musical timbres*
J. M. Grey
J. Acoust. Soc. Am. **61**, (1977) 1270–1277
- [40] *Entrained rhythmic activities of neuronal ensembles as perceptual memory of time interval*
G. Sumbre, A. Muto, H. Baier and M. Poo
Nature **456**, (2008) 102–106
- [41] *The amusic brain: in tune, out of key, and unaware*
I. Peretz, E. Brattico and M. Jarvenpaa
Brain **132**, (2009) 1277–1286
- [42] *Effects of auditory noise on the psychophysical detection of visual signals: Cross-modal stochastic resonance*
E. Manjarrez, I. Mendez, L. Martinez, A. Flores and C. R. Mirasso
Neuroscience Letters **415**, (2007) 231
- [43] *Modeling the influence of task on attention*
V. Navalpakkam and L. Itti
Vision Research **45**, (2005) 205–231
- [44] *Limit Distributions for Sums of Independent Random Variables*
B. V. Gnedenko and A. N. Kolmogorov
Addison-Wesley (1954) MA
- [45] *Multidimensional choice behavior in developmental psychophysics: Size, brightness, and color dimensions combined*
P. Hauf and V. Sarris
Journal of Vision **1** (2001) 363
- [46] *Psychophysiological investigation of vigilance decrement: Boredom or cognitive fatigue?*
N. Pattyn, X. Neyt and D. Herdiericlx
Physiology and Behavior **93** (2008) 369–378
- [47] *Noise-enhanced tactile sensation*
J. J. Collins, T. T. Imhoff, and P. Grigg
Nature **383**, (1996) 770

BIBLIOGRAPHY

- [48] *Numerical Recipes in C++*
W. H. Press, S. A. Teukolsky, W. T. Vetterling, and B. P. Flannery
Cambridge University Press (2003)

Masking effect

- [49] *The masking of pure tones and of speech by white noise*
J.E. Hawkins and S.S. Stevens
J. Acous. Soc. Am. **22/1**, (1950) 6–13
- [50] *Sentence intelligibility in noise for listeners with normal hearing and hearing impairment: Influence of measurement procedure and masking parameters*
K.C. Wagener and T. Brand
International Journal of Audiology **44/3**, (2005) 144–156
- [51] *Nonlinear Cochlear Signal Processing*
J.B. Allen
Physiology of the Ear, (2001)
- [52] *Masking potency and whiteness of noise at various noise check sizes*
H. Kukkonen, J. Rovamo and R. Näsänen
Investigative Ophthalmology & Visual Science **36/2**, (1995) 513–518
- [53] *The effect of noise check size and shape on grating detectability*
J. Rovamo and H. Kukkonen
Vision Res. **36/2**, (1996) 271–279
- [54] *Bayesian adaptive estimation of threshold versus contrast external noise function: The quick TvC method*
L. A. Lesmes, S. T. Jeon, Z-L Lu, and B. A. Doshier
Vision Res. **46**, (2006) 3160

Stochastic resonance: theory and reviews

- [55] *The mechanism of stochastic resonance*
R. Benzi, A. Sutera and A. Vulpiani
J. Phys. A, **14**, (1981) L453–L457
- [56] *Stochastic resonant damping in a noisy monostable system: theory and experiment*
G. Volpe, S. Perrone, J. M. Rubi and D. Petrov
Phys. Rev. **E77**, (2008) 051107

- [57] *Diversity-induced resonance*
C. J. Tessone, C. R. Mirasso, R. Toral and J. D. Gunton
Phys. Rev. Lett. **97** (2006) 194101
- [58] *Adding noise to improve measurement*
B. Ando' and S. Graziani
IEEE Instrumentation & Measurement Magazine (2001) 24
- [59] *Stochastic resonance as dithering*
R. A. Wannamaker, S. P. Lipshitz and J. Vanderkooy
Phys. Rev. E **61/1** (2000) 233
- [60] *Novel class of neural stochastic resonance and error-free information transfer*
H. Yasuda, T. Miyaoka, J. Horiguchi, A. Yasuda, P. Haenggi and Y. Yamamoto
Phys. Rev. Lett. **100** (2008) 118103
- [61] *Input-output gains for signal in noise in stochastic resonance*
F. Chapeau-Blondeau
Physics Letters A **232** (1997) 41
- [62] *Stochastic resonance in the heaviside nonlinearity with white noise and arbitrary periodic signal*
F. Chapeau-Blondeau
Phys. Rev. E **53/5** (1996) 53
- [63] *Stochastic resonance and signal detection in an energy detector – implication for biological receptor systems*
J. Tougaard
Biol. Cybern. **83** (2000) 471
- [64] *Generic noise-enhanced coding in neuronal arrays*
N. G. Stocks and R. Mannella
Phys. Rev. E **64** (2001) 030902
- [65] *Suprathreshold stochastic resonance in a single comparator*
R.-G. Wang and Z.-C. Long
Chin. Phys. Lett. **24/1** (2007) 275
- [66] *Optimal stimulus and noise distribution for information transmission via suprathreshold stochastic resonance*
M. D. McDonnell, N. G. Stocks and D. Abbott
Phys. Rev. E **75** (2007) 061105

BIBLIOGRAPHY

- [67] *Stochastic resonance and sensory information processing: a tutorial and review of application*
F. Moss, L. M. Ward and W. G. Sannita
Clinical Neurophysiology **115**, (2004) 267
- [68] *Stochastic resonance in the brain*
T. Mori and S. Kai
System and Computers in Japan **35/11** (2004) 39
- [69] *Stochastic resonance in climatic change*
R. Benzi, G. Parisi A. Sutera, and A. Vulpiani
Tellus, **34**, (1982) 10
- [70] *A Theory of Stochastic Resonance in Climatic Change*
R. Benzi, G. Parisi, A. Sutera and A. Vulpiani
SIAM Journal on Applied Mathematics, **43**, (1983) 565-578

Stochastic Resonance in non-biological systems

- [71] *Stochastic and coherence resonance in lasers: homoclinic chaos and polarization bistability*
F.T. Arecchi and R. Meucci
Eur. Phys. J. B **69** (2009) 93
- [72] *Noise color and asymmetry in stochastic resonance with silicon nanomechanical resonators*
T. Dunn, D.N. Guerra and P. Mohanty
Eur. Phys. J. B **69** (2009) 5
- [73] *Stochastic resonance phenomena in spin chains*
A. Rivas, N.P. Oxtoby and S.F. Huelga
Eur. Phys. J. B **69** (2009) 51

Stochastic Resonance in biological systems

- [74] *Stochastic resonance in the motor system: effects of noise on the monosynaptic reflex pathway of the cat spinal cord*
L. Martínez, T. Pérez, C. Mirasso, and E. Manjarrez
J. Neurophysiol. **97** (2007) 4007
- [75] *Stochastic resonance enhances the electrosensory information available to paddlefish for prey capture*

- P. E. Greenwood, L. M. Ward, D. F. Russell, A. Neiman, and F. Moss
Phys. Rev. Lett. **84/20** (2000) 4773
- [76] *Behavioural stochastic resonance: how a noisy army betrays its output*
J. A. Freund, J. Kienert, L. Schmimansky-Geier, B. Beisner, A. Neiman,
D. F. Russell, T. Yakusheva and F. Moss
Phys. Rev. E **63** (2001) 031910
- [77] *Evidence of stochastic resonance in the mating behaviour of *Nezara viridula* (L.)*
S. Spezia, L. Curcio, A. Fiasconaro, N. Pizzolato, D. Valenti, B. Spagnolo,
P. Lo Bue, E. Peri and S. Colazza
Eur. Phys. J. B **65** (2008) 453
- Medical application of stochastic resonance**
- [78] *Noise as therapy: a prelude to computationally-based neurology?*
J. C. Milton
Annals of Neurology **58/2** (2005) 173
- [79] *Health status and resonance in a model for living organisms under periodic stress and healing*
B.-G. Yoon, J. Choi and J.-Y. Fortin
Phys. Rev. E **73** (2006) 031905
- [80] *Effect of stochastic resonance on bone loss in osteopenic condition*
M. Rusconi, A. Zaikin, N. Marwan and J. Kurths
Phys. Rev. Lett. **100** (2008) 128101
- [81] *Noise and poise: enhancement of postural complexity in the elderly with stochastic-resonance-based therapy*
M. Costa, A. A. Priplata, L. A. Lipsitz, Z. Wu, N. E. Huang, A. L. Goldberger and C.-K. Peng
European Physics Letters **77** (2007) 68008
- [82] *Controlling posture using a plantar-based, tongue-placed tactile biofeedback system*
N. Vuillerme, O. Chenu, J. Demongeot and Y. Payan
Exp. Brain Res. **179** (2007) 409
- [83] *Noise-enhanced balance control in patients with diabetes and patients with stroke*
A. A. Priplata, B. L. Patritti, J. B. Niemi, R. Huges, D. C. Gravelle, L.

BIBLIOGRAPHY

A. Lipsitz, A. Veves, J. Stein, P. Bonato and J.J Collins
Annals of Neurology **59/1** (2006) 4

[84] *Noise-enhanced human sensorimotor function*
J.J Collins, A. A. Priplata, D. C. Gravelle, J. Niemi, J. Harry and L. A. Lipsitz
IEEE engineering in medicine and biology magazine **0739** (2003) 76

[85] *Stochastic heart-rate can reveal pathologic cardiac dynamics*
T. Kuusela
Phys. Rev. E **69** (2004) 031916

[86] *Noisy vestibular stimulation improves autonomic and motor responsiveness in central neurodegenerative disorders*
Y. Yamamoto, Z. R. Struzik, R. Soma, K. Ohashi and S. Kwak
Annals of Neurology **58/2** (2005) 175

Stochastic Resonance within the human brain

- Baroreflex system

[87] *Noise-enhanced human balance control*
A. A. Priplata, J. B. Niemi, M. Salen, J. Harry, L. A. Lipsitz and J.J Collins
Phys. Rev. Lett. **89/23** (2002) 238101

[88] *Noise-induced large-scale phase synchronization of human-brain activity associated with behavioural stochastic resonance*
K. Kitajo, S. M. Doesburg, K. Yamanaka, D. Nozaki, L. M. Ward and Y. Yamamoto
EPL **80** (2007) 40009

Stochastic Resonance in perceptual system

- Tactile perception

[89] *Noise-mediated enhancements and decrements in human tactile sensation*
J. J. Collins, T. T. Imhoff, and P. Grigg
Phys. Rev. E **56/1**, (1997) 923

-
- [90] *Touch noise increases vibrotactile sensitivity in old and young*
C. Wells, L. M. Ward, R. Chua and J. T. Inglis
Psychological Science, **16/4**, (2005) 313-320
- [91] *Stochastic resonance within the somatosensory system: effects of noise on evoked potentials elicited by tactile stimuli*
E. Manjarrez, g. Rojas-Piloni, I. Mendez and A. Flores
The journal of Neuroscience **23(6)**, (2003) 1997–2001
- Visual perception
- [92] *Visual perception of stochastic resonance*
E. Simonotto, M. Riani, C. Seife, M. Roberts, J. Twitty and F. Moss
Phys. Rev. Lett. **78/6**, (1997) 1186
- [93] *Same calculation efficiency but different internal noise for luminance- and contrast-modulated stimuli detection*
R. Allard and J. Flaubert
Journal of Vision **6**, (2006) 322–334
- [94] *Effect of noise on the contrast detection threshold in visual perception*
H. Sasaki, M. Todorokihara, T. Ishida, J. Miyachi, T. Kitamura and R. Aoki
Neurosci. Lett. **408**, (2006) 94
- [95] *Subthreshold noise facilitates the detection and discrimination of visual signals*
H. Sasaki, S. Sakane T. Ishida, M. Todorokihara, T. Kitamura and R. Aoki
Neurosci. Lett. **436**, (2008) 255
- [96] *Role of noise in image processing by the human perceptive system*
M. Piana, M. Canfora and M. Riani
Phys. Rev. E **62/1**, (2000) 1104
- [97] *Noise improves three-dimensional perception: Stochastic resonance and other impacts of noise to the perception of autostereograms*
T. Ditzinger, M. Stadler, D. Strüber, and J. A. S. Kelso
Phys. Rev. E **62**, (2000) 2566
- [98] *The impact of blurred vision on cognitive assessment*
A. Bertone, L. Bettinelli and J. Flaubert
Journal of Clinical and Experimental Neuropsychology **00**, (000) 00

BIBLIOGRAPHY

- [99] *Modulation of brain and behavioural responses to cognitive visual stimuli with varying signal-to-noise ratios*
A. Sorrentino, L. Parkkonen, M. Piana, A. M. Massone, L. Narici, S. Carozzo, M. Riani and W. G. Sannita
Clinical Neurophysiology **117**, (2006) 1098
- [100] *Behavioural stochastic resonance within the human brain*
K. Kitajo, D. Nozaki, L. M. Ward and Y. Yamamoto
Phys. Rev. Lett. **90/21**, (2003) 218103
- [101] *Internal noise determines external stochastic resonance in visual perception*
T. Aihara, K. Kitajo, D. Nozaki and Y. Yamamoto
Vision Research **48** (2008) 1569–1573
- [102] *Noise-improved signal detection in cat primary visual cortex via a well-balanced stochastic resonance-like procedure*
K. Funke, N. Kerscher and F. Wörgötter
European Journal of Neuroscience **26**, (2007) 1322–1332
- Stochastic Resonance and acoustic perception**
- [103] *Mechano-electrical transduction assisted by brownian motion: a role for noise in the auditory system*
F. Jaramillo and K. Wiesenfeld
Nature Neuroscience **1/5** (1998) 384
- [104]
J. F. Lindner, M. Bennett, and K. Wiesenfeld
Phys. Rev. E **72** (2005) 051911 ()
- [105] *Physiological noise level enhances mechano-electrical transduction in hair cells*
F. Jaramillo and K. Wiesenfeld
Chaos, Solitons and Fractals **11** (2000) 1869
- [106] *Human hearing enhanced by noise*
F. Zeng, Q. J. Fu, and R. Morse
Brain Research **869** (2000) 251
- [107] *Noise improves modulation detection by cochlear implant listeners at moderate carrier levels*
M. Chatterjee and S. I. Oba
J. Acoust. Soc. Am. **118/2** (2005) 993

- [108] *The effect of gaussian noise on the threshold, dynamic range, and loudness of analogue cochlear implant stimuli*
R. P. Morse, P. F. Morse, T. B. Nunn, K. A. M. Archer, and P. Boyle
JARO **8** (2007) 42
- [109] *Noise-enhanced hearing sensitivity*
Z. C. Long, F. Shao, Y. P. Zhang, and Y. G. Qin
Physics Letters A **323**, (2004) 434
- [110] *Lower hearing threshold by noise*
Z.-C. Long, F. Shao, Y.-P. Zhang and Y.-G. Qin
Chin. Phys. Lett. **21/4** (2004) 757
- [111] *The influence of noise type and level upon stochastic resonance in human audition*
D. T. Ries
Hearing Research **228**, (2007) 136

Signal Detection Theory

- [112] *A law of comparative judgment*
L. L. Thurstone
Psychol. Rev. **34**, (1927) 273
- [113] *Psychophysical analysis*
L. L. Thurstone
Am. J. Psychol. **38**, (1927) 368
- [114] *A new theory of visual detection*
W. P. Tanner and J. A. Swets
Tech. Rep. **18** (1953) University of Michigan, Electronic Defense Group
- [115] *The human use of information – I: Signal detection for the case of signal known exactly*
W. P. Tanner and J. A. Swets
Transaction IRE Professional Group of Information Theory **4**, (1953) 119
- [116] *A decision-making theory of visual detection*
W. P. Tanner and J. A. Swets
Psychol. Rev. **61**, (1953) 401
- [117] *Stimulus-oriented approach to detection*
L. A. Jeffress
J. Acoust. Soc. Am. **36**, (1964) 766

BIBLIOGRAPHY

- [118] *Receiver–operating characteristics determined by a mechanical analog to the rating scale*
C. S. Watson, M. E. Rilling and W. T. Bourbon
J. Acoust. Soc. Am. **36**, (1964) 766
- [119] *Neuronal correlates of a perceptual decision*
W. T. Newsome, K. H. Britten and J. A. Movshon
Nature **341**, (1989) 52–54
- [120] *The analysis of visual motion – A comparison of neuronal and psychophysical performance*
K. H. Britten, M. N. Shadlen and W. T. Newsome
Journal of Neuroscience **12**, (1992) 4745–4765
- [121] *A model of neuronal responses in visual area MT*
E. P. Simoncelli and D. J. Heeger
Vision Research **38**, (1998) 743–761
- [122] *Sense and the single neuron: Probing the physiology of perception*
A. J. Parker, W. T. Newsome
Annu. Rev. Neurosci. **21**, (1998) 227–277
- [123] *Saccade Target Selection in the Superior Colliculus: A Signal Detection Theory Approach*
B. Kim and M. Basso
J. Neurosci. **28**, (2008) 2991–3007
- [124] *Effects of biased feedback on learning and deciding in a vernier discrimination task*
H. M. Herzog and M. Fahle
Vision Res. **39**, (1999) 4232
- [125] *A theory of identification of complex stimuli with an application to word recognition*
M. Treisman
Psychol. Rev **85**, (1978) 525
- [126] *Model for stochastic–resonance–type behaviour in sensory perception*
Y. Gong, N. Matthews and N. Qian
Phys. Rev. E **65** (2002) 031904

Criterion Setting Dynamics

- [127] *The Art of Electronics*
P. Horowitz and W. Hill
Cambridge University Press (1989)
- [128] *A theory of criterion setting with an application to sequential dependencies*
M. Treisman and T.C. Williams
Psychol. Rev. **92**, (1984) 68
- [129] *The dynamics of experimentally induced criterion shifts*
S. Brown and M. Steyvers
J. Exp. Psychol. Learn. **31**, (2005) 587
- [130] *Stochastic resonance and the dithering effect in threshold physical systems*
L. Gammaitoni
Phys. Rev. E **52**, (1995) 4691
- [131] *Digital Signal Processing*
A. V. Oppenheim and R. W. Schaffer
Prentice Hall (1975)
- [132] *Psychology application note* from the web site www.qualisys.com
- [133] *Dissociation Between Judgments and Outcome-Expectancy Measures in Covariation Learning: A Signal Detection Theory Approach.*
C.J. Perales, A. Catena, D.R. Shanks and A.J. González
J. Exp. Psychol. Learn. **31**, (2005) 1105–1120

